

THE DYNAMICS OF SEMIGROUPS OF CONTRACTION SIMILARITIES ON
THE PLANE

A Dissertation

Submitted to the Faculty

of

Purdue University

by

Stefano Silvestri

In Partial Fulfillment of the

Requirements for the Degree

of

Doctor of Philosophy

August 2019

Purdue University

Indianapolis, Indiana

THE PURDUE UNIVERSITY GRADUATE SCHOOL
STATEMENT OF DISSERTATION APPROVAL

Dr. Rodrigo A. Pérez, Chair

Department of Mathematical Sciences

Dr. William Geller

Department of Mathematical Sciences

Dr. Michał Misiurewicz

Department of Mathematical Sciences

Dr. Roland K. Roeder

Department of Mathematical Sciences

Approved by:

Dr. Evgeny Mukhin

Head of the Graduate Program

Nature's beauty dies.
The day dawns when the nautilus is no more.
The rainbow passes, the flower fades, the mountains crumble, the stars grow cold.
But beauty in Mathematics endures for evermore.
- H. E. Huntley

ACKNOWLEDGMENTS

The completion of this Ph.D. is due to the invaluable help of the people around me. First on the list are the people closest to me: mom and dad, my brother, and my uncle Secondo for their unconditional love and unwavering support.

I am deeply thankful to my advisor Prof. Rodrigo A. Pérez for his help and guidance during this Ph.D. on both the academic and human levels. Thank you for persevering with me.

My sincere thanks also go to my Thesis Defense Committee Prof. William Geller, Prof. Michał Misiurewicz, Prof. Roland K. Roeder for their patience and support through the years.

I am also grateful to the new friends I made along this arduous journey for their encouragement, for the long-lasting chats, for the laughs, for the fun-times, and for making me pick up juggling again! Thank you for sharing this adventure with me, you made this *odyssey* very special.

Last but not least, I want to thank the administrative staff of the Math Department: Jami, Tina, John, Jamie, and Cindy for always being so kind and understanding.

TABLE OF CONTENTS

	Page
LIST OF FIGURES	vii
ABSTRACT	ix
1 INTRODUCTION	1
2 GENERAL THEORY OF IFS	4
2.1 Iterated Function Systems	4
2.2 Examples	5
2.2.1 The Cantor Set	5
2.2.2 The Sierpiński Triangle	6
2.3 Symbolic Representation of an Attractor	7
2.4 Geometry of the Attractor	9
3 PARAMETRIC FAMILIES OF IFS	15
3.1 Notation	17
3.2 The Disconnectivity Algorithm	19
3.3 Geometry of the Connectedness Locus	20
3.4 The Overlap Set	23
4 THE BOUNDARY OF THE CONNECTEDNESS LOCUS	28
4.1 Self and Asymptotic Similarity	28
4.2 Proof of the Main Theorems	32
4.3 Examples: Landmark Points	38
4.3.1 $+(++-)^{\infty}$	38
4.3.2 $+--(+)^{\infty}$	43
4.3.3 $+---(+)^{\infty}$	46
4.3.4 $+--0(+)^{\infty}$	48
4.3.5 $+--00(+)^{\infty}$	50

	Page
4.4 Thunderstorm in No Man's Land	52
4.4.1 Alignment Condition	53
4.4.2 Shape Conditions at λ_0	56
4.4.3 Stack Contents of the Disconnectivity Algorithm	58
4.4.4 Different Shapes	59
4.4.5 Proof of the Proposition	63
4.5 Connection to Quadratic Dynamics	64
REFERENCES	69
VITA	71

LIST OF FIGURES

Figure	Page
2.1 The first four steps in the construction of the Cantor Set.	6
2.2 The first six steps in the construction of the Sierpiński Triangle. The dashed circle has radius 2. The colors represent which map has been applied first.	7
2.3 A feasible open set V , in gray, and its images for the Sierpiński Triangle. .	10
2.4 Two non trivial examples of IFS satisfying OSC.	11
2.5 The IFS $\{\mathfrak{s}_0, \mathfrak{s}_1\}$ on \mathbb{R} with contraction ratio the reciprocal of the golden ratio fails the overlap set condition. The red interval represents the overlap of $\mathfrak{s}_0(A)$ with $\mathfrak{s}_1(A)$, which are drawn above A in blue and orange respectively.	14
3.1 The connectivity locus \mathcal{M} , in blue, and its subset \mathcal{M}_0 , in fuchsia. The outer circle for both of them has radius 1.	16
3.2 Top row: the Twin-Dragon and the associated parameter $\lambda = 2^{-1}(1+i)$ in \mathcal{M} and \mathcal{M}_0 . Bottom row: the Tame Twin-Dragon and the corresponding parameter $\lambda' = 4^{-1}(1 + \sqrt{7}i)$ in \mathcal{M} and \mathcal{M}_0	27
4.1 \mathcal{M} is blue while \mathcal{M}_0 is fuchsia. Calegari and his collaborators showed that $\lambda \approx 0.371859 + 0.519411i$, marked in cyan, is a buried point of $\partial\mathcal{M}$	30
4.2 Construction of B_n , an element in the connected chain of open sets in $\mathbb{C} \setminus \tilde{A}_\lambda$. The dotted circle has half the radius of $\tilde{D}^{b n}$	35
4.3 The attractor A_{λ_0} inside $\tilde{\mathcal{I}}^\mathfrak{b}$. The green discs are part of the chain whose existence is provided by Theorem 4.1.3.	43
4.4 The attractor A_{λ_1} inside $\tilde{\mathcal{I}}^\mathfrak{b}$. The green discs are part of the chain whose existence is provided by Theorem 4.1.3.	46
4.5 The attractor A_{λ_2} inside $\tilde{\mathcal{I}}^\mathfrak{b}$. The green discs are part of the chain whose existence is provided by Theorem 4.1.3.	48
4.6 The attractor A_{λ_3} inside $\tilde{\mathcal{I}}^\mathfrak{b}$. The green discs are part of the chain whose existence is provided by Theorem 4.1.3.	50
4.7 The attractor A_{λ_4} inside $\tilde{\mathcal{I}}^\mathfrak{b}$. The green discs are part of the chain whose existence is provided by Theorem 4.1.3.	52

Figure	Page
4.8 In the background is \mathbb{I}^2 . Highlighted are the nodal discs of level 3 with centers $\pm f_2(\lambda_0) \pm \lambda_0^3$. The origin is colored in yellow.	54
4.9 Plots of the level curves $\text{Im}(\Xi_k(z)) = 0$ inside the disc of radius $2^{-1/2}$ for $k = 1, 2, 3, 4$. The parameter λ_0 is drawn in red.	55
4.10 Local picture around the origin of \mathbb{I}^2 and \mathbb{I}^5 for the parameter λ_0 . The cloud \mathbb{N}^- is highlighted in blue, while \mathbb{N}^+ is in orange.	57
4.11 Diagram representing how the stack entries change as we run Algorithm 1 for λ_0 . The integer $j \geq 0$ also indicates the level of the stack.	58
4.12 The instar at level 2 for λ_0 (top left), η_1 (top right), η_2 (bottom left), and η_3 (bottom right). The extra intersections are highlighted in red. For λ_0 and η_1 the aligned nodal discs of the next level are also drawn.	60
4.13 Table illustrating the self similar set A_λ and the corresponding Julia set J_c	68

ABSTRACT

Silvestri, Stefano Ph.D., Purdue University, August 2019. The Dynamics of Semigroups of Contraction Similarities on the Plane. Major Professor: Rodrigo A. Pérez.

Consider two objects associated to the Iterated Function System (IFS) $\{\lambda z + 1, \lambda z - 1\}$: the locus \mathcal{M} of parameters $\lambda \in \mathbb{D} \setminus \{0\}$ for which the corresponding attractor is connected; and the locus \mathcal{M}_0 of parameters for which the related attractor contains 0. The set \mathcal{M} can also be characterized as the locus of parameters for which the attractor of the IFS $\{\lambda z + 1, \lambda z, \lambda z - 1\}$ contains $1/\lambda$. Exploiting the asymptotic similarity of \mathcal{M} and \mathcal{M}_0 with the respective associated attractors, we give sufficient conditions on $\lambda \in \partial\mathcal{M}$ or $\partial\mathcal{M}_0$ to guarantee it is accessible (not buried). Moreover, for a specific parameter $\lambda \in \partial\mathcal{M} \cap \partial\mathcal{M}_0$ we describe a method to show it is accessible from the connected component of $\mathbb{D} \setminus \mathcal{M}$ containing the origin.

1. INTRODUCTION

The focus of this thesis is on a pair of mathematical objects, denoted by \mathcal{M} and \mathcal{M}_0 , whose study relates to several areas of mathematics. There is interest from the number theory point of view, since β -expansions (non-integer representation) of real numbers and Parry polynomials have been used [1, 2] to study \mathcal{M}_0 . Moreover, \mathcal{M} and \mathcal{M}_0 can be viewed as subsets of the closure of the roots of polynomials with (restricted) integer coefficients. The set \mathcal{M}_0 can also be seen from a dynamical point of view as the closure of the set (restricted to the unit disc) of Galois conjugates of entropies of real quadratic polynomials [3, 4].

We will investigate the sets \mathcal{M} and \mathcal{M}_0 via two other interpretations: as the closure of the roots of power series with restricted coefficients, and as the connectedness locus for a pair of linear transformations.

There is a compelling motivation, especially for analysts, to use the above interpretations of \mathcal{M} and \mathcal{M}_0 . The limit set A_λ , obtained by iteration of the aforementioned linear transformations, is the support of a probability measure, an infinite Bernoulli convolution. Such measure ν_λ is the distribution of the random sum $\sum_{n \geq 0} \pm \lambda^n$ where the signs are chosen with equal probability. The main concern is to find for which values of λ the measure ν_λ is absolutely continuous with respect to the Lebesgue measure. This problem dates back to Erdős [5] in 1939. In the real case, $\lambda \in (0, 1)$ and ν_λ is only known to be singular when λ is the reciprocal of a Pisot number in $(1, 2)$. This is proved by showing that the Fourier transform $\widehat{\nu}_\lambda(x)$ does not tend to zero as $x \rightarrow \infty$. In the complex case, ν_λ is singular whenever $|\lambda| < 2^{-1/2}$. The proof is a simple argument on the Hausdorff dimension of the support of ν_λ . See [6–8] for further background and results on this topic.

Our approach does not tackle this issue. The focus is on the boundary of \mathcal{M} and \mathcal{M}_0 . It was proven [9, 10] that both $\mathbb{D} \setminus \mathcal{M}$ and $\mathbb{D} \setminus \mathcal{M}_0$ are disconnected, i.e. that there

exists holes in \mathcal{M} and \mathcal{M}_0 . Moreover, these holes appear to be very well-organized as there are sequences of holes in \mathcal{M} accumulating to points on $\partial\mathcal{M}$. The question of classifying these connected components of $\mathbb{D} \setminus \mathcal{M}$ is still open, however our results are a step in that direction. Let \mathcal{P} denote the set of all power series with coefficients in $\{-1, 0, +1\}$, i.e.

$$\mathcal{P} := \left\{ f(z) = \sum_{j=0}^{\infty} c_j z^j \mid c_j \in \{-1, 0, +1\}, c_0 = 1 \right\}$$

then

Theorem 1.0.1 (Pérez-Silvestri) *Suppose f is the unique power series in \mathcal{P} that vanishes at $\lambda \in \mathcal{M} \setminus \mathbb{R}$ with $|\lambda| \leq 2^{-1/2}$. If f has finitely many zero coefficients and its Taylor polynomials satisfy certain conditions then λ is on the boundary of a hole of \mathcal{M} .*

and, with minor adjustments to the conditions on the Taylor polynomials,

Theorem 1.0.2 (Pérez-Silvestri) *Suppose f is the unique power series in \mathcal{P} that vanishes at $\lambda \in \mathcal{M} \setminus \mathbb{R}$ with $|\lambda| \leq 2^{-1/2}$. If f has no zero coefficients and its Taylor polynomials satisfy certain conditions then λ is on the boundary of a hole of \mathcal{M}_0 .*

We refer to points on the boundary of holes as *accessible* points, for obvious reasons. For a specific point on $\partial\mathcal{M} \cap \partial\mathcal{M}_0$, we further describe a method to determine the connected component of $\mathbb{D} \setminus \mathcal{M}$ from which it is accessible.

Proposition 1.0.1 (Pérez-Silvestri) *Let $\lambda_0 \approx -0.366+0.520i$ be the root of $f(z) = 1 + (z + z^2 - z^3)(1 - z^3)^{-1}$ then λ_0 is accessible from the connected component of $\mathbb{D} \setminus \mathcal{M}$ containing the origin.*

Further motivation to study boundary points of \mathcal{M}_0 is provided by the results in [11, 12]. It is possible to define quadratic dynamics on the limit set \mathbf{A}_λ so that it is quasymmetrically conjugate to the dynamics of $z^2 + c$ on the Julia set for Misiurewicz parameter c . We overview this connection in Section 4.5.

The thesis is organized as follows. Chapter 2 introduces the framework of our study, the Iterated Function Systems, abbreviated as IFS. An IFS is a finite collection of linear transformations on a complete metric space. Their study has formally begun with John E. Hutchinson in his highly influential paper [13] in 1981. Michael F. Barnsley and Kenneth Falconer popularized the theory of IFS with their books [14,15].

Chapters 3 and 4 describe the aforementioned sets. \mathcal{M} and \mathcal{M}_0 arise from a family of IFS parameterized by a complex number in the punctured unit disc. In the sections of Chapter 3, we set the notation and overview some known results about the sets \mathcal{M} and \mathcal{M}_0 . Our main theorems are proven in Chapter 4. Using these results we obtain explicit accessible parameters on the boundaries of both \mathcal{M} and \mathcal{M}_0 .

2. GENERAL THEORY OF IFS

2.1 Iterated Function Systems

Let (X, d) be a complete metric space and let \mathcal{X} be the space of nonempty compact subsets of X , endowed with the Hausdorff metric d_H . Recall that for any compact sets $E, F \in \mathcal{X}$ the Hausdorff distance between them is defined as

$$d_H(E, F) := \inf \{ \varepsilon > 0 \mid E \subset F^{(\varepsilon)} \text{ and } F \subset E^{(\varepsilon)} \}$$

where $F^{(\varepsilon)} := \{x \in X \mid d(x, y) < \varepsilon \text{ for some } y \in F\}$ is an ε -neighborhood of F .

An Iterated Function System (IFS) is a finite collection of contractions $\{\mathfrak{s}_j\}_{j=1}^m$

$$\mathfrak{s}_j : (X, d) \rightarrow (X, d) \quad \text{with} \quad d(\mathfrak{s}_j(x), \mathfrak{s}_j(y)) \leq d(x, y) \quad \text{for all } x, y \text{ in } X.$$

If we let $\mathbf{S} : (\mathcal{X}, d_H) \rightarrow (\mathcal{X}, d_H)$ be defined by

$$\mathbf{S}(K) := \bigcup_{j=1}^m \mathfrak{s}_j(K)$$

then a tedious but straightforward exercise shows \mathbf{S} is also a contraction. Hutchinson realized that the Contraction Fixed Point Theorem of Banach guarantees that \mathbf{S} has a unique fixed point:

Definition 2.1.1 (Hutchinson [13]) *Given a finite collection of contractions $\{\mathfrak{s}_j\}_{j=1}^m$ on a complete metric space (X, d) , there exists a unique compact set $\mathbf{A} \in \mathcal{X}$, called the limit set or attractor, such that*

$$\mathbf{S}(\mathbf{A}) = \bigcup_{j=1}^m \mathfrak{s}_j(\mathbf{A}) = \mathbf{A}.$$

Equivalently, for any $K \in \mathcal{X}$

$$\mathbf{A} = \lim_{n \rightarrow \infty} \mathbf{S}^n(K),$$

where $\mathbf{S}^k = \mathbf{S} \circ \mathbf{S}^{k-1}$ denotes the k -fold composition of \mathbf{S} with itself.

The attractor of an IFS can, in fact, be obtained in another way:

Proposition 2.1.1 (Hutchinson [13]) *If a non-empty closed set $C \subset X$ is forward invariant (i.e. $\mathfrak{s}_j(C) \subseteq C$) under the contraction mappings \mathfrak{s}_j , ($1 \leq j \leq m$) then C contains the attractor A of the IFS $\{\mathfrak{s}_j\}_{j=1}^m$ and*

$$A = \bigcap_{n \geq 0} S^n(C).$$

2.2 Examples

In what follows we provide a few classic examples of IFS. They will support the discussions of the properties of IFS in the next sections of this chapter. Furthermore, the first example actually belongs to the particular family of IFS on which we will focus in the following chapters.

2.2.1 The Cantor Set

Consider the contraction similarities

$$\mathfrak{s}_0(x) = \frac{1}{3}x - 1 \quad \mathfrak{s}_1(x) = \frac{1}{3}x + 1$$

on \mathbb{R} . Let $C_0 = [-3/2, 3/2]$, then simple calculations show that $\mathfrak{s}_0(C_0) = [-3/2, -1/2]$ and $\mathfrak{s}_1(C_0) = [1/2, 3/2]$, thus $C_1 := S(C_0) = \mathfrak{s}_0(C_0) \cup \mathfrak{s}_1(C_0)$ is a subset of C_0 , which by Proposition 2.1.1 implies the attractor is a subset of C_0 . Note that C_1 is equivalent to the interval C_0 with the open middle third removed. In the next iteration, the images $\mathfrak{s}_0(C_1)$ and $\mathfrak{s}_1(C_1)$ are simply the intervals $\mathfrak{s}_0(C_0)$ and $\mathfrak{s}_1(C_0)$ with their open middle third removed. Repeating this process infinitely many times will then lead us to the Cantor Set, $\mathfrak{C} = \bigcap_{n \geq 0} C_n$ where $C_k = S(C_{k-1})$ for $k \geq 1$. A few steps of the construction are shown in the figure below.

Note that the n th iterate, C_n , consists of 2^n disjoint closed intervals, each of length $(\frac{1}{3})^{n-1}$, so the total length of C_n is $3(\frac{2}{3})^n$ which tends to 0 as we increase n to infinity. However, the points $\pm 3/2$ are indeed in \mathfrak{C} , since they belong to C_n for every n . By

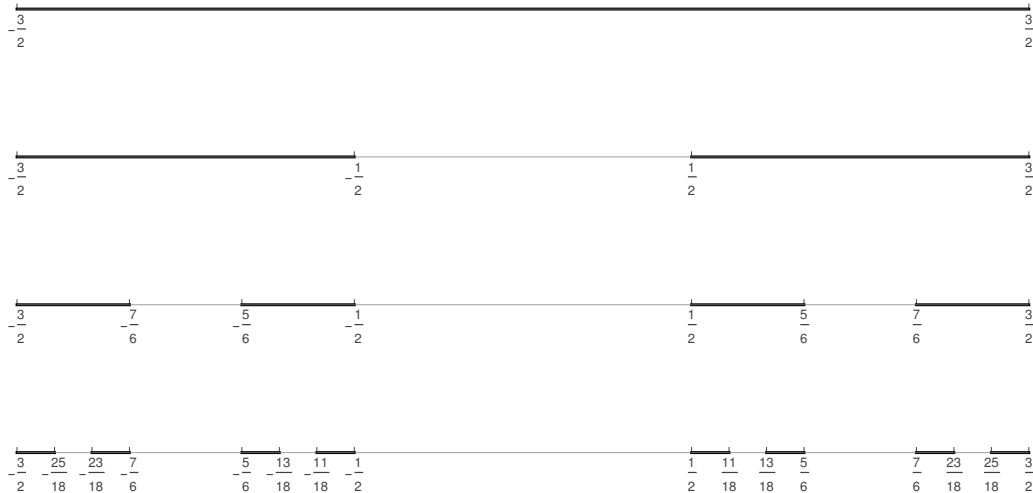


Fig. 2.1. The first four steps in the construction of the Cantor Set.

the same argument taking the endpoints of all the intervals of all the approximations C_n , we get a countable set of points, all belonging to \mathfrak{C} .

In fact, as we will see in Section 2.3, \mathfrak{C} can be put in bijection with the set of one-sided infinite binary words, so it is uncountable. The endpoints of every C_n correspond to eventually repeating words, and are precisely those points of \mathfrak{C} that are *accessible* from $\mathbb{R} \setminus \mathfrak{C}$.

We remark also that we can also consider the maps $\{\mathfrak{s}_0, \mathfrak{s}_1\}$ as contraction similarities on \mathbb{C} and obtain the same limit set, since by Definition 2.1.1, $\mathfrak{C} = \lim_{n \rightarrow \infty} S^n(K)$ for any non-empty compact set K .

2.2.2 The Sierpiński Triangle

Another standard example is the *Sierpiński Triangle*, \mathfrak{T} . In this case we consider three contraction similarities on \mathbb{C} :

$$\mathfrak{s}_0(z) = \frac{1}{2}z + \xi_3^0, \quad \mathfrak{s}_1(z) = \frac{1}{2}z + \xi_3^1, \quad \mathfrak{s}_2(z) = \frac{1}{2}z + \xi_3^2$$

where $\xi_3 = \exp(2\pi i/3)$ is a third root of unity. Let T_0 be the equilateral triangle with vertices at $2\xi_3^0$, $2\xi_3^1$, and $2\xi_3^2$. Joining the images \mathfrak{s}_0 , \mathfrak{s}_1 , and \mathfrak{s}_2 of T_0 is equivalent to removing the interior of the triangle with vertices at the midpoints of the sides of T_0 . Similarly, in the next iteration we remove the inner triangle from each of the three remaining triangles, and so on, in analogy to our description of the Cantor Set. Note however that \mathfrak{T} is a connected set, while \mathfrak{C} is not.

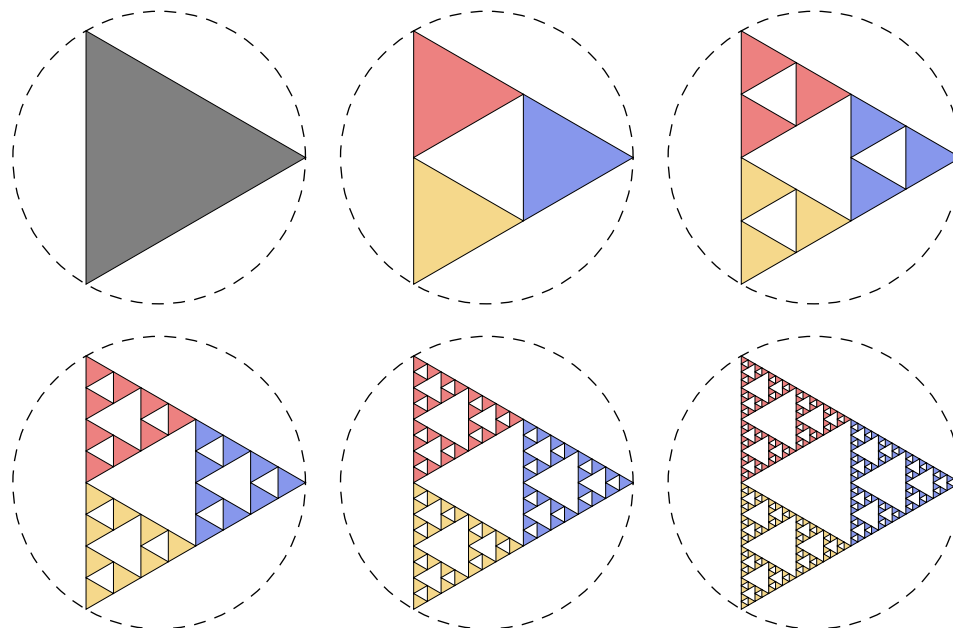


Fig. 2.2. The first six steps in the construction of the Sierpiński Triangle. The dashed circle has radius 2. The colors represent which map has been applied first.

2.3 Symbolic Representation of an Attractor

This last section introduces a convenient way to describe limit sets of iterated function systems. This interpretation is a consequence of the following result.

Theorem 2.3.1 (Hutchinson [13]) *The attractor A of an IFS $\{\mathfrak{s}_j\}_{j=1}^m$ is the closure of the set of fixed points of every finite composition of the maps $\{\mathfrak{s}_j\}_{j=1}^m$.*

Given an IFS $\{\mathfrak{s}_j\}_{j=1}^m$ we will describe points in the attractor A by assigning them a “name” consisting of a sequence of symbols from $\{1, 2, \dots, m\}$. For any finite word $\mathfrak{w} = w_0 w_1 \cdots w_{n-1} \in \{1, 2, \dots, m\}^n$ we will denote the finite composition

$$\mathfrak{s}_{\mathfrak{w}} = \mathfrak{s}_{w_0} \circ \mathfrak{s}_{w_1} \circ \dots \circ \mathfrak{s}_{w_{n-1}}$$

so that $A^{\mathfrak{w}} := \mathfrak{s}_{\mathfrak{w}}(A)$ and $A = \bigcup \{A^{\mathfrak{w}} \mid \mathfrak{w} \in \{1, 2, \dots, m\}^n\}$. When n tends to infinity, this induces a continuous map, called the *address map*, $\pi : \{1, 2, \dots, m\}^\infty \rightarrow A$ from the set $\{1, 2, \dots, m\}^\infty$ of all infinite words $\mathfrak{w} = w_0 w_1 \cdots$ onto the attractor, defined by

$$\pi(\mathfrak{w}) := \lim_{n \rightarrow \infty} \mathfrak{s}_{w_0} \circ \dots \circ \mathfrak{s}_{w_{n-1}}(x)$$

where the choice of $x \in X$ does not matter. The infinite word \mathfrak{w} will then be called an *itinerary* of the point $\pi(\mathfrak{w}) \in A$.

It is important to note that itineraries are often not unique. As seen from the discussion in Section 2.2.1 the address map $\pi_1 : \{0, 1\}^\infty \rightarrow \mathfrak{C}$ is, in fact, a bijection since \mathfrak{C} is totally disconnected. However, for an attractor A each nonempty intersection $\mathfrak{s}_{\mathfrak{w}_1}(A) \cap \mathfrak{s}_{\mathfrak{w}_2}(A)$, where the words \mathfrak{w}_1 and \mathfrak{w}_2 start differently, gives rise to dual itineraries for a common point. In the Sierpiński Triangle \mathfrak{T} , where the address map $\pi_2 : \{0, 1, 2\}^\infty \rightarrow \mathfrak{T}$ is not injective: for example, consider the words

$$\mathfrak{a} = 011111 \cdots = 0(1)^\infty \quad \mathfrak{b} = 100000 \cdots = 1(0)^\infty.$$

The repeating words $(0)^\infty$ and $(1)^\infty$ correspond to the fixed points $2\xi_3^0, 2\xi_3^1$ of \mathfrak{s}_0 and \mathfrak{s}_1 which are vertices of the starting triangle T_0 . Consequently, their images $\mathfrak{s}_0(2\xi_3^1)$ and $\mathfrak{s}_1(2\xi_3^0)$, with itineraries \mathfrak{a} and \mathfrak{b} respectively, are both sent to the midpoint between them:

$$\begin{aligned} \mathfrak{s}_0(2\xi_3^1) &= \frac{1}{2}(2\xi_3^1) + \xi_3^0 = \xi_3^1 + \xi_3^0 \\ \mathfrak{s}_1(2\xi_3^0) &= \frac{1}{2}(2\xi_3^0) + \xi_3^1 = \xi_3^0 + \xi_3^1 \end{aligned}$$

In general, whenever the limit set of an IFS is connected the address map π cannot possibly be a bijection.

2.4 Geometry of the Attractor

The geometry of the limit set associated to an IFS is quite irregular. However, the same “irregularities” appear at different scales as the attractor is magnified. In what follows, we introduce some useful tools that will help in obtaining a better handle on the geometric structure of the attractor.

We have already discussed the (non) connectivity of the Cantor Set. This can be extended, using Proposition 2.1.1, to the following standard exercise:

Lemma 2.4.1 *Consider the IFS of contraction similarities $\{\mathfrak{s}_i\}_{i=1}^m$. Then \mathbf{A} is totally disconnected if and only if $\mathfrak{s}_j(\mathbf{A}) \cap \mathfrak{s}_k(\mathbf{A}) = \emptyset$ for all $j \neq k$.*

The above lemma hints that the geometric structure of the attractor \mathbf{A} is determined by the overlap set $\bigcap_{j=1}^m \mathfrak{s}_j(\mathbf{A})$. There is a historically important property of an IFS which ensures that there is not “too much” overlap.

Definition 2.4.1 (Moran [16]) *An IFS of contraction similarities $\{\mathfrak{s}_i\}_{i=1}^m$ is said to have the open set condition (OSC) if there exists a nonempty open set $V \subset \mathbb{C}$ with*

$$\bigcup_{j=1}^m \mathfrak{s}_j(V) \subseteq V \text{ and } \bigcap_{j=1}^m \mathfrak{s}_j(V) = \emptyset.$$

A set V satisfying the OSC condition for the IFS $\{\mathfrak{s}_i\}_{i=1}^m$ is called a feasible open set.

There are various possibilities for a feasible set depending on the attractor. For instance, if the pieces $\mathfrak{s}_j(\mathbf{A})$ are all disjoint, then there is a minimum distance $\epsilon > 0$ between all of them, so a δ -neighborhood of \mathbf{A} with $\delta < \epsilon/2$ is a feasible open set. In other situations, it might be even easier to find: consider the Cantor Set \mathfrak{C} , then any disc (or interval, if we restrict to maps on \mathbb{R}) centered at the origin with radius $r \in [3/2, 3]$ is a feasible open set.

However, difficulties in finding a suitable V arise when the attractor is connected. For starters, it is easy to see that the feasible open set must avoid certain points of \mathbf{A} : for any point ξ in the nonempty overlap $\mathfrak{s}_j(\mathbf{A}) \cap \mathfrak{s}_k(\mathbf{A})$, $\mathfrak{s}_j^{-1}(\xi)$ and $\mathfrak{s}_k^{-1}(\xi)$ cannot

possibly be in V since otherwise $\xi \in \mathfrak{s}_j(V) \cap \mathfrak{s}_k(V)$. As an example, consider the Sierpiński Triangle, then the interior of the starting triangle is a feasible open set. In this way, V does not contain not only the preimages of the points in the overlap set, but also the preimages of all points accessible from $\mathbb{C} \setminus \mathfrak{T}$. Alternatively, one can choose V to be the interior of the hexagon with vertices at the scaled sixth roots of unity $2\xi_6^k = 2 \exp(2k\pi i/6)$ for $k \in \{0, 1, 2, 3, 4, 5\}$ (see Fig. 2.3).

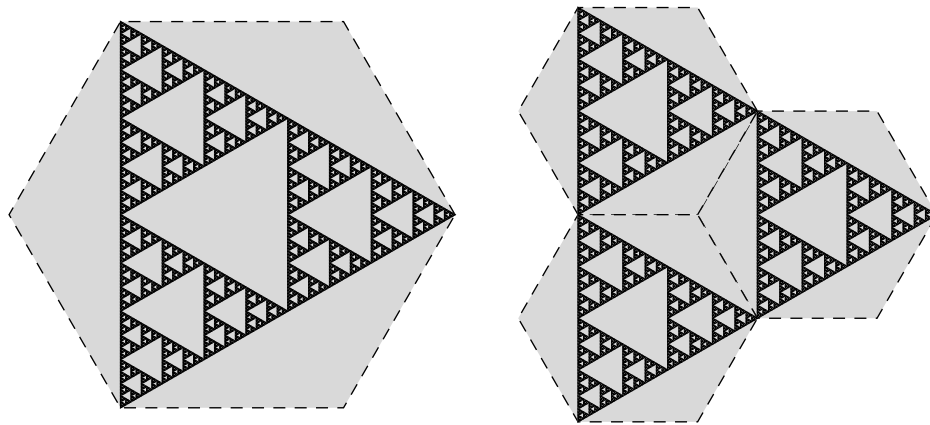


Fig. 2.3. A feasible open set V , in gray, and its images for the Sierpiński Triangle.

In [17] there are examples of IFS satisfying the OSC where the feasible open set has a complicated structure which is revealed only under magnification. Two of them are shown in Fig. 2.4: the attractor on the left is generated by the maps

$$\mathfrak{s}_0(z) = -\frac{i}{2}z, \quad \mathfrak{s}_1(z) = -\frac{1}{2}z - \frac{1}{2}, \quad \mathfrak{s}_2(z) = -\frac{1}{2}z + \frac{1+i}{2};$$

while the limit set on the right is obtained from the maps

$$\mathfrak{s}_0(z) = \frac{i}{2}z - \frac{5i}{2}, \quad \mathfrak{s}_1(z) = -\frac{1}{2}z, \quad \mathfrak{s}_2(z) = \frac{i}{2}z - \frac{1+4i}{2}.$$

The open set condition is important in the measure-theoretic study of IFS as it is a useful tool in establishing the dimension of the limit set. The dimension of a set is

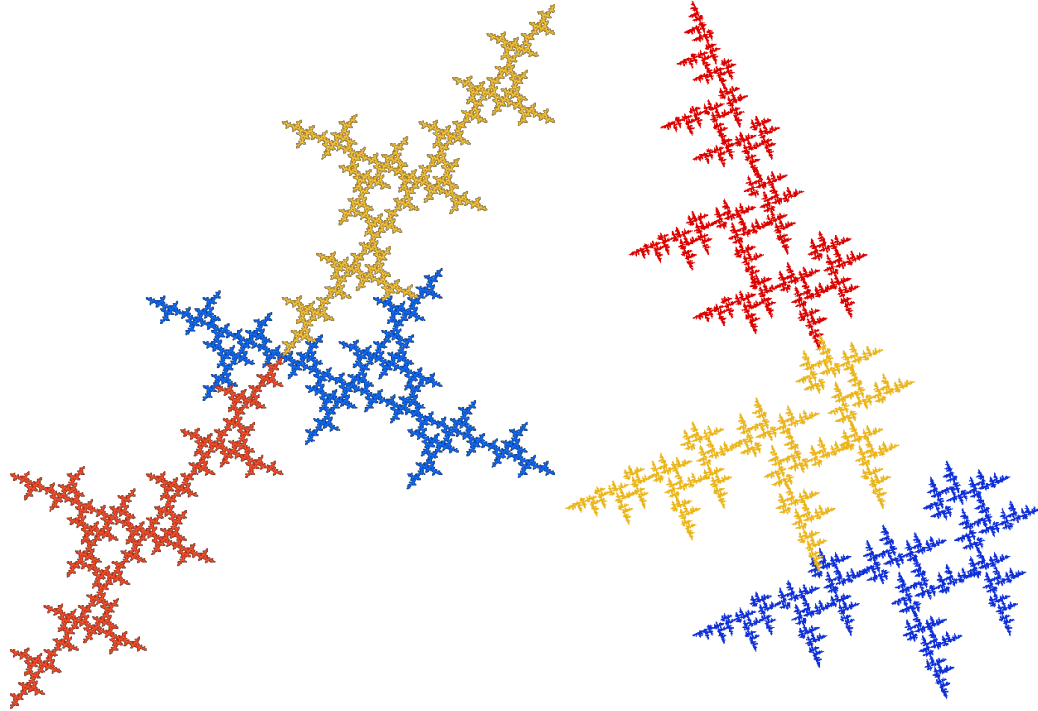


Fig. 2.4. Two non trivial examples of IFS satisfying OSC.

a quantity that determines its size in the sense of how much it fills up the space in which it lives.

There exists a variety of notions of dimension for the attractor of an IFS, but we will only describe two of the most common ones: the *Hausdorff dimension* and the *similarity dimension*. We first need the concept of Hausdorff measure

Definition 2.4.2 Suppose F is a subset of \mathbb{R}^d and let $s > 0$. For any $\delta > 0$ define

$$\mathcal{H}_\delta^s(F) = \inf \left\{ \sum_{i=1}^{\infty} \text{diam}(U_i)^s \mid \{U_i\} \text{ is a cover of } F \text{ and } \text{diam}(U_i) < \delta \right\},$$

where $\text{diam}(U) = \sup \{|x - y| \mid x, y \in U\}$. The s -dimensional Hausdorff measure of F is

$$\mathcal{H}^s(F) = \lim_{\delta \rightarrow 0} \mathcal{H}_\delta^s(F).$$

Hausdorff measures generalize the familiar ideas of length, area, and volume. It may be shown that, the n -dimensional Hausdorff measure for subsets of \mathbb{R}^n is, up to a constant multiple, just the n -dimensional volume.

The limit in the definition above exists for any subset F of \mathbb{R}^n , though the limiting value can be 0 or ∞ . For a simple example, take F to be a disc in \mathbb{R}^3 , then an exercise shows $\mathcal{H}^1(F) = \text{length}(F) = \infty$, $\mathcal{H}^2(F) = \frac{4}{\pi} \text{area}(F) = 4$, and $\mathcal{H}^3(F) = \frac{6}{\pi} \text{vol}(F) = 0$. In particular, $\mathcal{H}^s(F) = \infty$ for every $s < 2$ and $\mathcal{H}^s(F) = 0$ for every $s > 2$.

The jump discontinuity of $\mathcal{H}^s(F)$ as a function of s is the Hausdorff dimension of F . More precisely,

Definition 2.4.3 For any F subset of \mathbb{R}^d , its Hausdorff dimension is

$$\dim_{\text{H}}(F) = \inf \{s \geq 0 \mid \mathcal{H}^s(F) = 0\} = \sup \{s \mid \mathcal{H}^s(F) = \infty\}.$$

It follows the disc $F \subset \mathbb{R}^3$, discussed above, has Hausdorff dimension equal to 2.

The other related notion of dimension is the similarity dimension

Definition 2.4.4 Given an IFS of contraction similarities $\{\mathfrak{s}_j\}_{j=1}^m$ with contraction ratios $0 < r_j < 1$, the similarity dimension of the attractor is the unique number α such that

$$\sum_{j=1}^m r_j^\alpha = 1.$$

This notion of dimension is only useful in the context of IFS. Nonetheless, it is a powerful tool in calculating the Hausdorff dimension of the attractor:

Theorem 2.4.1 Consider the IFS $\{\mathfrak{s}_j\}_{j=1}^m$ with contraction ratios $0 < r_j < 1$. Let \mathbf{A} be the attractor of the IFS and let α be its similarity dimension. Then $\dim_{\text{H}}(\mathbf{A}) \leq \alpha$, with equality if the IFS satisfies the OSC.

For a proof see Falconer [15].

As mentioned before, the OSC turns out to be a favorable property of IFS. In fact, three more equivalent definitions of OSC have been found.

Theorem 2.4.2 Consider the IFS of contraction similarities $\{\mathfrak{s}_j\}_{j=1}^m$ and let A be the associated attractor. The following are equivalent

- (a) The IFS satisfies the OSC.
- (b) (Moran [16] and Schief [18]) $\mathcal{H}^\alpha(A) > 0$ where α is the similarity dimension of A .
- (c) The finite clustering property (Schief [18]): there exists an integer N such that for every $A^{\mathfrak{w}}$ of diameter ε , for a finite length word \mathfrak{w} , there are at most N incomparable pieces $A^{\mathfrak{v}}$ of diameter $\geq \varepsilon$ that can intersect the ε -neighborhood of $A^{\mathfrak{w}}$. We say that $A^{\mathfrak{w}}$ and $A^{\mathfrak{v}}$ are incomparable if \mathfrak{w} is not a prefix \mathfrak{v} and viceversa.
- (d) The neighbor map condition (Bandt-Graf [19]): the identity map is not an accumulation point of the set of neighbor maps of A . A neighbor map has the form $h = \mathfrak{s}_{\mathfrak{w}}^{-1}\mathfrak{s}_{\mathfrak{v}}$ where $\mathfrak{w}, \mathfrak{v} \in \{1, 2, \dots, m\}^n$ with $w_0 \neq v_0$.

How does the attractor of an IFS which fails the OSC look like? The above theorem implies that OSC fails when the similarity dimension is larger than the ambient space on which the IFS operates. Roughly speaking, it is equivalent to saying that the overlap set of the attractor is “too large”.

Consider the contraction similarities on \mathbb{R}

$$\mathfrak{s}_0(x) = \frac{\sqrt{5}-1}{2}x - 1 \quad \mathfrak{s}_1(x) = \frac{\sqrt{5}-1}{2}x + 1$$

its associated attractor A is the closed interval $\left[-\frac{3+\sqrt{5}}{2}, \frac{3+\sqrt{5}}{2}\right]$ since

$$\begin{aligned} \mathfrak{s}_0(A) \cup \mathfrak{s}_1(A) &= \left[-\frac{3+\sqrt{5}}{2}, \frac{\sqrt{5}-1}{2}\right] \cup \left[-\frac{\sqrt{5}-1}{2}, \frac{3+\sqrt{5}}{2}\right] \\ &= \left[-\frac{3+\sqrt{5}}{2}, \frac{3+\sqrt{5}}{2}\right] = A. \end{aligned}$$

Its similarity dimension, α is the solution to the equation $2\left(\frac{\sqrt{5}-1}{2}\right)^\alpha = 1$, i.e.

$$\alpha = -\frac{\ln(2)}{\ln\left(\frac{\sqrt{5}-1}{2}\right)} \approx 1.44042$$

but the dimension of \mathbb{R} is $1 < \alpha$.

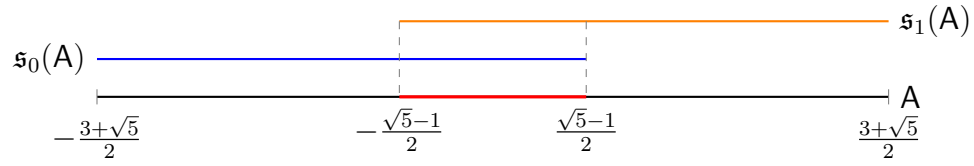


Fig. 2.5. The IFS $\{\mathfrak{s}_0, \mathfrak{s}_1\}$ on \mathbb{R} with contraction ratio the reciprocal of the golden ratio fails the overlap set condition. The red interval represents the overlap of $\mathfrak{s}_0(A)$ with $\mathfrak{s}_1(A)$, which are drawn above A in blue and orange respectively.

We will refer back to the OSC property in Section 3.4, when analyzing our particular family of IFS.

3. PARAMETRIC FAMILIES OF IFS

The rest of this thesis will be focused on two families of IFS parametrized in the punctured disc. Let $\lambda \in \mathbb{D}^* := \mathbb{D} \setminus \{0\}$, and consider the contraction similarities

$$\mathfrak{s}_-(z) := \lambda z - 1, \quad \mathfrak{s}_0(z) := \lambda z, \quad \mathfrak{s}_+(z) := \lambda z + 1.$$

Let A_λ and \tilde{A}_λ be the attractors of the IFS $\{\mathfrak{s}_-, \mathfrak{s}_+\}$ and $\{\mathfrak{s}_-, \mathfrak{s}_0, \mathfrak{s}_+\}$, respectively. The use of the symbols $\{-, 0, +\}$, rather than the indices $\{0, 1, 2\}$, is justified since each symbol suggests the direction of the translation applied by the corresponding map.

Remember that we obtain the attractor of an IFS by iterating the union of the defining maps starting with *any* nonempty compact set. Since \mathfrak{s}_- , \mathfrak{s}_0 , and \mathfrak{s}_+ are affine maps we obtain the following descriptions of the limit sets

$$A_\lambda = \left\{ \sum_{n=0}^{\infty} a_n \lambda^n \mid a_n \in \{-1, +1\} \right\}, \quad \tilde{A}_\lambda = \left\{ \sum_{n=0}^{\infty} a_n \lambda^n \mid a_n \in \{-1, 0, +1\} \right\}.$$

Both attractors are symmetric about 0, and clearly $A_\lambda \subseteq \tilde{A}_\lambda$. It is advantageous to study them together because, contrary to what happens with the Mandelbrot set, the parameter regions

$$\mathcal{M} := \{\lambda \in \mathbb{D} \mid A_\lambda \text{ is connected}\} \quad \text{and} \quad \mathcal{M}_0 := \{\lambda \in \mathbb{D} \mid 0 \in A_\lambda\}.$$

are not equal, see Fig. 3.1. Rather, \mathcal{M} coincides with the set $\{\lambda \in \mathbb{D} \mid \lambda^{-1} \in \tilde{A}_\lambda\}$ or, equivalently, $\{\lambda \in \mathbb{D} \mid 0 \in \mathfrak{s}_-(\tilde{A}_\lambda) \cap \mathfrak{s}_0(\tilde{A}_\lambda) \cap \mathfrak{s}_+(\tilde{A}_\lambda)\}$.

Interest in these IFS families spiked recently, after Tiozzo [4] (inspired by a conjecture of Thurston [3]) proved that \mathcal{M}_0 equals the closure of the set of Galois conjugates of entropies of superattracting real quadratic polynomials. Both \mathcal{M} and \mathcal{M}_0 were first introduced by Barnsley and Harrington [20] in the mid 1980s. In 1988–92,

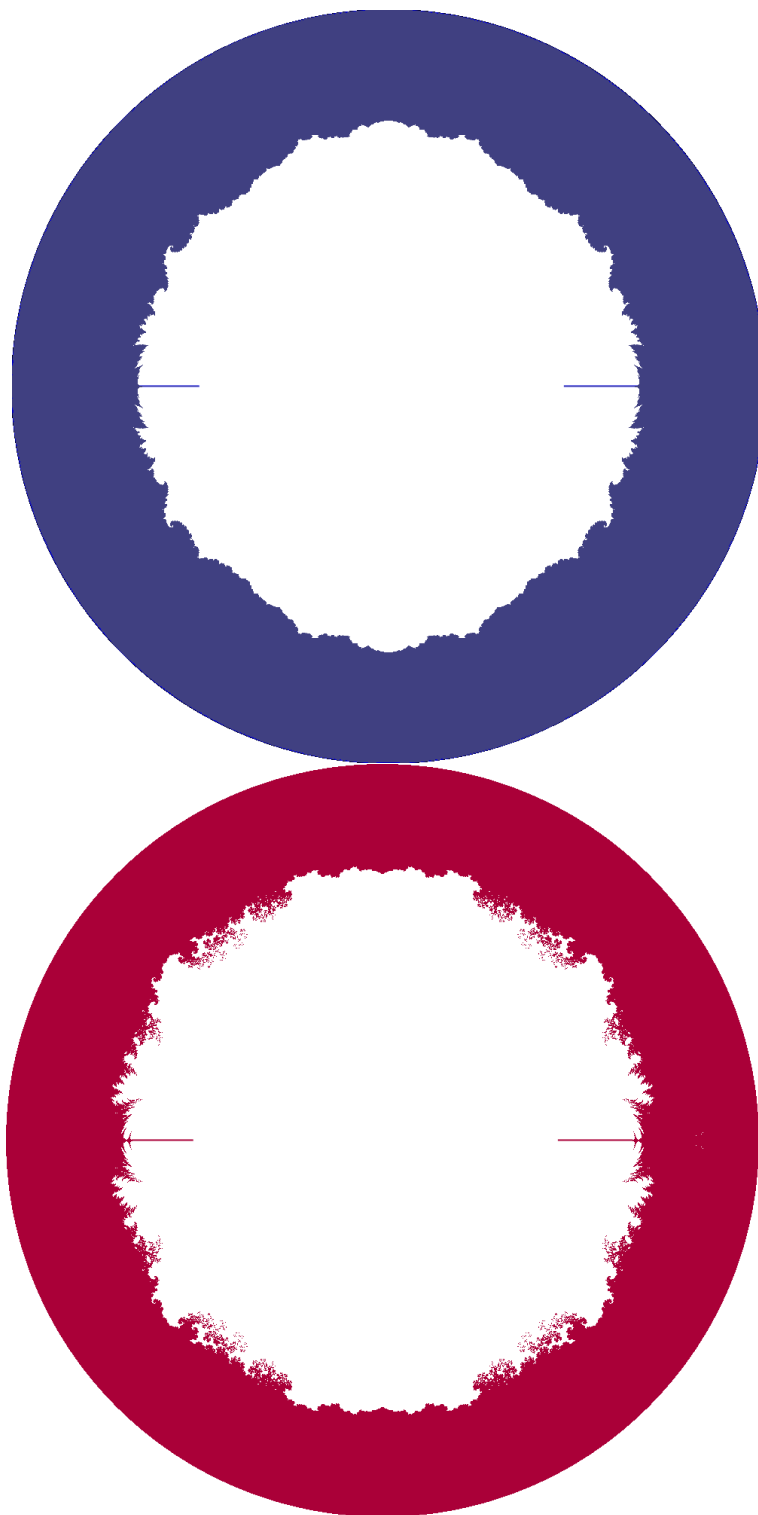


Fig. 3.1. The connectivity locus \mathcal{M} , in blue, and its subset \mathcal{M}_0 , in fuchsia. The outer circle for both of them has radius 1.

Bousch [21, 22] proved \mathcal{M} and \mathcal{M}_0 are connected and locally connected. In 2002, Bandt [9] proved the existence of a hole in \mathcal{M} , and conjectured that there are in fact infinitely many holes. In 2014 Calegari, Koch, and Walker [10] gave a positive answer to the conjecture, for both \mathcal{M} and \mathcal{M}_0 , and in fact constructed infinite sequences of holes accumulating at certain parameters in $\partial\mathcal{M}$. These are buried points of $\partial\mathcal{M}$, i.e. not accessible from $\mathbb{D} \setminus \mathcal{M}$.

This thesis focuses on those parameters $\lambda \in \partial\mathcal{M}$ or $\partial\mathcal{M}_0$ that are not buried, however, their discussion is delayed to chapter 4. In this chapter we formalize notation and show basic facts and properties of \mathcal{M} and \mathcal{M}_0 . We will also prove some technical lemmas and propositions which will be used later to prove the main results.

3.1 Notation

As in Chapter 2, let Σ^n be the set of all words $\mathbf{w} = a_0 \cdots a_{n-1}$ of length n in $\{-, +\}$. Define $\mathfrak{s}_{\mathbf{w}} = \mathfrak{s}_{a_0} \circ \cdots \circ \mathfrak{s}_{a_{n-1}}$ so that $A_{\lambda}^{\mathbf{w}} = \mathfrak{s}_{\mathbf{w}}(A_{\lambda})$ and

$$A_{\lambda} = \bigcup_{\mathbf{w} \in \Sigma^n} A_{\lambda}^{\mathbf{w}}.$$

The natural projection from the space Σ^{∞} of infinite words, $\mathbf{w} = a_0 a_1 \cdots$ in $\{-, +\}$, onto the attractor, A_{λ} is given by

$$\pi_{\lambda} : \Sigma^{\infty} \rightarrow A_{\lambda} \quad \pi_{\lambda}(\mathbf{w}) = \sum_{n=0}^{\infty} a_n \lambda^n.$$

As before, the word $\mathbf{w} \in \Sigma^{\infty}$ is called the *itinerary* of $\pi_{\lambda}(\mathbf{w})$ in A_{λ} . Remember that if A_{λ} is connected, then there could be multiple itineraries for a given point in A_{λ} . Nevertheless, elements $\omega \in A_{\lambda}$ that are in $A_{\lambda}^{a_0 a_1 \cdots a_k}$ can be written as

$$\omega = a_0 + a_1 \lambda + \cdots + a_k \lambda^k + \sum_{n=k+1}^{\infty} a_n \lambda^n, \quad a_n \in \{-1, +1\}.$$

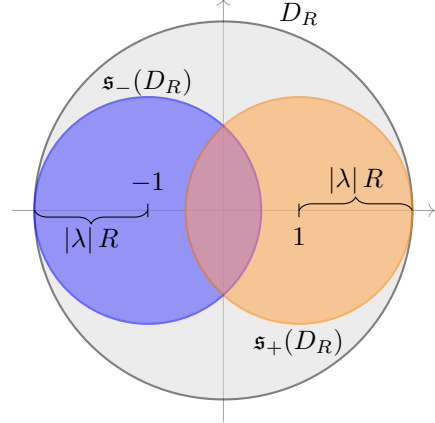
We will use $\mathbf{w}|k$ to denote the finite word $a_0 a_1 \cdots a_k$ coming from the truncation of the infinite word $\mathbf{w} = a_0 a_1 \cdots$. The notation $|\mathbf{w}|$ will indicate the length of the finite word \mathbf{w} .

Let $D_r(z)$ denote the closed disc centered at z with radius r and, when $z = 0$, we will abbreviate $D_r = D_r(0)$.

Lemma 3.1.1 *Let $R \geq (1 - |\lambda|)^{-1}$, then $A_\lambda \subset D_R$ and $\tilde{A}_\lambda \subset D_R$.*

Proof By Proposition 2.1.1, we only have to show that $\mathfrak{s}_-(D_R) \cup \mathfrak{s}_+(D_R) \subset D_R$. But $\mathfrak{s}_-(D_R)$ and $\mathfrak{s}_+(D_R)$ are discs of radius $|\lambda|R$ centered at -1 and 1 , respectively. For them to be inside D_R , we need

$$|(-1) - 1| + 2|\lambda|R \leq 2R \iff \frac{1}{1 - |\lambda|} \leq R.$$



Since the disc $\mathfrak{s}_0(D_r)$ is centered at the origin with radius $|\lambda|R < R$, \tilde{A}_λ is also contained in D_R . \square

From here on, we let $R := (1 - |\lambda|)^{-1}$. Let $I^{-1} = \tilde{I}^{-1}$ be the disc D_R , and consider the recursive constructions $I^n = \mathfrak{s}_-(I^{n-1}) \cup \mathfrak{s}_+(I^{n-1})$, and $\tilde{I}^n = \mathfrak{s}_-(\tilde{I}^{n-1}) \cup \mathfrak{s}_0(\tilde{I}^{n-1}) \cup \mathfrak{s}_+(\tilde{I}^{n-1})$ for $n \in \mathbb{N}$. From Lemma 3.1.1, it is clear that

$$A_\lambda = \bigcap_{n=0}^{\infty} I^n \quad \text{and} \quad \tilde{A}_\lambda = \bigcap_{n=0}^{\infty} \tilde{I}^n.$$

As before, for any finite word $\mathbf{w} = a_0 a_1 \cdots a_k$ in Σ^{k+1} we can identify the discs in I^{k+1} as $D^{\mathbf{w}} := \mathfrak{s}_{\mathbf{w}}(I^{-1})$. Each of these discs will then be centered at $\mathfrak{s}_{\mathbf{w}}(0) = a_0 + a_1 \lambda + \cdots + a_k \lambda^k$, and have a radius of $|\lambda|^{k+1} R$. If $\mathbf{w} \in \Sigma^\infty$ is an infinite word, then $\mathfrak{s}_{\mathbf{w}}(0) \in A_\lambda^{\mathbf{w}/k} \subset D^{\mathbf{w}/k}$ for all $k \geq 0$. Analogously, if $\mathbf{w} \in \tilde{\Sigma}^\infty$, then $\mathfrak{s}_{\mathbf{w}}(0) \in \tilde{A}_\lambda^{\mathbf{w}/k} \subset \tilde{D}^{\mathbf{w}/k}$ for all $k \geq 0$.

From now on, we will refer to I^k and \tilde{I}^k as the *instar*¹ at level k of the IFS $\{\mathfrak{s}_-, \mathfrak{s}_+\}$ and $\{\mathfrak{s}_-, \mathfrak{s}_0, \mathfrak{s}_+\}$, respectively. Given that I^k is the union of the copies of the instar at

¹ The word “instar” is used in biology to describe the developmental stage of arthropods, such as insects, between each molt until sexual maturity. We chose it because the limit set is obtained by going through (infinitely many) developmental stages.

level $k - 1$, $\mathfrak{s}_+(I^{k-1})$ and $\mathfrak{s}_-(I^{k-1})$ will be respectively called the *positive* and *negative instars* at level k . Similarly, we refer to $\mathfrak{s}_+(\tilde{I}^{k-1})$, $\mathfrak{s}_0(\tilde{I}^{k-1})$, and $\mathfrak{s}_-(\tilde{I}^{k-1})$ as the *positive*, *central*, and *negative instar* of level k .

It will also be useful to have a name for each of the discs and their centers in the instar. The center $\mathfrak{s}_{\mathfrak{w}|k}(0) = \sum_{j=0}^k a_j \lambda^j$ will be called a *node* with itinerary $\mathfrak{w}|k$ and generally denoted by $\nu_{\mathfrak{w}|k}$, while the closed disc $D^{\mathfrak{w}|k}$ (or $\tilde{D}^{\mathfrak{w}|k}$) surrounding it will be referred to as a *nodal disc* with itinerary $\mathfrak{w}|k$.

3.2 The Disconnectivity Algorithm

The authors in [10] introduced a fast algorithm to determine whether λ is not in \mathcal{M} . We replicate it here, adjusted to our notation, as we will make use of it later in Chapter 4.

Recall that the attractor A_λ equals the intersection $\bigcap_{n \geq 0} I^n$ of all instars. Thus A_λ is a Cantor set (i.e. $\lambda \notin \mathcal{M}$) if and only if I^n is disconnected from some level $n \geq 0$ onward. Since I^n is defined as the union $\mathfrak{s}_-(I^{n-1}) \cup \mathfrak{s}_+(I^{n-1})$ of the negative and positive instars, then it is disconnected if and only if these do not intersect. A problem arises because verifying that none of the 2^{n-1} nodal discs of $\mathfrak{s}_-(I^{n-1})$ intersect any of the 2^{n-1} nodal discs of $\mathfrak{s}_+(I^{n-1})$ becomes a prohibitive computation as n increases.

However, if $D^{\mathfrak{w}} \cap D^{\mathfrak{v}} = \emptyset$, then it is superfluous to verify whether $D^{\mathfrak{w}x} \cap D^{\mathfrak{v}y}$ is empty for any combination $x, y \in \{-, +\}$. Therefore, we only need to check for possible intersections that have not been ruled out at a previous level, and even better, we may restrict only to words $\mathfrak{w}, \mathfrak{v} \in \Sigma^n$ with $w_0 \neq v_0$.

If $|\mathfrak{w}| = n$, the disc $D^{\mathfrak{w}}$, of level $n - 1$, is given by $\mathfrak{s}_{\mathfrak{w}}(I^{-1}) = \mathfrak{s}_{\mathfrak{w}}(0) + \lambda^n I^{-1} = \nu_{\mathfrak{w}} + \lambda^n I^{-1}$, i.e. it is centered at the node $\nu_{\mathfrak{w}}$ and has radius $|\lambda^n| R$. Thus, if two discs of level $n - 1$ intersect, the distance between the centers is $|\nu_{\mathfrak{w}} - \nu_{\mathfrak{v}}| < 2|\lambda^n| R$.

The algorithm begins by verifying that the nodal discs at level 0 intersect, i.e. it checks whether

$$\left| \frac{\nu_+ - \nu_-}{\lambda} \right| = \left| \frac{2}{\lambda} \right| < 2R.$$

If so (i.e. when $|\lambda| > 1/2$), the element $2\lambda^{-1}$ is stored in the stack V and the algorithm enters its recursive phase: at each level $n \geq 0$, the stack V will contain the entry $(\nu_{\mathbf{w}} - \nu_{\mathbf{v}})\lambda^{-(n+1)}$, if and only if the discs $D^{\mathbf{w}}$ and $D^{\mathbf{v}}$ of level n intersect.

To be more precise, let \mathbf{w}, \mathbf{v} be words of length n , starting with opposite symbols, such that $\alpha := (\nu_{\mathbf{w}} - \nu_{\mathbf{v}})\lambda^{-n-1}$ is in the stack V . For the next level, the algorithm only needs to search for possible intersections between elements of $\{D^{\mathbf{w}^-}, D^{\mathbf{w}^+}\}$ and elements of $\{D^{\mathbf{v}^-}, D^{\mathbf{v}^+}\}$; that is, it computes the values

$$\begin{aligned} \frac{\nu_{\mathbf{w}^+} - \nu_{\mathbf{v}^+}}{\lambda^{n+2}} &= \frac{\nu_{\mathbf{w}} - \nu_{\mathbf{v}} + \lambda^{n+1} - \lambda^{n+1}}{\lambda^{n+2}} = \frac{\alpha}{\lambda} \\ \frac{\nu_{\mathbf{w}^+} - \nu_{\mathbf{v}^-}}{\lambda^{n+2}} &= \frac{\nu_{\mathbf{w}} - \nu_{\mathbf{v}} + \lambda^{n+1} + \lambda^{n+1}}{\lambda^{n+2}} = \frac{\alpha + 2}{\lambda} \\ \frac{\nu_{\mathbf{w}^-} - \nu_{\mathbf{v}^+}}{\lambda^{n+2}} &= \frac{\nu_{\mathbf{w}} - \nu_{\mathbf{v}} - \lambda^{n+1} - \lambda^{n+1}}{\lambda^{n+2}} = \frac{\alpha - 2}{\lambda} \\ \frac{\nu_{\mathbf{w}^-} - \nu_{\mathbf{v}^-}}{\lambda^{n+2}} &= \frac{\nu_{\mathbf{w}} - \nu_{\mathbf{v}} - \lambda^{n+1} + \lambda^{n+1}}{\lambda^{n+2}} = \frac{\alpha}{\lambda} \end{aligned}$$

and compares them to $2R$. The next level stack is then comprised of these values less than $2R$.

If the algorithm returns *true* then the attractor is certifiably totally disconnected. On the other hand, if it returns *false*, A_λ might still be disconnected but the algorithm will not discover it unless the maxlevel is increased.

3.3 Geometry of the Connectedness Locus

In this section we give a quick, hand-waving account of the features of \mathcal{M} and \mathcal{M}_0 . In Fig. 3.1 we can see how the two sets look like. Since $A_{-\lambda} = A_\lambda$ and $A_{\bar{\lambda}} = A_\lambda$, for any $\lambda \in \mathbb{D}$, both \mathcal{M} and \mathcal{M}_0 are symmetric about the origin. Interestingly, the sets \mathcal{M} and \mathcal{M}_0 can be defined using other pairs of similarities. Indeed, for any $c \neq d \in \mathbb{C}$ consider the contraction similarities

$$\mathfrak{s}_c(z) = \lambda z + c \quad \text{and} \quad \mathfrak{s}_d(z) = \lambda z + d,$$

then the map

$$\phi(z) = \frac{1}{d-c} \left(z - \frac{c}{1-\lambda} \right)$$

Algorithm 1: Disconnected($\lambda, \text{maxlevel}$)

 $V \leftarrow \{2\lambda^{-1}\}$
 $n \leftarrow 0$
while $V \neq \emptyset$ *or* $n \leq \text{maxlevel}$ **do**
 $W \leftarrow \emptyset$
forall $\alpha \in V$ **do**
if $|\lambda^{-1}\alpha| < 2R$ **then** $W \leftarrow W \cup \lambda^{-1}\alpha$
if $|\lambda^{-1}(\alpha + 2)| < 2R$ **then** $W \leftarrow W \cup \lambda^{-1}(\alpha + 2)$
if $|\lambda^{-1}(\alpha - 2)| < 2R$ **then** $W \leftarrow W \cup \lambda^{-1}(\alpha - 2)$
 $V \leftarrow W$
 $n \leftarrow n + 1$
if $V = \emptyset$ **then return** *true*
else return *false*

conjugates \mathfrak{s}_c to \mathfrak{s}_0 and \mathfrak{s}_d to \mathfrak{s}_+ . It follows that if $\mathbf{B} = \mathfrak{s}_c(\mathbf{B}) \cup \mathfrak{s}_d(\mathbf{B})$ is the attractor of the IFS $\{\mathfrak{s}_c, \mathfrak{s}_d\}$, then $\phi(\mathbf{B}) = \mathbf{A}_\lambda$. Therefore, it is up to one's preference which contraction similarities to use to determine \mathcal{M} and \mathcal{M}_0 . For example, many authors (e.g [9, 10, 23]) use the pair $\{\mathfrak{s}_0, \mathfrak{s}_+\}$ to describe \mathcal{M} .

Notice that $\lambda = 1/3$ generates the Cantor Set we described in Section 2.2.1. As $\lambda \in \mathbb{R}$ increases towards $1/2$, the gap between the generating intervals decreases until, at $\lambda = 1/2$ the attractor fuses into the interval $[-2, 2]$. A striking feature of \mathcal{M} and \mathcal{M}_0 are the clearly visible isolated whiskers on the real axis starting at $\lambda = \pm 1/2$. Barnsley and Harrington [20] were the first to rigorously prove that \mathcal{M} is entirely real in some definite neighborhood of the endpoints of these whiskers. In fact, they gave a rough estimate of the size of the interval which was later improved by Calegari, Koch, and Walker in [10].

Theorem 3.3.1 ([10, 20]) *There is some $\alpha > 1/2$ so that the intersection of \mathcal{M} with some open subset of \mathbb{C} is equal to the interval $[1/2, \alpha)$.*

The approximate value of α is 0.6684755322100605954110550451436814.

The picture of \mathcal{M} suggests that there is an entire annulus in its interior. Indeed, using an argument with the similarity dimension (see Definition 2.4.4) and an application of Lemma 3.1.1 it is possible to prove

Theorem 3.3.2 (Bousch [21]) *The annulus $\frac{1}{\sqrt{2}} \leq |\lambda| \leq 1$ is entirely contained in \mathcal{M} . The open disc of radius $1/2$ is completely contained in $\mathbb{D} \setminus \mathcal{M}$.*

If $\lambda^2 \in \mathcal{M}$, then $\lambda \in \mathcal{M}_0$. Consequently, \mathcal{M}_0 contains the annulus $2^{-1/4} \leq |\lambda| < 1$.

The proof of the second statement needs an interpretation of both sets as the zero locus of power series with certain prescribed coefficients. We will see this interpretation in the next section.

Note that the bounds in the theorem are actually sharp. If we move along the imaginary axis, the attractor for any $y \in (0, 2^{-1/2})$ is a cartesian product of Cantor sets, $\mathbf{A}_{y^i} = \mathbf{A}_{y^2} \times y\mathbf{A}_{y^2}$. When $y = 2^{-1/2}$ we actually get the rectangle with vertices

at $\pm 2 \pm \sqrt{2}i$. From the above theorem it follows that the boundary of \mathcal{M} has to be contained in the closed disc of radius $2^{-1/2}$.

Bousch obtained another significant result about the sets \mathcal{M} and \mathcal{M}_0 :

Theorem 3.3.3 (Bousch [22]) *The sets \mathcal{M} and \mathcal{M}_0 are both connected and locally connected.*

Again the proof is based on the other definitions of the sets.

The last important property of \mathcal{M} , conjectured by Bandt [9] and proved by Calegari et al. [10], is

Theorem 3.3.4 *The set \mathcal{M} is regular-closed; that is*

$$\mathcal{M} = \overline{\text{int}(\mathcal{M})} \cup (\mathcal{M} \cap \mathbb{R}).$$

3.4 The Overlap Set

Recall from Lemma 2.4.1 that O_λ plays a key role in the geometric structure of A_λ . If it is empty then A_λ is simply a Cantor set and consequently $\lambda \in \mathbb{D} \setminus \mathcal{M}$. However, if O_λ is “large” then it becomes difficult to distinguish the smaller affine copies that constitute A_λ . Moreover, if the large size of the overlap is resilient to a small change of λ , then the parameter is in the interior of \mathcal{M} . Intuitively, $\lambda \in \partial\mathcal{M}$ whenever O_λ is in some sense “thin”.

Whenever O_λ is nonempty there exist itineraries $\mathbf{a}, \mathbf{b} \in \Sigma^\infty$ with $a_0 = -$ and $b_0 = +$ such that

$$\pi_\lambda(\mathbf{w}) := \sum_{j=0}^{\infty} a_j \lambda^j = \sum_{j=0}^{\infty} b_j \lambda^j = \pi_\lambda(\mathbf{v}) \iff \sum_{j=0}^{\infty} (a_j - b_j) \lambda^j = 0$$

Observe that $a_j - b_j \in \{-2, 0, +2\}$ for every $j \geq 0$. Consequently, denote the set of all power series with coefficients from the set $\{-1, 0, +1\}$ as

$$\mathcal{P} = \left\{ f(z) = \sum_{j=0}^{\infty} c_j z^j \mid c_j \in \{-1, 0, +1\}, c_0 = 1 \right\}$$

and define the set of power series which have λ as a root by

$$\mathcal{F}_\lambda = \{f \in \mathcal{P} \mid f(\lambda) = 0\}.$$

Then for $\lambda \in \mathbb{D}$ the overlap set, O_λ is nonempty whenever there exists $f \in \mathcal{P}$ such that it has coefficients $c_j = (a_j - b_j)/2$ and $f(\lambda) = 0$. Conversely, if for a particular $\lambda \in \mathbb{D}$ the set \mathcal{F}_λ is nonempty, then so is O_λ , and each element in it has an itinerary associated to some $f \in \mathcal{F}_\lambda$. We have just shown that

$$\mathcal{M} = \{\lambda \in \mathbb{D} \mid \mathbf{A}_\lambda \text{ is connected}\} = \{\lambda \in \mathbb{D} \mid |\mathcal{F}_\lambda| \neq 0\}.$$

Moreover, since \mathbf{A}_λ is symmetric with respect to 0, having the origin in the overlap implies that the coefficients c_j of at least one of the power series $f \in \mathcal{F}_\lambda$ must all be nonzero (see Lemma 3.4.1). It follows that

$$\mathcal{M}_0 = \{\lambda \in \mathbb{D} \mid 0 \in \mathbf{A}_\lambda\} = \left\{ \lambda \in \mathbb{D} \mid \exists f \in \mathcal{P}, f(\lambda) = \sum_{j=0}^{\infty} c_j \lambda^j = 0, c_j \in \{-1, 1\} \right\}$$

from which it is clear that $\mathcal{M}_0 \subset \mathcal{M}$.

The following result is important, as it gives more insight on the relationship between elements in O_λ and the power series which have λ as a root. We have adjusted the proof to our setting (and notation).

Lemma 3.4.1 (Solomyak [23]) $|O_\lambda| = 1$ or 2 if and only if $|\mathcal{F}_\lambda| = 1$. Moreover,

- (i.) $|O_\lambda| = 1$ if and only if $f \in \mathcal{F}_\lambda$ has no zero coefficients.
- (ii.) $|O_\lambda| = 2$ if and only if $f \in \mathcal{F}_\lambda$ has exactly one zero coefficients.

Proof (\Rightarrow) Suppose $|O_\lambda| = 1$ then, since \mathbf{A}_λ is symmetric with respect to 0, we must have $O_\lambda = \{0\}$. Let $f(z) = \sum_{j=0}^{\infty} c_j z^j$ be in \mathcal{F}_λ then we will show that $c_j \neq 0$ for all $j \geq 0$. Assume otherwise, then there exist $j \geq 1$ such that $c_j = 0$. Without loss of generality, assume that only $c_1 = 0$. Then

$$\begin{aligned}
c_0 + 0 \cdot \lambda + \sum_{j=2}^{\infty} c_j \lambda^j &= 0 \\
2c_0 + 0 \cdot \lambda + \sum_{j=2}^{\infty} 2c_j \lambda^j &= 0 \\
a_0 + a_1 \lambda + \sum_{j=2}^{\infty} a_j \lambda^j &= b_0 + b_1 \lambda + \sum_{j=2}^{\infty} b_j \lambda^j
\end{aligned}$$

where $a_1 = b_1$ and $a_j = -b_j \in \{-1, +1\}$ for all $j \neq 1$. Therefore, since $\sum_{j=0}^{\infty} a_j \lambda^j \in \mathbf{A}_\lambda^+$ and $\sum_{j=0}^{\infty} b_j \lambda^j \in \mathbf{A}_\lambda^-$ (or viceversa), then $\pm \lambda \in O_\lambda$, a contradiction.

To show uniqueness of f in \mathcal{F}_λ , suppose there is $g \in \mathcal{F}_\lambda$. By the argument above, all the coefficients of g are also ± 1 . Now since both $f(\lambda) = 0$ and $g(\lambda) = 0$, then $h(\lambda) = 0$ where $h = \frac{1}{2}(f + g)$. It follows that $h \in \mathcal{F}_\lambda$ and it has all its coefficients equal to 1 or -1 , but this is only possible if $f \equiv g$.

Assume $O_\lambda = \{y_1, y_2\}$. Then, since \mathbf{A}_λ is symmetric with respect to 0, we must have $y_1 = -y_2$. Let $f(z) = \sum_{j=0}^{\infty} c_j z^j$ be in \mathcal{F}_λ , then we will show that exactly one coefficient is 0. We already know from the argument above that we must have at least one zero coefficient to have two symmetric points in O_λ . Without loss of generality, suppose that only $c_1 = c_2 = 0$. Then,

$$\begin{aligned}
c_0 + 0 \cdot \lambda + 0 \cdot \lambda^2 + \sum_{j=3}^{\infty} c_j \lambda^j &= 0 \\
2c_0 + 0 \cdot \lambda + 0 \cdot \lambda^2 + \sum_{j=2}^{\infty} 2c_j \lambda^j &= 0 \\
a_0 + a_1 \lambda + a_2 \lambda^2 + \sum_{j=3}^{\infty} a_j \lambda^j &= b_0 + b_1 \lambda + b_2 \lambda^2 + \sum_{j=3}^{\infty} b_j \lambda^j
\end{aligned}$$

where $a_1 = b_1$, $a_2 = b_2$, and $a_j = -b_j \in \{-1, +1\}$ for all $j \neq 1, 2$. Therefore, since $\sum_{j=0}^{\infty} a_j \lambda^j \in \mathbf{A}_\lambda^+$ and $\sum_{j=0}^{\infty} b_j \lambda^j \in \mathbf{A}_\lambda^-$ (or viceversa), then $(\pm \lambda \pm \lambda^2) \in O_\lambda$, giving a contradiction.

The uniqueness of f in \mathcal{F}_λ is proved in the same way as before: suppose there is $g \in \mathcal{F}_\lambda$. By the argument above, exactly one of the coefficients of g is 0. Now

since both $f(\lambda) = 0$ and $g(\lambda) = 0$, then $h(\lambda) = 0$ where $h = \frac{1}{2}(f + g)$. It follows that $h \in \mathcal{F}_\lambda$ and it has exactly one of its coefficients equal to 0, but this is only possible if $f \equiv g$.

(\Leftarrow) Let $f \in \mathcal{F}_\lambda$. We have seen above that the number of zero coefficients of f determines the elements in the overlap. Since f is assumed to be unique, then $|O_\lambda| = 1$ or 2 .

□

Using Rouché's Theorem and careful estimates Solomyak was also able to prove that

Theorem 3.4.1 (Solomyak [23]) *There exist uncountably many $\lambda \in \mathcal{M}$ for which $|O_\lambda| = 1$. The itinerary of $0 \in A_\lambda$ is different for different λ .*

Recall that in Section 2.4 we introduced the Open Set Condition (OSC) for an IFS as a possible tool to investigate the associated attractor. How does the size of O_λ relate to the OSC? Unfortunately, it is not completely clear. However, Bandt and his collaborators have recently shown that

Theorem 3.4.2 (Bandt-Rao [24]) *If $0 < |O_\lambda| < \infty$ then the OSC is satisfied.*

and subsequently expanded Solomyak's result to

Theorem 3.4.3 (Bandt-Hung [25]) *For every $m \in \mathbb{N}$ there are uncountably many $\lambda \in \mathcal{M}$ for which OSC holds, and the overlap set consists of 2^m points. For each λ there exists a unique $f \in \mathcal{P}$ such that $\mathcal{F}_\lambda = \{f\}$.*

It must be noted that the proof of the above lemma cannot be easily extended to the case of $|O_\lambda| = 2^m$ for $m \geq 2$. Indeed, Bandt and Hung used a different argument to show the uniqueness of the power series.

As previously mentioned, $\lambda = i/\sqrt{2}$ is on the boundary of \mathcal{M} . However, there are uncountable many power series that vanish at that parameter, since the overlap set

is a segment on the imaginary axis, $[-\sqrt{2}i, \sqrt{2}i]$. It can be easily shown that, for any $k \geq 0$, the power series $(1 \pm z^{2k+1})(1 + 2z^2)(1 + z^2)^{-1}$ is in $\mathcal{F}_{i/\sqrt{2}}$. Nonetheless, the IFS $\left\{ \frac{i}{\sqrt{2}}z - 1, \frac{i}{\sqrt{2}}z + 1 \right\}$ satisfies the OSC, since a feasible open set is the interior of $A_{i/\sqrt{2}}$.

Furthermore, consider the parameters $\lambda = \frac{1}{2}(1 + i)$ and $\lambda' = \frac{1}{4}(1 + \sqrt{7}i)$, both with norm $1/\sqrt{2}$, whose corresponding attractors are shown in Fig. 3.2. These are, respectively, the well studied “twin-dragon” and “tame twin-dragon”, and they are part of a larger family of “rep-tiles” (“rep” stands for “replication”, and “tiles” since these sets can tile the whole plane). In both cases, the overlap set is uncountable (in fact a rectifiable curve) and consequently so are \mathcal{F}_λ and $\mathcal{F}_{\lambda'}$. Both IFS satisfy the OSC, however, it seems that both parameters are on $\partial\mathcal{M}_0$ but not $\partial\mathcal{M}$.

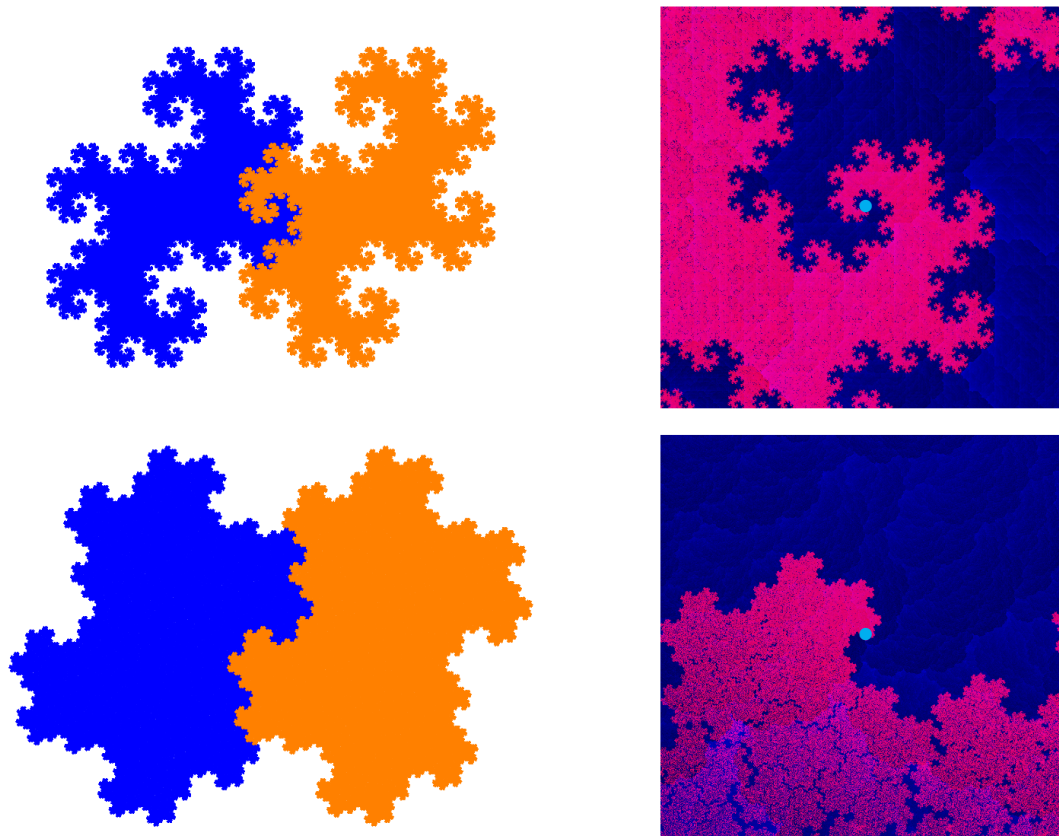


Fig. 3.2. Top row: the Twin-Dragon and the associated parameter $\lambda = 2^{-1}(1 + i)$ in \mathcal{M} and \mathcal{M}_0 . Bottom row: the Tame Twin-Dragon and the corresponding parameter $\lambda' = 4^{-1}(1 + \sqrt{7}i)$ in \mathcal{M} and \mathcal{M}_0 .

4. THE BOUNDARY OF THE CONNECTEDNESS LOCUS

In the previous chapter we saw the importance of knowing the elements of the set \mathcal{F}_λ and the overlap set O_λ to understand which parameters λ lie in the boundary of \mathcal{M} . It was pointed out by Barnsley [14] and Bandt [9] that the local structure of \mathcal{M} seems to reflect the one of the attractor. Solomyak [23] was the first to show this connection rigorously and it was later improved by Calegari et al. [10]. This property is the key to prove our results about accessible points on $\partial\mathcal{M}$.

In this chapter we will first overview some of the known results (section 4.1) and explain how our results fit in. In Section 4.2, we prove the main theorems. We also provide parameters satisfying the assumptions of the main theorems in Section 4.3. Finally, in Section 4.4 we propose a method on how to prove that a certain parameter is on $\partial\mathcal{M}$. Unfortunately, there is a technical issue that we were not able to prove, but we strongly believe it to be true. Finally, in Section 4.5 we point out why parameters on the shared boundary $\partial\mathcal{M} \cap \partial\mathcal{M}_0$ are interesting to study from a Complex Dynamics perspective.

4.1 Self and Asymptotic Similarity

Before describing the old and new results about $\partial\mathcal{M}$, we recall some definitions which can be found in [26]. Remember that $D_r(z)$ denotes a closed disc centered at z with radius r and $D_r = D_r(0)$. For compact sets $E, F \subset \mathbb{C}$ denote

$$[E]_r = (E \cap D_r) \cup \partial D_r; \quad d_r(E, F) = d_{\mathbb{H}}([E]_r, [F]_r)$$

where $d_{\mathbb{H}}$ is the Hausdorff distance defined at the beginning of Section 2.1.

Definition 4.1.1 (i.) *A compact set F is ρ -self-similar about $z \in F$, for $\rho \in \mathbb{C} \setminus \overline{\mathbb{D}}$, if there is $r > 0$ such that $[\rho(F - z)]_r = [F - z]_r$.*

- (ii.) Two compact sets E and F are asymptotically similar about $z \in E$ and $w \in F$ if there is $r > 0$ such that

$$\lim_{t \in \mathbb{C}, |t| \rightarrow \infty} d_r(t(E - z), t(F - w)) = 0.$$

- (iii.) A compact set E is asymptotically ρ -self similar about a point $z \in E$ if there is $r > 0$ and a compact set F such that

$$d_r(\rho^n(E - z), F) \rightarrow 0 \quad n \rightarrow \infty.$$

We can now state the result of Solomyak:

Theorem 4.1.1 (Solomyak [23]) Suppose $\lambda \in \mathcal{M} \setminus \mathbb{R}$, with $|\lambda| \leq 2^{-1/2}$, is such that $\mathcal{F}_\lambda = \{f\}$ with

$$f(z) = \sum_{n=0}^{\ell} c_n z^n + \frac{c_{\ell+1} z^{\ell+1} + \dots + c_{\ell+p} z^{\ell+p}}{1 - z^p}.$$

Then $f'(\lambda) \neq 0$ and

- (i.) $\tilde{\mathbf{A}}_\lambda$ is λ^{-p} -self similar about $-\lambda^{-(\ell+1)} \sum_{n=0}^{\ell} c_n \lambda^n =: \zeta$.
- (ii.) \mathcal{M} about λ is asymptotically similar to $\frac{\lambda^{\ell+1}}{f'(\lambda)} \tilde{\mathbf{A}}_\lambda$ about $\frac{\lambda^{\ell+1}}{f'(\lambda)} \zeta$.
- (iii.) \mathcal{M} is asymptotically λ^{-p} -self similar about λ .

An important remark is that if the coefficients of f are all non zero, then the theorem holds true if we substitute $\tilde{\mathbf{A}}_\lambda$ with \mathbf{A}_λ and \mathcal{M} with \mathcal{M}_0 . However, the above theorem is not enough to certify that parameters λ satisfying the hypothesis of the theorem lie on $\partial\mathcal{M}$, because points in a neighborhood of ζ , not in $\tilde{\mathbf{A}}_\lambda$, are not necessarily also outside of \mathcal{M} in a neighborhood of λ .

Theorem 4.1.2 (Calegari-Koch-Walker [10]) Suppose $\lambda \in \mathcal{M} \setminus \mathbb{R}$, with $|\lambda| \leq 2^{-1/2}$, is a root of

$$f(z) = \sum_{n=0}^{\ell} c_n z^n + \frac{c_{\ell+1} z^{\ell+1} + \dots + c_{\ell+p} z^{\ell+p}}{1 - z^p}, \quad c_j \in \{-1, 0, +1\}.$$

- (i.) If $C \in \frac{\lambda^{\ell+1}}{f'(\lambda)} \left(\tilde{\mathbf{A}}_\lambda - \zeta \right)$, then for every $\varepsilon > 0$, there is a C' such that $|C - C'| < \varepsilon$ and for all sufficiently large n , a neighborhood of $C'\lambda^{pn} + \lambda$ is contained in \mathcal{M} .
- (ii.) If $\mathcal{F}_\lambda = \{f\}$, then there is $\delta > 0$ such that for every $C \notin \frac{\lambda^{\ell+1}}{f'(\lambda)} \left(\tilde{\mathbf{A}}_\lambda - \zeta \right)$ with $|C| < \delta$, the parameter $C\lambda^{pn} + \lambda$ is not in \mathcal{M} for all sufficiently large n .

The first part of this theorem says that if λ is a root of a rational function then there is an increasing union of open subsets of \mathcal{M} limiting to the asymptotically scaled copy of \mathcal{M} centered at λ . It is therefore a stronger result than Theorem 4.1.1. The second part of Theorem 4.1.2 implies that if $|\mathcal{F}_\lambda| = 1$, it is possible to find a sequence of parameters in $\mathbb{D} \setminus \mathcal{M}$ converging to λ and, therefore, establishing $\lambda \in \partial\mathcal{M}$.

However, the theorem does not exclude the possibility that λ is the limit of a sequence of connected components of $\mathbb{D} \setminus \mathcal{M}$ with diameter going to zero, i.e. λ is a buried point of $\partial\mathcal{M}$. The question of whether there is a way to recognize accessible and buried points of $\partial\mathcal{M}$ remained open. The following theorem, which is our main result, gives a partial answer.

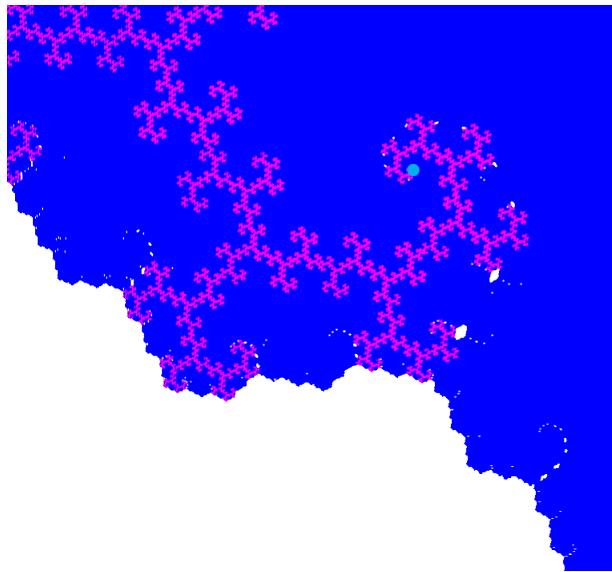


Fig. 4.1. \mathcal{M} is blue while \mathcal{M}_0 is fuchsia. Calegari and his collaborators showed that $\lambda \approx 0.371859 + 0.519411i$, marked in cyan, is a buried point of $\partial\mathcal{M}$.

Theorem 4.1.3 Suppose $\lambda \in \mathcal{M} \setminus \mathbb{R}$ with $|\lambda| \leq 2^{-1/2}$, is such that $\mathcal{F}_\lambda = \{f\}$ with

$$f(z) = \sum_{n=0}^{\ell} c_n z^n + \frac{c_{\ell+1} z^{\ell+1} + \dots + c_{\ell+p} z^{\ell+p}}{1 - z^p}.$$

Assume also that $f(z)$ has finitely many zero coefficient and that its Taylor polynomials, $f_k(z) = \sum_{j=0}^k c_j z^j$ satisfy the following conditions for every $0 \leq n \leq p-1$:

(i.) $|f_{\ell+1+n}(\lambda)| > \frac{1}{2} \frac{|\lambda^{\ell+1+n+1}|}{1 - |\lambda|};$

(ii.) $|f_{\ell+1+n}(\lambda)| + |f_{\ell+1+n+1}(\lambda)| > \frac{|\lambda^{\ell+1+n+1}|}{1 - |\lambda|};$

(iii.) $2|f_{\ell+1+n}(\lambda)| < |2f_\ell(\lambda) + \lambda^{\ell+1}P(\lambda)|$, where P is any polynomial of degree less or equal to n with coefficients from the set $\{-2, -1, 0, +1, +2\}$. Except, of course, for the polynomial P such that $2f_\ell(z) + z^{\ell+1}P(z) = 2f_{\ell+1+n}(z)$.

Then λ is accessible from a connected component of $\mathbb{D} \setminus \mathcal{M}$.

An immediate corollary is then

Corollary 4.1.4 Suppose $\lambda \in \mathcal{M} \setminus \mathbb{R}$ with $|\lambda| \leq 2^{-1/2}$, is such that $\mathcal{F}_\lambda = \{f\}$ where f satisfies the hypothesis of Theorem 4.1.3 and has no zero coefficients. Then $\lambda \in \partial\mathcal{M} \cap \partial\mathcal{M}_0$ and it is accessible from a connected component of $\mathbb{D} \setminus \mathcal{M}$.

Restricting the assumptions on the coefficients on the power series, f we also obtain

Theorem 4.1.5 Suppose $\lambda \in \mathcal{M} \setminus \mathbb{R}$ with $|\lambda| \leq 2^{-1/2}$, is such that $\mathcal{F}_\lambda = \{f\}$ with

$$f(z) = \sum_{n=0}^{\ell} c_n z^n + \frac{c_{\ell+1} z^{\ell+1} + \dots + c_{\ell+p} z^{\ell+p}}{1 - z^p}.$$

Assume also that $f(z)$ has no zero coefficient and that its Taylor polynomials, $f_k(z) = \sum_{j=0}^k c_j z^j$ satisfy the following conditions for every $0 \leq n \leq p-1$:

(i.) $|f_{\ell+1+n}(\lambda)| > \frac{1}{2} \frac{|\lambda^{\ell+1+n+1}|}{1 - |\lambda|};$

(ii.) $|f_{\ell+1+n}(\lambda)| + |f_{\ell+1+n+1}(\lambda)| > \frac{|\lambda^{\ell+1+n+1}|}{1 - |\lambda|};$

(iii.) $|f_{\ell+1+n}(\lambda)| < |f_\ell(\lambda) + \lambda^{\ell+1}P(\lambda)|$, where P is any polynomial of degree less or equal to n with coefficients from the set $\{-1, 0, +1\}$. Except, of course, for the polynomial P such that $f_\ell(z) + z^{\ell+1}P(z) = f_{\ell+1+n}(z)$.

Then λ is accessible from a connected component of $\mathbb{D} \setminus \mathcal{M}_0$.

In lieu of Corollary 4.1.4 and experimental evidence, we believe that if the assumptions on Theorem 4.1.5 are satisfied, then also condition (iii.) of Theorem 4.1.3 must hold. Moreover, we conjecture that the parameters on $\partial\mathcal{M} \cap \partial\mathcal{M}_0$ are actually on the boundary of the main connected component of $\mathbb{D} \setminus \mathcal{M}_0$. However, we decided to leave the study of these conjectures for future work.

4.2 Proof of the Main Theorems

We will prove theorems 4.1.3 and 4.1.5 in this section. The idea of the proof, for both theorems, is to construct, locally, a connected chain of open discs outside $\tilde{\mathbf{A}}_\lambda$ (or \mathbf{A}_λ) that converges to $\zeta = -\lambda^{-(\ell+1)} \sum_{n=0}^{\ell} c_j \lambda^j$ and conclude by Theorem 4.1.2(ii.) that λ is accessible, hence on the boundary of a hole. The restrictions on the Taylor polynomials show up when deducing the conditions for such a chain to exist.

We first need a lemma

Lemma 4.2.1 *Let $\lambda \in \mathcal{M}$ be such that $\mathcal{F}_\lambda = \{f\}$ with*

$$f(z) = \sum_{n=0}^{\ell} c_j z^j + \frac{c_{\ell+1} z^{\ell+1} + \dots + c_{\ell+p} z^{\ell+p}}{1 - z^p},$$

where $c_j = 0$ only for some $0 < j \leq \ell$. Let $\xi \in O_\lambda$ have itineraries $\mathbf{a} = a_0 a_1 a_2 \dots$ and $\bar{\mathbf{a}} = \bar{a}_0 \bar{a}_1 \bar{a}_2 \dots$ where $a_j = -\bar{a}_j = c_j$ if $c_j \neq 0$, and otherwise $a_j = \bar{a}_j = -$ or $+$.

Then for every $0 \leq n \leq p-1$ the set $\mathbf{D}^{\mathbf{a}|\ell+n+p} \cup \mathbf{D}^{\bar{\mathbf{a}}|\ell+n+p}$ about ξ is λ^{-p} -self similar to $\mathbf{D}^{\mathbf{a}|\ell+n} \cup \mathbf{D}^{\bar{\mathbf{a}}|\ell+n}$ about ξ .

Proof Since the set in question is the union of two intersecting closed discs, to prove the lemma is equivalent to showing that

$$\frac{1}{\lambda^p} \left((\mathbf{D}^{\mathbf{a}|\ell+n+p} \cup \mathbf{D}^{\bar{\mathbf{a}}|\ell+n+p}) - \xi \right) = (\mathbf{D}^{\mathbf{a}|\ell+n} \cup \mathbf{D}^{\bar{\mathbf{a}}|\ell+n}) - \xi.$$

We will only show it for the case $n = 0$ to simplify the expressions, but the proof is easily generalized to $0 < n < p$.

Observe that since λ is a root of $f(z)$ then

$$c_{\ell+1}\lambda^{\ell+1} + \dots + c_{\ell+p}\lambda^{\ell+p} = (\lambda^p - 1)(c_0 + c_1\lambda + \dots + c_\ell\lambda^\ell).$$

Consequently,

$$\begin{aligned} \left| (a_0 + a_1\lambda + \dots + a_{\ell+p}\lambda^{\ell+p}) - (\bar{a}_0 + \bar{a}_1\lambda + \dots + \bar{a}_{\ell+p}\lambda^{\ell+p}) \right| &= 2 \left| c_0 + c_1\lambda + \dots + c_{\ell+p}\lambda^{\ell+p} \right| \\ &= 2 |\lambda^p| \left| c_0 + c_1\lambda + \dots + c_\ell\lambda^\ell \right| \end{aligned}$$

and

$$\left| (a_0 + a_1\lambda + \dots + a_\ell\lambda^\ell) - (\bar{a}_0 + \bar{a}_1\lambda + \dots + \bar{a}_\ell\lambda^\ell) \right| = 2 \left| c_0 + c_1\lambda + \dots + c_\ell\lambda^\ell \right|$$

which proves that the distance of the nodes at level $\ell + p$ and at level ℓ are multiple of each other.

Finally, the center of the disc $D^{a_0 a_1 \dots a_{\ell+p}}$ is

$$\begin{aligned} a_0 + a_1\lambda + \dots + a_{\ell+p}\lambda^{\ell+p} &= c_0 + c_1\lambda + \dots + c_{\ell+p}\lambda^{\ell+p} + \sum_{0 < j \leq \ell : c_j=0} a_j\lambda^j \\ &= \lambda^p(c_0 + c_1\lambda + \dots + c_\ell\lambda^\ell) + \sum_{0 < j \leq \ell : c_j=0} a_j\lambda^j \\ \implies \sum_{j=0}^{\ell+p} a_j\lambda^j - \sum_{0 < j \leq \ell : c_j=0} a_j\lambda^j &= \lambda^p \sum_{j=0}^{\ell} c_j\lambda^j = \lambda^p \left(\sum_{j=0}^{\ell} a_j\lambda^j - \sum_{0 < j \leq \ell : c_j=0} a_j\lambda^j \right). \end{aligned}$$

Notice that by definition $\xi = \sum_{0 < j \leq \ell : c_j=0} a_j\lambda^j$, so the above equation becomes

$$a_0 + a_1\lambda + \dots + a_{\ell+p}\lambda^{\ell+p} - \xi = \lambda^p(a_0 + a_1\lambda + \dots + a_\ell\lambda^\ell - \xi).$$

Analogous arguments are done for the other disc. \square

Remember from Lemma 3.1.1 we have that $A_\lambda \subset D_R$ and that $A_\lambda^{\mathbf{w}} \subset D^{\mathbf{w}}$ for any finite word $\mathbf{w} \in \Sigma^n$. Consequently, the above lemma proves the self-similarity of the attractor A_λ at its overlap:

Corollary 4.2.1 *Let $\lambda \in \mathcal{M}$ be such that $\mathcal{F}_\lambda = \{f\}$ with*

$$f(z) = \sum_{n=0}^{\ell} c_n z^n + \frac{c_{\ell+1} z^{\ell+1} + \dots + c_{\ell+p} z^{\ell+p}}{1 - z^p},$$

where $c_j = 0$ only for some $0 < j \leq \ell$. Let $\xi \in O_\lambda$ have itineraries $\mathbf{a} = a_0 a_1 a_2 \dots$ and $\bar{\mathbf{a}} = \bar{a}_0 \bar{a}_1 \bar{a}_2 \dots$ where $a_j = -\bar{a}_j = c_j$ if $c_j \neq 0$, and otherwise $a_j = \bar{a}_j = -$ or $+$.

Then for every $0 \leq n \leq p-1$ the set $A_\lambda^{\mathbf{a}|\ell+p+n} \cup A_\lambda^{\bar{\mathbf{a}}|\ell+p+n}$ about ξ is λ^{-p} -self similar to $A_\lambda^{\mathbf{a}|\ell+n} \cup A_\lambda^{\bar{\mathbf{a}}|\ell+n}$ about ξ .

Remark 4.2.1 *The above result can be directly extended to the attractor \tilde{A}_λ of the IFS $\{\mathfrak{s}_-, \mathfrak{s}_0, \mathfrak{s}_+\}$ with the coefficients a_n also allowed to be 0. For any finite word $\mathbf{w} \in \tilde{\Sigma}^n$, since $\mathfrak{s}_\mathbf{w}(\tilde{A}_\lambda^0)$ will always be in between $\mathfrak{s}_\mathbf{w}(\tilde{A}_\lambda^+)$ and $\mathfrak{s}_\mathbf{w}(\tilde{A}_\lambda^-)$ then we have the following inclusion of the overlap sets: $A_\lambda^+ \cap A_\lambda^- \subseteq \tilde{A}_\lambda^+ \cap \tilde{A}_\lambda^-$.*

We now proceed to the construction of the chain in the complement of \tilde{A}_λ . We will exploit the recursive construction of \tilde{A}_λ to find each disc in the chain: for each $n \geq 0$ we find an open disc tangent to the instar \tilde{I}^n . Moreover, two consecutive discs in the chain must intersect non trivially. Finally, this chain must converge to $\zeta \in \tilde{A}_\lambda$.

Recall that λ is the root of a unique power series $f \in \mathcal{P}$ whose non-zero coefficients eventually repeat: say

$$f(z) = \sum_{j=0}^{\ell} c_j z^j + \frac{c_{\ell+1} z^{\ell+1} + \dots + c_{\ell+p} z^{\ell+p}}{1 - z^p}.$$

Now, ζ is defined to be $-\lambda^{-(\ell+1)} \sum_{j=0}^{\ell} c_j \lambda^j$ which means it can be described with the periodic itinerary $(c_{\ell+1} \dots c_{\ell+p})^\infty \in \Sigma^\infty$. This itinerary will be the unique one associated to ζ as long as $|\mathcal{F}_\lambda| = 1$. Since we assume so in the statement of the theorems, there is a unique sequence of nodes converging to ζ , namely the ones whose itinerary is the truncation of $(c_{\ell+1} \dots c_{\ell+p})^\infty$ at some index.

Set $\mathbf{b} = b_0 b_1 \dots \in \tilde{\Sigma}^\infty$ where $b_j = c_{\ell+1+j}$ and let $\zeta_n := \nu_{\mathbf{b}|n}$ be the node in \tilde{I}^n . Observe that ζ_n is by definition the center of the disc $\tilde{D}^{\mathbf{b}|n}$ and ζ is a point inside such disc. Therefore, if ζ_n is far enough from ζ , then $\omega_n = -\zeta_n + 2\zeta$, i.e. the reflection of

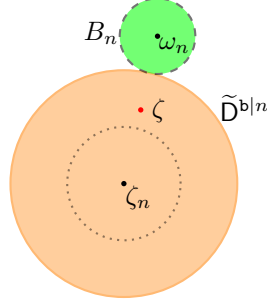


Fig. 4.2. Construction of B_n , an element in the connected chain of open sets in $\mathbb{C} \setminus \tilde{A}_\lambda$. The dotted circle has half the radius of $\tilde{D}^{b|n}$.

ζ_n about ζ , will be outside $\tilde{D}^{b|n}$. We can then find an open disc, B_n centered at ω_n tangent to $\tilde{D}^{b|n}$ (see Figure 4.2).

Recall that each nodal disc in \tilde{I}^n has a radius of $|\lambda^{n+1}|(1 - |\lambda|)^{-1}$. Thus, the radius, r_n of B_n is easily found to be

$$r_n := |\omega_n - \zeta_n| - \frac{|\lambda^{n+1}|}{1 - |\lambda|} = 2|\zeta - \zeta_n| - \frac{|\lambda^{n+1}|}{1 - |\lambda|}.$$

Proof [of Theorem 4.1.3]: We shall show that the chain of open discs $\bigcup_{n \geq 0} B_n$ is a connected subset of $\mathbb{C} \setminus \tilde{A}_\lambda$. In fact, it is enough to prove $\tilde{I}^{p-1} \cap \bigcup_{n=0}^{p-1} B_n = \emptyset$, since by Theorem 4.1.1 the attractor \tilde{A}_λ is λ^{-p} -self similar about ζ . Moreover, we will prove that $C\lambda^{pm} \in \frac{\lambda^{\ell+1}}{f'(\lambda)} (\bigcup_{n \geq 0} B_n - \zeta)$ for every $C \in \frac{\lambda^{\ell+1}}{f'(\lambda)} (\bigcup_{n \geq 0} B_n - \zeta)$ and m large enough. The claim of the theorem will then follow from Theorem 4.1.2(ii).

We consider only the case $|O_\lambda| = 2$ to simplify the notation and the explanation of the proof. The condition of $|O_\lambda|$ being finite implies that the zero coefficients of the power series are the non repeating ones. The choice of which $\xi \in O_\lambda$ to consider is arbitrary but ζ is always unique because $|\mathcal{F}_\lambda| = 1$.

By assumption, the coefficients of f are strictly preperiodic and exactly one of them must be zero. Hence, there exists $0 < k \leq \ell$ such that $c_k = 0$ which implies $O_\lambda = \{\pm\lambda^k\} = \{\pm\xi\}$. We deduce that the itinerary of ζ is a word in Σ^∞ and, thus, $\zeta \in A_\lambda \subset \tilde{A}_\lambda$.

Let $\mathbf{a}, \bar{\mathbf{a}} \in \Sigma^\infty$ be such that $\pi_\lambda(\mathbf{a}) = \pi_\lambda(\bar{\mathbf{a}}) = \xi$. Therefore, $a_j = -\bar{a}_j = c_j$ for all $j \neq k$ and $a_k = \bar{a}_k = +1$ or -1 (since $c_k = 0$). In particular, $\xi = f(\lambda) + a_k \lambda^k$. Denote by ξ_n the nodes with itinerary $\mathbf{a}|n$, i.e. $\xi_n = \nu_{\mathbf{a}|n} = \sum_{j=0}^n a_j \lambda^j$. The Taylor polynomial $f_{\ell+1+n}(\lambda)$ for $n \geq 0$ can then be written as $\xi_{\ell+1+n} - \xi$.

Observe that the itinerary of ζ is the (left) shift of \mathbf{a} by ℓ terms. Indeed, we claim that

$$\zeta = \mathfrak{s}_{\mathbf{a}|\ell}^{-1}(\xi) \quad \text{and} \quad \zeta_n = \mathfrak{s}_{\mathbf{a}|\ell}^{-1}(\xi_{\ell+1+n}).$$

Since $\mathfrak{s}_{a_0 a_1}(z) = \mathfrak{s}_{a_0}(\mathfrak{s}_{a_1}(z)) = \lambda^2 z + \nu_{a_0 a_1}$ then $\mathfrak{s}_{a_0 a_1}^{-1}(z) = \mathfrak{s}_{a_1}^{-1}(\mathfrak{s}_{a_0}^{-1}(z)) = \frac{1}{\lambda^2}(z - \nu_{a_0 a_1})$. Consequently,

$$\begin{aligned} \mathfrak{s}_{\mathbf{a}|\ell}^{-1}(\xi) &= \frac{1}{\lambda^{\ell+1}}(\xi - \xi_\ell) = -\frac{1}{\lambda^{\ell+1}}f_\ell(\lambda) = \zeta \\ \mathfrak{s}_{\mathbf{a}|\ell}^{-1}(\xi_{\ell+1+n}) &= \frac{1}{\lambda^{\ell+1}}(\xi_{\ell+1+n} - \xi_\ell) = \frac{1}{\lambda^{\ell+1}}(f_{\ell+1+n}(\lambda) - f_\ell(\lambda)) = \zeta_n. \end{aligned}$$

The centers of the discs B_n were defined in terms of ζ_n and ζ , but we can now rewrite them in terms of the Taylor polynomials

$$\omega_n = -\zeta_n + 2\zeta = -\frac{1}{\lambda^{\ell+1}}(f_{\ell+1+n}(\lambda) + f_\ell(\lambda)).$$

Using the above equations, we also rewrite the radius of B_n in terms of a Taylor polynomial:

$$r_n = |\omega_n - \zeta_n| - \frac{|\lambda^{n+1}|}{1 - |\lambda|} = \frac{2}{|\lambda^{\ell+1}|} |f_{\ell+1+n}(\lambda)| - \frac{|\lambda^{n+1}|}{1 - |\lambda|}.$$

We are now practically done: for each $0 \leq n \leq p-1$

(i.) the disc B_n exists if and only if $r_n > 0$, namely

$$\frac{2}{|\lambda^{\ell+1}|} |f_{\ell+1+n}(\lambda)| - \frac{|\lambda^{n+1}|}{1 - |\lambda|} > 0 \iff |f_{\ell+1+n}(\lambda)| > \frac{1}{2} \frac{|\lambda^{\ell+1+n+1}|}{1 - |\lambda|}$$

which is true by assumption;

(ii.) $B_n \cap B_{n+1} \neq \emptyset$ if and only if $r_n + r_{n+1} > |\omega_n - \omega_{n+1}| = |\lambda^{n+1}|$, namely

$$\begin{aligned} \frac{2}{|\lambda^{\ell+1}|} (|f_{\ell+1+n}(\lambda)| + |f_{\ell+1+n+1}(\lambda)|) - \frac{|\lambda^{n+1}|}{1 - |\lambda|} - \frac{|\lambda^{n+2}|}{1 - |\lambda|} &> |\lambda^{n+1}| \\ \iff |f_{\ell+1+n}(\lambda)| + |f_{\ell+1+n+1}(\lambda)| &> \frac{|\lambda^{\ell+1+n+1}|}{1 - |\lambda|} \end{aligned}$$

which is true by assumption;

- (iii.) the disc B_n is tangent to $\tilde{\Gamma}^n$ if and only if for every node $\nu_{\mathbf{w}|n} \in \tilde{\Gamma}^n$ with $\mathbf{w} \in \tilde{\Sigma}^\infty$ we have $r_n + |\lambda^{n+1}|(1 - |\lambda|)^{-1} < |\omega_n - \nu_{\mathbf{w}|n}|$, namely

$$\begin{aligned} \frac{2}{|\lambda^{\ell+1}|} |f_{\ell+1+n}(\lambda)| &< \left| -\frac{1}{\lambda^{\ell+1}} (f_{\ell+1+n}(\lambda) + f_\ell(\lambda)) - \nu_{\mathbf{w}|n} \right| \\ \iff 2 |f_{\ell+1+n}(\lambda)| &< |f_\ell(\lambda) + f_{\ell+1+n}(\lambda) + \lambda^{\ell+1} \nu_{\mathbf{w}|n}| \\ &< |2f_\ell(\lambda) + \lambda^{\ell+1} P(\lambda)| \end{aligned}$$

where P is a polynomial of degree at most n with coefficients taken from the set $\{-2, -1, 0, +1, +2\}$. Again, the inequality is true by assumption.

Finally, we claim that $C\lambda^{pm} \in \frac{\lambda^{\ell+1}}{f'(\lambda)} (\bigcup_{n \geq 0} B_n - \zeta)$ for every $C \in \frac{\lambda^{\ell+1}}{f'(\lambda)} (\bigcup_{n \geq 0} B_n - \zeta)$ and $m \geq 1$. We will show that, after a translation by $-\zeta$, the chain is forward invariant under $z \mapsto \lambda^p z$.

Observe that $\omega_n - \zeta = -\lambda^{-\ell-1} f_{\ell+1+n}(\lambda)$ and since $(\lambda^p - 1)f_\ell(\lambda) = \sum_{j=\ell+1}^{\ell+p} c_j \lambda^j$, then

$$\begin{aligned} \lambda^p(\omega_n - \zeta) &= -\frac{1}{\lambda^{\ell+1}} \lambda^p f_{\ell+1+n}(\lambda) \\ &= -\frac{1}{\lambda^{\ell+1}} \lambda^p \left(f_\ell(\lambda) + \sum_{j=\ell+1}^{\ell+1+n} c_j \lambda^j \right) \\ &= -\frac{1}{\lambda^{\ell+1}} \left(\lambda^p f_\ell(\lambda) + \lambda^p \sum_{j=\ell+1}^{\ell+1+n} c_j \lambda^j \right) \\ &= -\frac{1}{\lambda^{\ell+1}} \left(f_\ell(\lambda) + \sum_{j=\ell+1}^{\ell+p} c_j \lambda^j + \sum_{j=\ell+1+p}^{\ell+1+n+p} c_j \lambda^j \right) \\ &= -\frac{1}{\lambda^{\ell+1}} f_{\ell+1+n+p}(\lambda) = \omega_{n+p} - \zeta \end{aligned}$$

where the second to last equality is due to the fact that $c_{\ell+k} = c_{\ell+k+p}$ for every $k \geq 1$. Hence, the claim follows. \square

The proof of Theorem 4.1.5 is exactly the same, except we only have to show $\bigcup_{n \geq 0} B_n$ is outside A_λ . Therefore, in step (iii.) we need to check that B_n does not intersect the instar Γ^n , rather than $\tilde{\Gamma}^n$.

4.3 Examples: Landmark Points

In this section we present examples of parameters λ satisfying the hypothesis of Theorem 4.1.3 and 4.1.5. In [23], Solomyak provided parameters λ , referred by him as landmark points, with $|\mathcal{F}_\lambda| = 1$. We will prove that they are all accessible points on the boundary of \mathcal{M} .

Each example is denoted by a word in $\tilde{\Sigma}^\infty$ corresponding to the coefficients of the power series associated to the parameter.

4.3.1 $+(+ + -)^\infty$

Let $\mathbf{c} = c_0c_1 \cdots = +(+ + -)^\infty \in \Sigma^\infty$ and $f(z) := \sum_{k=0}^\infty c_k z^k = \frac{1 + z + z^2 - 2z^3}{1 - z^3}$. Solomyak proved in [23] that¹ f is the unique power series for which $\lambda_0 \approx -0.366 + 0.520i$ is a root. Using the notations of Theorem 4.1.3 we have $\ell = 0$, $p = 3$, $\xi = 0$, $\xi_n = f_n(\lambda_0)$, and $\zeta = -\frac{1}{\lambda_0} \in \mathbf{A}_{\lambda_0} \subset \tilde{\mathbf{A}}_{\lambda_0}$ which has itinerary $\mathbf{b} = (+ + -)^\infty$.

We begin with proving hypothesis (i.) of Theorem 4.1.3 is satisfied:

Lemma 4.3.1 *Let λ_0 and $f(z)$ be as above. Then for every $0 \leq n \leq p - 1$*

$$2|f_n(\lambda_0)| > \frac{|\lambda_0^{n+1}|}{1 - |\lambda_0|}.$$

Proof First notice that

$$(i.) \quad \frac{\sqrt{5} - 1}{2} < |\lambda_0| < \frac{2}{3} \text{ and}$$

$$(ii.) \quad \frac{2}{3}\pi < \arg(\lambda_0) < \frac{23}{32}\pi.$$

Then from (i.) we get

$$2|f_0(\lambda_0)| = 2|1| > \frac{|\lambda_0|}{1 - |\lambda_0|}.$$

¹Solomyak considered the word $+(- + + + -)^\infty$ which gives the power series $\frac{1 - z + z^2 + 2z^3}{1 + z^3}$, or in other words, he considered $f(-z)$. The symmetry of \mathcal{M} allows us to consider $f(z)$ instead.

From (ii.) and the Law of Cosines we get

$$\begin{aligned}
2|f_1(\lambda_0)| = 2|1 + \lambda_0| &> 2\sqrt{1 + |\lambda_0|^2 - 2|\lambda_0| \cos\left(\frac{9\pi}{32}\right)} \\
&> 2\sqrt{1 + \frac{(\sqrt{5}-1)^2}{4} - (\sqrt{5}-1) \cos\left(\frac{9\pi}{32}\right)} \\
&> 2\frac{1}{\sqrt{2}} > 2|\lambda_0| > \frac{|\lambda_0^2|}{1 - |\lambda_0|}.
\end{aligned}$$

Since $f(\lambda_0) = 0$ then $f_2(\lambda_0) = 1 + \lambda_0 + \lambda_0^2 = 2\lambda_0^3$ and consequently

$$2|f_2(\lambda_0)| = 2|2\lambda_0^3| > \frac{|\lambda_0^3|}{1 - |\lambda_0|}$$

because $4 > (1 - |\lambda_0|)^{-1}$. □

Remember that satisfying Theorem 4.1.3(i.) is equivalent to saying that, the discs B_n in the chain exists for every $n \geq 0$. We will now show that $B_n \cap B_{n+1} \neq \emptyset$ and that $B_n \subset \mathbb{C} \setminus \tilde{I}^n$, namely the remaining two hypothesis of Theorem 4.1.3. Recall that each disc B_n is centered at ω_n and has radius r_n :

$$\omega_n = -\frac{1}{\lambda_0}(f_{n+1}(\lambda_0) + f_0(\lambda_0)), \quad r_n = \frac{2}{|\lambda_0|}|f_{n+1}(\lambda_0)| - \frac{|\lambda_0^{n+1}|}{1 - |\lambda_0|}$$

Lemma 4.3.2 *For $\lambda_0 \approx -0.366 + 0.520i$, the set $\bigcup_{n \geq 0} B_n$ is connected and lies in the complement of \tilde{A}_{λ_0} .*

Proof By the self-similarity of the attractor A_{λ_0} at ζ it is enough to prove that $\bigcup_{0 \leq n \leq 2} B_n$ is connected and lies outside the instar \tilde{I}^2 . We will first show that B_n lies outside the instar \tilde{I}^n and then prove that $B_n \cap B_{n+1} \neq \emptyset$ for each $n = 0, 1, 2$.

$n = 0$: The instar \tilde{I}^0 is the union of the discs D^+ , D^0 , and D^- . We already know that B_0 is outside D^+ , we want to show that the distances between ω_0 and the nodes $\nu_0 = 0$ and $\nu_- = -1$ is larger than the sum of the radii of B_0 and the nodal disc of level 0. In other words, we need that $r_0 + |\lambda_0|(1 - |\lambda_0|)^{-1} < |\omega_0 - 0|$ and

$r_0 + |\lambda_0|(1 - |\lambda_0|)^{-1} < |\omega_0 - (-1)|$. Using that $2^{-1}(\sqrt{5} - 1) < |\lambda_0| < 2/3$ and $\arg(\lambda_0) > \frac{2}{3}\pi$, the Law of Cosine tells us

$$|1 + \lambda_0| < \sqrt{1 + |\lambda_0|^2 - 2|\lambda_0| \cos\left(\frac{\pi}{3}\right)} < \sqrt{1 + \frac{4}{9} - \frac{4}{3} \cos\left(\frac{\pi}{3}\right)} < 1$$

so

$$|\omega_0 - (-1)| = 2 \left| \frac{1}{\lambda_0} \right| > 2 \left| \frac{1 + \lambda_0}{\lambda_0} \right| = r_0 + \frac{|\lambda_0|}{1 - |\lambda_0|}.$$

Moreover, using the better estimate $\frac{11}{16}\pi < \arg(\lambda_0) < \frac{45}{64}\pi$,

$$2|1 + \lambda_0| < 2\sqrt{1 + \frac{4}{9} - \frac{4}{3} \cos\left(\frac{5\pi}{16}\right)} < \sqrt{2^2 + \frac{4}{9} - 2\frac{4}{3} \cos\left(\frac{19\pi}{64}\right)} < |2 + \lambda_0|$$

implying that

$$|\omega_0 - 0| = \left| \frac{2 + \lambda_0}{\lambda_0} \right| > 2 \left| \frac{1 + \lambda_0}{\lambda_0} \right| = r_0 + \frac{|\lambda_0|}{1 - |\lambda_0|}.$$

$n = 1$: The instar $\tilde{\Gamma}^1$ is the union of the discs $\tilde{\mathcal{D}}^{w_0^+}$, $\tilde{\mathcal{D}}^{w_0^0}$, and $\tilde{\mathcal{D}}^{w_0^-}$ where $w_0 \in \{+, 0, -\}$. Instead of checking that eight more inequalities are satisfied, we use the fact that $\arg(\lambda_0) \in (2\pi/3, 23\pi/32)$ to show $0 < \operatorname{Re}(\zeta_1) < \operatorname{Re}(\zeta)$. Given that $\zeta_1 = \frac{1}{\lambda_0}(f_{1+1}(\lambda_0) - f_0(\lambda_0)) = 1 + \lambda_0$ we need to check

$$-\frac{1}{|\lambda_0|} \cos(\arg(\lambda_0)) > 1 + |\lambda_0| \cos(\arg(\lambda_0)) \iff -\cos(\arg(\lambda_0)) > \frac{|\lambda_0|}{1 + |\lambda_0|^2}$$

Indeed, $-\cos(\arg(\lambda_0)) \in (0.55, 0.64)$ and $\frac{|\lambda_0|}{1 + |\lambda_0|^2} \in (0.44, 0.47)$. Moreover, we have $\operatorname{Re}(\zeta_1) > 0$ because $\cos(\arg(\lambda_0)) > -3/2 > -|\lambda_0|^{-1}$. Consequently, ω_1 is in the first quadrant with $\operatorname{Re}(\omega_1) > \operatorname{Re}(\zeta_1)$. It follows that B_1 has a chance to intersect only the discs $\tilde{\mathcal{D}}^{+0}$ and $\tilde{\mathcal{D}}^{+-}$. However, in Lemma 4.3.1 we showed that $|1 + \lambda_0| > 2^{-1/2}$, therefore, since $2^{-1/2} > 2|\lambda_0|^3$ we have

$$|\omega_1 - (1 - \lambda_0)| = 2 \left| \frac{1 + \lambda_0}{\lambda_0} \right| > 4|\lambda_0|^2 = r_1 + \frac{|\lambda_0|^2}{1 - |\lambda_0|}.$$

so $B_1 \cap \tilde{\mathcal{D}}^{+-} = \emptyset$.

Finally, B_1 does not intersect $\tilde{\mathcal{D}}^{+0}$ because

$$\begin{aligned} |\omega_1 - (1 + 0 \cdot \lambda_0)| &= \left| \frac{-\lambda_0^2 + 4\lambda_0^3}{\lambda_0} \right| = |\lambda_0| |1 - 4\lambda_0| > |\lambda_0| (1 + 4|\lambda_0| \cos(\pi/4)) \\ &> |\lambda_0| \frac{8}{3} > 4|\lambda_0|^2 = r_1 + \frac{|\lambda_0|^2}{1 - |\lambda_0|}. \end{aligned}$$

In the first equality we used the fact that $1 + \lambda_0 = -\lambda_0^2 + 2\lambda_0^3$ and in the second line that $1 + \sqrt{2}(\sqrt{5} - 1) > 8/3 > 4|\lambda_0|$.

$n = 2$: In this case we shall prove that $B_2 \subset B_1$ which implies that B_2 is outside $\tilde{\Gamma}^2$ because of the containment $\tilde{\Gamma}^2 \subset \tilde{\Gamma}^1$. Firstly, we have $|\omega_1 - \omega_2| = |\lambda_0^2|$ and that the radius of B_1 is $r_1 = 4|\lambda_0^2| - \frac{|\lambda_0^2|}{1-|\lambda_0|} > |\lambda_0^2|$ because $3 > (1 - |\lambda_0|)^{-1}$. Secondly, the radius of B_2 is $r_2 = 2|\lambda_0^2| - \frac{|\lambda_0^3|}{1-|\lambda_0|}$, so for the containment to hold we must have

$$4|\lambda_0^2| - \frac{|\lambda_0^2|}{1-|\lambda_0|} > 2\left(2|\lambda_0^2| - \frac{|\lambda_0^3|}{1-|\lambda_0|}\right),$$

which holds since $2|\lambda_0| > 1$.

We have shown that B_0, B_1 , and B_2 do not intersect their respective instar and, therefore, their union lies outside the instar $\tilde{\Gamma}^2 \supset \tilde{\mathbf{A}}_{\lambda_0}$. We have also proved that $B_2 \subset B_1$ so it remains to show that $B_1 \cap B_0 \neq \emptyset$ and $B_2 \cap B_3 \neq \emptyset$.

We will prove that $\omega_1 \in B_0$, i.e. $|\omega_0 - \omega_1| = |\lambda_0| < r_0$: recall that $r_0 = 2\left|\frac{1+\lambda_0}{\lambda_0}\right| - \frac{|\lambda_0|}{1-|\lambda_0|}$ and $0.63 < |\lambda_0| < 0.64$ then

$$2|1 - 2\lambda_0| > 2(1 + 2(0.63)\cos(\pi/4)) > \frac{1}{1 - (0.64)} + 1 > \frac{1}{1 - |\lambda_0|} + 1$$

which implies

$$2\left|\frac{1 + \lambda_0}{\lambda_0}\right| = 2\left|\frac{-\lambda_0^2 + 2\lambda_0^3}{\lambda_0}\right| = 2|\lambda_0||1 - 2\lambda_0| > |\lambda_0|\left(\frac{1}{1 - |\lambda_0|} + 1\right).$$

Finally, we want to show that $|\omega_2 - \omega_3||\lambda_0^3| = |\lambda_0^3| < r_2 + r_3$. By definition $r_3 = 2|\lambda_0^2||1 + \lambda_0| - \frac{|\lambda_0^4|}{1-|\lambda_0|}$ and since

$$\begin{aligned} |\lambda_0| + \frac{|\lambda_0^2|}{1 - |\lambda_0|} &< 0.639 + \frac{(0.639)^2}{1 - 0.639} < 1 + \sqrt{1 + \frac{(\sqrt{5} - 1)^2}{4} - (\sqrt{5} - 1)\cos\left(\frac{9\pi}{32}\right)} \\ &< 1 + |1 + \lambda_0| \end{aligned}$$

then

$$\begin{aligned}
|\lambda_0| &< 1 + |1 + \lambda_0| - \frac{|\lambda_0^2|}{1 - |\lambda_0|} \\
\iff |\lambda_0| &< 2 + 2|1 + \lambda_0| - |\lambda_0| - \frac{2|\lambda_0^2|}{1 - |\lambda_0|} \\
&= 2 - \frac{|\lambda_0|}{1 - |\lambda_0|} + 2|1 + \lambda_0| - \frac{|\lambda_0^2|}{1 - |\lambda_0|} \\
\iff |\lambda_0^3| &< r_2 + r_3.
\end{aligned}$$

The equality in the third line holds because $\frac{|\lambda_0|}{1 - |\lambda_0|} = |\lambda_0| + \frac{|\lambda_0^2|}{1 - |\lambda_0|}$.

□

We can now prove

Proposition 4.3.1 *The parameter $\lambda_0 \approx -0.366 + 0.520i$, root of the rational function $f(z) = 1 + (z + z^2 - z^3)(1 - z^3)^{-1}$, is an accessible point of $\partial\mathcal{M} \cap \partial\mathcal{M}_0$.*

Proof By Lemma 4.3.2 the chain $\bigcup_{n \geq 0} B_n$ is connected and lies in the complement of \tilde{A}_{λ_0} . Then by Theorem 4.1.3 $\lambda_0 \in \partial\mathcal{M}$ is an accessible point. Because $f(z)$ is unique and has no zero coefficients, by Corollary 4.1.4, λ_0 is an accessible point of $\partial\mathcal{M} \cap \partial\mathcal{M}_0$. □

It must be noted that the uncountable set \mathcal{T} of parameters mentioned in Theorem 3.4.1 and Theorem 3.4.3 contains $\lambda_0 \approx -0.366 + 0.520i$. In fact, such set was found by perturbing the number of repeating coefficients in the power series f and by allowing that some of the perturbed repeating coefficients to be 0. The way Bandt and Hung proved that no other power series $g \in \mathcal{P}$ has a root in \mathcal{T} , entailed finding a uniform lower bound in a neighborhood of \mathcal{T} on the normalized difference

$$\frac{g(z) - h(z)}{z^k} = \sum_{j=0}^{\infty} \epsilon_j z^j, \quad \epsilon_j \in \{-2, -1, 0, +1, +2\}; \quad \epsilon_0 \neq 0$$

where $k \geq 1$ and $h(z)$ a power series with a root in \mathcal{T} . We are working on extending Proposition 4.3.1 to parameters in \mathcal{T} .

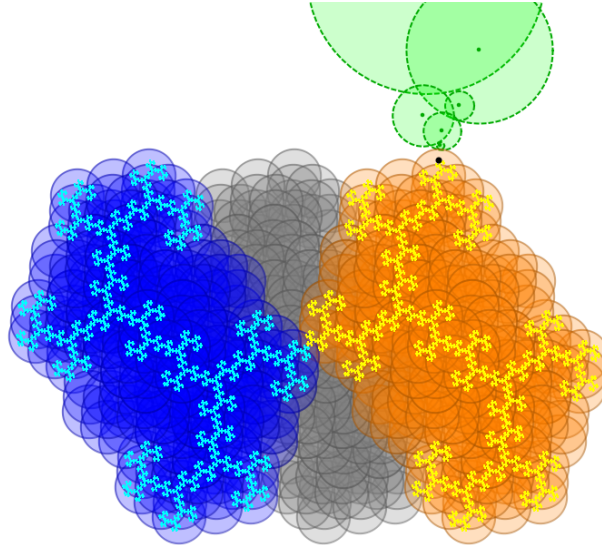


Fig. 4.3. The attractor A_{λ_0} inside $\tilde{\Gamma}^5$. The green discs are part of the chain whose existence is provided by Theorem 4.1.3.

4.3.2 $+ - -(+)\infty$

The remaining landmark points are all inside the following sector:

$$\frac{\sqrt{5}-1}{2} < |z| < \frac{2}{3} \quad \text{with} \quad 0 < \arg(z) < \frac{5\pi}{32}.$$

Therefore, we will first prove, by simple geometric arguments, certain inequalities for all points in the above sector.

Lemma 4.3.3 *Suppose $\frac{\sqrt{5}-1}{2} < |\lambda| < \frac{2}{3}$ and $0 < \arg(\lambda) < \frac{5\pi}{32}$. Then the following holds:*

(a.) $1 - |\lambda| > \frac{1}{2} |1 - \lambda|;$

(b.) $1 - |\lambda|^2 > |1 - \lambda|;$

(c.) $|\lambda| < |2 - \lambda|;$

(d.) $2|\lambda| < |3 - \lambda|;$

(e.) $2|\lambda| < |1 + \lambda|.$

Proof From the Law of Cosine we obtain

$$\begin{aligned} 0.541 &> \sqrt{1^2 + \left(\frac{\sqrt{5}-1}{2}\right)^2 - 2\left(\frac{\sqrt{5}-1}{2}\right)\cos\left(\frac{5\pi}{32}\right)} \\ &> |1-\lambda| > \sqrt{1^2 + \left(\frac{2}{3}\right)^2 - 2\left(\frac{2}{3}\right)\cos(0)} = \frac{1}{3}. \end{aligned}$$

It follows that

$$1 - |\lambda| > 1 - \frac{2}{3} > \frac{1}{2}(0.541) > \frac{1}{2}|1 - \lambda|$$

and

$$1 - |\lambda|^2 > 1 - \frac{4}{9} > 0.541 > |1 - \lambda|,$$

which gives **(a.)** and **(b.)**.

Similarly,

$$\begin{aligned} |2 - \lambda| &> \sqrt{2^2 + \left(\frac{2}{3}\right)^2 - 2\left(\frac{2}{3}\right)2\cos(0)} = \frac{4}{3} > 2|\lambda| > |\lambda| \\ |3 - \lambda| &> \sqrt{3^2 + \left(\frac{2}{3}\right)^2 - 2\left(\frac{2}{3}\right)3\cos(0)} = \frac{7}{3} > 2|\lambda|, \end{aligned}$$

which gives **(c.)** and **(d.)**.

Finally,

$$|1 + \lambda| > \sqrt{1^2 + \left(\frac{\sqrt{5}-1}{2}\right)^2 + 2\left(\frac{\sqrt{5}-1}{2}\right)\cos\left(\frac{5\pi}{32}\right)} > 1.572 > \frac{4}{3} > 2|\lambda|,$$

giving **(e.)** and concluding the proof of the lemma. \square

Let $\mathbf{c} = c_0c_1\cdots = + - -(+)\infty \in \Sigma^\infty$ and $f(z) := \sum_{k=0}^\infty c_k z^k = \frac{1 - 2z + 2z^3}{1 - z}$. Solomyak proved in [23] that f is the unique power series for which $\lambda_1 \approx 0.5957439 + 0.2544259i$ is a root. Using the notations of Theorem 4.1.3 we have $\ell = 2$, $p = 1$, $n = 0$, and $\zeta = \frac{1}{1-\lambda_1} \in \mathbf{A}_{\lambda_1} \subset \tilde{\mathbf{A}}_{\lambda_1}$ which has itinerary $\mathbf{b} = (+)^\infty$.

We are now ready to prove

Proposition 4.3.2 *The parameter $\lambda_1 \approx 0.5957439 + 0.2544259i$, root of the rational function $f(z) = (1 - 2z + 2z^3)(1 - z)^{-1}$, is an accessible point of $\partial\mathcal{M} \cap \partial\mathcal{M}_0$.*

Proof Observe that since λ_1 is the root of the power series f , we can write

$$\begin{aligned} f_\ell(\lambda_1) &= 1 - \lambda_1 - \lambda_1^2 = -\frac{\lambda_1^3}{1 - \lambda_1}, \\ f_{\ell+1}(\lambda_1) &= 1 - \lambda_1 - \lambda_1^2 + \lambda_1^3 = -\frac{\lambda_1^4}{1 - \lambda_1}, \\ f_{\ell+2}(\lambda_1) &= 1 - \lambda_1 - \lambda_1^2 + \lambda_1^3 + \lambda_1^4 = -\frac{\lambda_1^5}{1 - \lambda_1}. \end{aligned}$$

Condition **(i.)** in Theorem 4.1.3 is satisfied since

$$|f_{\ell+1}(\lambda_1)| > \frac{1}{2} \frac{|\lambda_1^{\ell+2}|}{1 - |\lambda_1|} \iff \left| \frac{1}{1 - \lambda_1} \right| > \frac{1}{2} \frac{1}{1 - |\lambda_1|} \iff 1 - |\lambda_1| > \frac{1}{2} |1 - \lambda_1|$$

holds by Lemma 4.3.3 part **(a.)**.

Condition **(ii.)** in Theorem 4.1.3 is satisfied since

$$\begin{aligned} |f_{\ell+1}(\lambda_1)| + |f_{\ell+2}(\lambda_1)| &> \frac{|\lambda_1^{\ell+2}|}{1 - |\lambda_1|} \iff \left| \frac{1}{1 - \lambda_1} \right| + \left| \frac{\lambda_1}{1 - \lambda_1} \right| > \frac{1}{1 - |\lambda_1|} \\ &\iff 1 - |\lambda_1|^2 > |1 - \lambda_1| \end{aligned}$$

holds by Lemma 4.3.3 part **(b.)**.

Condition **(iii.)** in Theorem 4.1.3 has four cases since the polynomial P can only be either -2 , -1 , 0 , or 1 . The case $P(z) = -2$ is satisfied because

$$\begin{aligned} |2f_{\ell+1}(\lambda_1)| < |2f_\ell(\lambda_1) + \lambda_1^3(-2)| &\iff \left| \frac{-2\lambda_1^4}{1 - \lambda_1} \right| < \left| \frac{-4\lambda_1^3 + 2\lambda_1^4}{1 - \lambda_1} \right| \\ &\iff |\lambda_1| < |2 - \lambda_1| \end{aligned}$$

holds by Lemma 4.3.3 part **(c.)**.

The case $P(z) = -1$ is satisfied because

$$\begin{aligned} |2f_{\ell+1}(\lambda_1)| < |2f_\ell(\lambda_1) + \lambda_1^3(-1)| &\iff \left| \frac{-2\lambda_1^4}{1 - \lambda_1} \right| < \left| \frac{-3\lambda_1^3 + \lambda_1^4}{1 - \lambda_1} \right| \\ &\iff |2\lambda_1| < |3 - \lambda_1| \end{aligned}$$

holds by Lemma 4.3.3 part **(d.)**.

The case $P(z) = 0$ is trivial since

$$|2f_{\ell+1}(\lambda_1)| < |2f_\ell(\lambda_1) + \lambda_1^3(0)| \iff \left| \frac{-2\lambda_1^4}{1 - \lambda_1} \right| < \left| \frac{-2\lambda_1^3}{1 - \lambda_1} \right| \iff |\lambda_1| < 1$$

The case $P(z) = 1$ is satisfied because

$$\begin{aligned} |2f_{\ell+1}(\lambda_1)| < |2f_\ell(\lambda_1) + \lambda_1^3(1)| &\iff \left| \frac{-2\lambda_1^4}{1-\lambda_1} \right| < \left| \frac{-\lambda_1^3 - \lambda_1^4}{1-\lambda_1} \right| \\ &\iff |2\lambda_1| < |1 + \lambda_1| \end{aligned}$$

holds by Lemma 4.3.3 part (e.).

Therefore, $\lambda_1 \in \partial\mathcal{M}$ is accessible since all the assumption of Theorem 4.1.3 are satisfied. Moreover, because $f(z)$ is unique and has no zero coefficients, by Corollary 4.1.4, λ_1 is an accessible point of $\partial\mathcal{M} \cap \partial\mathcal{M}_0$. \square

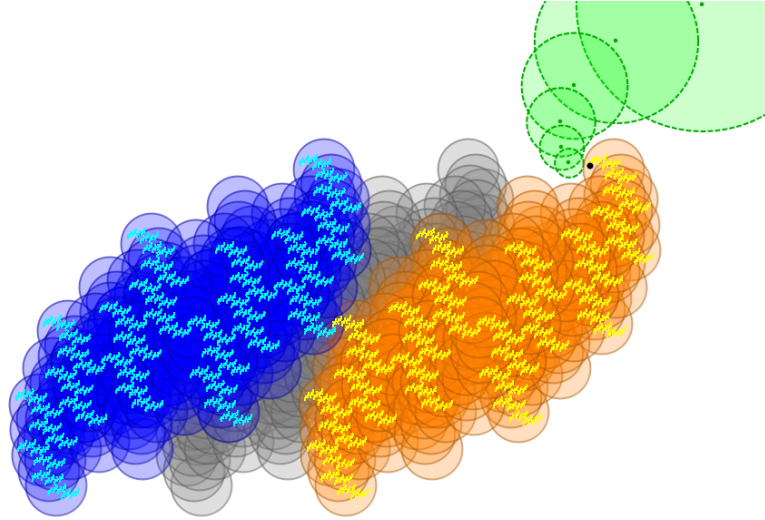


Fig. 4.4. The attractor A_{λ_1} inside $\tilde{\Gamma}^5$. The green discs are part of the chain whose existence is provided by Theorem 4.1.3.

4.3.3 $+ - - - (+)^\infty$

Let $\mathbf{c} = c_0c_1\cdots = + - - - (+)^\infty \in \Sigma^\infty$ and $f(z) := \sum_{k=0}^\infty c_k z^k = \frac{1 - 2z + 2z^4}{1 - z}$. Solomyak proved in [23] that f is the unique power series for which $\lambda_2 \approx 0.63601 + 0.106924i$ is a root. Using the notations of Theorem 4.1.3 we have $\ell = 3$, $p = 1$, $n = 0$, and $\zeta = \frac{1}{1-\lambda_2} \in A_{\lambda_2} \subset \tilde{A}_{\lambda_2}$ which has itinerary $\mathbf{b} = (+)^\infty$.

We are now ready to prove

Proposition 4.3.3 *The parameter $\lambda_2 \approx 0.63601 + 0.106924i$, root of the rational function $f(z) = (1 - 2z + 2z^4)(1 - z)^{-1}$, is an accessible point of $\partial\mathcal{M} \cap \partial\mathcal{M}_0$.*

Proof Observe that since λ_2 is the root of the power series f , we can write

$$\begin{aligned} f_\ell(\lambda_2) &= 1 - \lambda_2 - \lambda_2^2 - \lambda_2^3 = -\frac{\lambda_2^4}{1 - \lambda_2}, \\ f_{\ell+1}(\lambda_2) &= 1 - \lambda_2 - \lambda_2^2 - \lambda_2^3 + \lambda_2^4 = -\frac{\lambda_2^5}{1 - \lambda_2}, \\ f_{\ell+2}(\lambda_2) &= 1 - \lambda_2 - \lambda_2^2 - \lambda_2^3 + \lambda_2^4 + \lambda_2^5 = -\frac{\lambda_2^6}{1 - \lambda_2}. \end{aligned}$$

Condition (i.) in Theorem 4.1.3 is satisfied since

$$|f_{\ell+1}(\lambda_2)| > \frac{1}{2} \frac{|\lambda_2^{\ell+2}|}{1 - |\lambda_2|} \iff \left| \frac{1}{1 - \lambda_2} \right| > \frac{1}{2} \frac{1}{1 - |\lambda_2|} \iff 1 - |\lambda_2| > \frac{1}{2} |1 - \lambda_2|$$

holds by Lemma 4.3.3 part (a.).

Condition (ii.) in Theorem 4.1.3 is satisfied

$$\begin{aligned} |f_{\ell+1}(\lambda_2)| + |f_{\ell+2}(\lambda_2)| &> \frac{|\lambda_2^{\ell+2}|}{1 - |\lambda_2|} \iff \left| \frac{1}{1 - \lambda_2} \right| + \left| \frac{\lambda_2}{1 - \lambda_2} \right| > \frac{1}{1 - |\lambda_2|} \\ &\iff 1 - |\lambda_2|^2 > |1 - \lambda_2| \end{aligned}$$

holds by Lemma 4.3.3 part (b.).

Condition (iii.) in Theorem 4.1.3 has four cases since the polynomial P can only be either $-2, -1, 0$, or 1 . The case $P(z) = -2$ is satisfied because

$$\begin{aligned} |2f_{\ell+1}(\lambda_2)| < |2f_\ell(\lambda_2) + \lambda_2^4(-2)| &\iff \left| \frac{-2\lambda_2^5}{1 - \lambda_2} \right| < \left| \frac{-4\lambda_2^4 + 2\lambda_2^5}{1 - \lambda_2} \right| \\ &\iff |\lambda_2| < |2 - \lambda_2| \end{aligned}$$

holds by Lemma 4.3.3 part (c.).

The case $P(z) = -1$ is satisfied because

$$\begin{aligned} |2f_{\ell+1}(\lambda_2)| < |2f_\ell(\lambda_2) + \lambda_2^4(-1)| &\iff \left| \frac{-2\lambda_2^5}{1 - \lambda_2} \right| < \left| \frac{-3\lambda_2^4 + \lambda_2^5}{1 - \lambda_2} \right| \\ &\iff |2\lambda_2| < |3 - \lambda_2| \end{aligned}$$

holds by Lemma 4.3.3 part (d.).

The case $P(z) = 0$ is trivial since

$$|2f_{\ell+1}(\lambda_2)| < |2f_{\ell}(\lambda_2) + \lambda_2^4(0)| \iff \left| \frac{-2\lambda_2^5}{1-\lambda_2} \right| < \left| \frac{-2\lambda_2^4}{1-\lambda_2} \right| \iff |\lambda_2| < 1$$

The case $P(z) = 1$ is satisfied because

$$\begin{aligned} |2f_{\ell+1}(\lambda_2)| < |2f_{\ell}(\lambda_2) + \lambda_2^4(1)| &\iff \left| \frac{-2\lambda_2^5}{1-\lambda_2} \right| < \left| \frac{-\lambda_2^3 - \lambda_2^5}{1-\lambda_2} \right| \\ &\iff |2\lambda_2| < |1 + \lambda_2| \end{aligned}$$

holds by Lemma 4.3.3 part (e.).

Therefore, $\lambda_2 \in \partial\mathcal{M}$ is accessible since all the assumption of Theorem 4.1.3 are satisfied. Moreover, because $f(z)$ is unique and has no zero coefficients, by Corollary 4.1.4, λ_2 is an accessible point of $\partial\mathcal{M} \cap \partial\mathcal{M}_0$. \square

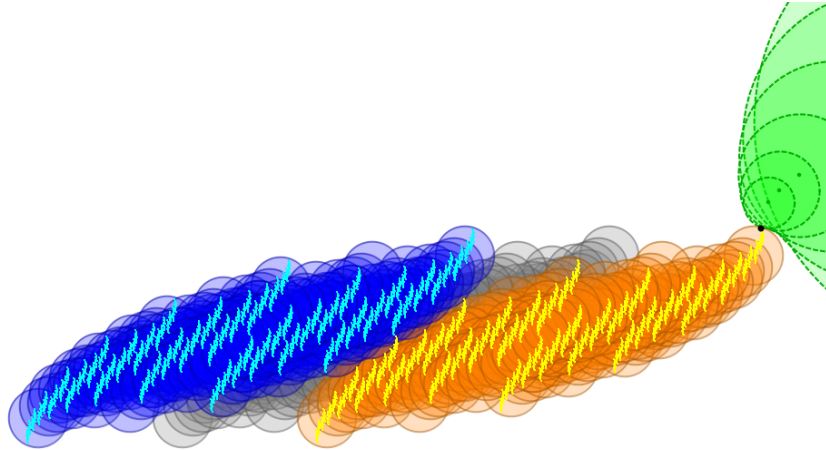


Fig. 4.5. The attractor A_{λ_2} inside $\tilde{\Gamma}^5$. The green discs are part of the chain whose existence is provided by Theorem 4.1.3.

4.3.4 $+ - -0(+)^{\infty}$

Let $\mathbf{c} = c_0c_1 \cdots = + - -0(+)^{\infty} \in \tilde{\Sigma}^{\infty}$ and $f(z) := \sum_{k=0}^{\infty} c_k z^k = \frac{1 - 2z + z^3 + z^4}{1 - z}$. Solomyak proved in [23] that f is the unique power series for which $\lambda_3 \approx 0.6219644 +$

$0.1877304i$ is a root. Using the notations of Theorem 4.1.3 we have $\ell = 3$, $p = 1$, $n = 0$, and $\zeta = \frac{1}{1-\lambda_3} \in \mathbf{A}_{\lambda_3} \subset \tilde{\mathbf{A}}_{\lambda_3}$ which has itinerary $\mathbf{b} = (+)^\infty$.

We are now ready to prove

Proposition 4.3.4 *The parameter $\lambda_3 \approx 0.6219644 + 0.1877304i$, root of the rational function $f(z) = (1 - 2z + z^3 + z^4)(1 - z)^{-1}$, is an accessible point of $\partial\mathcal{M}$.*

Proof Observe that since λ_3 is the root of the power series f , we can write

$$\begin{aligned} f_\ell(\lambda_3) &= 1 - \lambda_3 - \lambda_3^2 = -\frac{\lambda_3^4}{1 - \lambda_3}, \\ f_{\ell+1}(\lambda_3) &= 1 - \lambda_3 - \lambda_3^2 + \lambda_3^4 = -\frac{\lambda_3^5}{1 - \lambda_3}, \\ f_{\ell+2}(\lambda_3) &= 1 - \lambda_3 - \lambda_3^2 + \lambda_3^4 + \lambda_3^5 = -\frac{\lambda_3^6}{1 - \lambda_3}. \end{aligned}$$

Condition (i.) in Theorem 4.1.3 is satisfied since

$$|f_{\ell+1}(\lambda_3)| > \frac{1}{2} \frac{|\lambda_3^{\ell+2}|}{1 - |\lambda_3|} \iff \left| \frac{1}{1 - \lambda_3} \right| > \frac{1}{2} \frac{1}{1 - |\lambda_3|} \iff 1 - |\lambda_3| > \frac{1}{2} |1 - \lambda_3|$$

holds by Lemma 4.3.3 part (a.).

Condition (ii.) in Theorem 4.1.3 is satisfied since

$$\begin{aligned} |f_{\ell+1}(\lambda_3)| + |f_{\ell+2}(\lambda_3)| &> \frac{|\lambda_3^{\ell+2}|}{1 - |\lambda_3|} \iff \left| \frac{1}{1 - \lambda_3} \right| + \left| \frac{\lambda_3}{1 - \lambda_3} \right| > \frac{1}{1 - |\lambda_3|} \\ &\iff 1 - |\lambda_3|^2 > |1 - \lambda_3| \end{aligned}$$

holds by Lemma 4.3.3 part (b.).

Condition (iii.) in Theorem 4.1.3 has four cases since the polynomial P can only be either -2 , -1 , 0 , or 1 . The case $P(z) = -2$ is satisfied because

$$\begin{aligned} |2f_{\ell+1}(\lambda_3)| < |2f_\ell(\lambda_3) + \lambda_3^4(-2)| &\iff \left| \frac{-2\lambda_3^5}{1 - \lambda_3} \right| < \left| \frac{-4\lambda_3^4 + 2\lambda_3^5}{1 - \lambda_3} \right| \\ &\iff |\lambda_3| < |2 - \lambda_3| \end{aligned}$$

holds by Lemma 4.3.3 part (c.).

The case $P(z) = -1$ is satisfied because

$$\begin{aligned} |2f_{\ell+1}(\lambda_3)| < |2f_\ell(\lambda_3) + \lambda_3^4(-1)| &\iff \left| \frac{-2\lambda_3^5}{1 - \lambda_3} \right| < \left| \frac{-3\lambda_3^4 + \lambda_3^5}{1 - \lambda_3} \right| \\ &\iff |2\lambda_3| < |3 - \lambda_3| \end{aligned}$$

holds by Lemma 4.3.3 part (d.).

The case $P(z) = 0$ is trivial since

$$|2f_{\ell+1}(\lambda_3)| < |2f_{\ell}(\lambda_3) + \lambda_3^4(0)| \iff \left| \frac{-2\lambda_3^5}{1-\lambda_3} \right| < \left| \frac{-2\lambda_3^4}{1-\lambda_3} \right| \iff |\lambda_3| < 1$$

The case $P(z) = 1$ is satisfied because

$$\begin{aligned} |2f_{\ell+1}(\lambda_3)| < |2f_{\ell}(\lambda_3) + \lambda_3^4(1)| &\iff \left| \frac{-2\lambda_3^5}{1-\lambda_3} \right| < \left| \frac{-\lambda_3^3 - \lambda_3^5}{1-\lambda_3} \right| \\ &\iff |2\lambda_3| < |1 + \lambda_3| \end{aligned}$$

holds by Lemma 4.3.3 part (e.).

Therefore, $\lambda_3 \in \partial\mathcal{M}$ is accessible since all the assumption of Theorem 4.1.3 are satisfied. \square

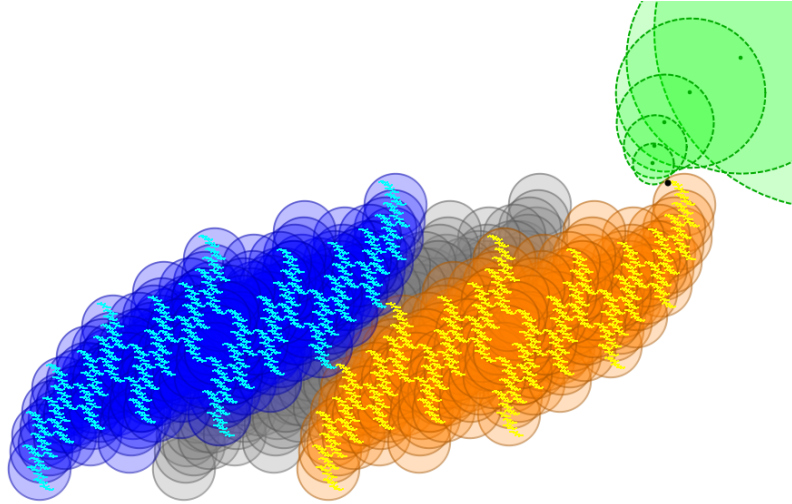


Fig. 4.6. The attractor A_{λ_3} inside $\tilde{\Gamma}^5$. The green discs are part of the chain whose existence is provided by Theorem 4.1.3.

4.3.5 $+ - -00(+)^{\infty}$

Let $\mathbf{c} = c_0c_1 \cdots = + - -00(+)^{\infty} \in \tilde{\Sigma}^{\infty}$ and $f(z) := \sum_{k=0}^{\infty} c_k z^k = \frac{1 - 2z + z^3 + z^5}{1 - z}$. Solomyak proved in [23] that f is the unique power series for which $\lambda_4 \approx 0.643703 +$

0.140749i is a root. Using the notations of Theorem 4.1.3 we have $\ell = 4$, $p = 1$, $n = 0$, and $\zeta = \frac{1}{1-\lambda_4} \in \mathbf{A}_{\lambda_4} \subset \tilde{\mathbf{A}}_{\lambda_4}$ which has itinerary $\mathbf{b} = (+)^\infty$.

We are now ready to prove

Proposition 4.3.5 *The parameter $\lambda_4 \approx 0.643703 + 0.140749i$, root of the rational function $f(z) = (1 - 2z + z^3 + z^5)(1 - z)^{-1}$, is an accessible point of $\partial\mathcal{M}$.*

Proof Observe that since λ_4 is the root of the power series f , we can write

$$\begin{aligned} f_\ell(\lambda_4) &= 1 - \lambda_4 - \lambda_4^2 = -\frac{\lambda_4^5}{1 - \lambda_4}, \\ f_{\ell+1}(\lambda_4) &= 1 - \lambda_4 - \lambda_4^2 + \lambda_4^5 = -\frac{\lambda_4^6}{1 - \lambda_4}, \\ f_{\ell+2}(\lambda_4) &= 1 - \lambda_4 - \lambda_4^2 + \lambda_4^5 + \lambda_4^6 = -\frac{\lambda_4^7}{1 - \lambda_4}. \end{aligned}$$

Condition (i.) in Theorem 4.1.3 is satisfied since

$$|f_{\ell+1}(\lambda_4)| > \frac{1}{2} \frac{|\lambda_4^{\ell+2}|}{1 - |\lambda_4|} \iff \left| \frac{1}{1 - \lambda_4} \right| > \frac{1}{2} \frac{1}{1 - |\lambda_4|} \iff 1 - |\lambda_4| > \frac{1}{2} |1 - \lambda_4|$$

holds by Lemma 4.3.3 part (a.).

Condition (ii.) in Theorem 4.1.3 is satisfied since

$$\begin{aligned} |f_{\ell+1}(\lambda_4)| + |f_{\ell+2}(\lambda_4)| &> \frac{|\lambda_4^{\ell+2}|}{1 - |\lambda_4|} \iff \left| \frac{1}{1 - \lambda_4} \right| + \left| \frac{\lambda_4}{1 - \lambda_4} \right| > \frac{1}{1 - |\lambda_4|} \\ &\iff 1 - |\lambda_4|^2 > |1 - \lambda_4| \end{aligned}$$

holds by Lemma 4.3.3 part (b.).

Condition (iii.) in Theorem 4.1.3 has four cases since the polynomial P can only be either -2 , -1 , 0 , or 1 . The case $P(z) = -2$ is satisfied because

$$\begin{aligned} |2f_{\ell+1}(\lambda_4)| < |2f_\ell(\lambda_4) + \lambda_4^4(-2)| &\iff \left| \frac{-2\lambda_4^5}{1 - \lambda_4} \right| < \left| \frac{-4\lambda_4^4 + 2\lambda_4^5}{1 - \lambda_4} \right| \\ &\iff |\lambda_4| < |2 - \lambda_4| \end{aligned}$$

holds by Lemma 4.3.3 part (c.).

The case $P(z) = -1$ is satisfied because

$$\begin{aligned} |2f_{\ell+1}(\lambda_4)| < |2f_\ell(\lambda_4) + \lambda_4^4(-1)| &\iff \left| \frac{-2\lambda_4^5}{1 - \lambda_4} \right| < \left| \frac{-3\lambda_4^4 + \lambda_4^5}{1 - \lambda_4} \right| \\ &\iff |2\lambda_4| < |3 - \lambda_4| \end{aligned}$$

holds by Lemma 4.3.3 part (d.).

The case $P(z) = 0$ is trivial since

$$|2f_{\ell+1}(\lambda_4)| < |2f_{\ell}(\lambda_4) + \lambda_4^4(0)| \iff \left| \frac{-2\lambda_4^5}{1-\lambda_4} \right| < \left| \frac{-2\lambda_4^4}{1-\lambda_4} \right| \iff |\lambda_4| < 1$$

The case $P(z) = 1$ is satisfied because

$$\begin{aligned} |2f_{\ell+1}(\lambda_4)| < |2f_{\ell}(\lambda_4) + \lambda_4^4(1)| &\iff \left| \frac{-2\lambda_4^5}{1-\lambda_4} \right| < \left| \frac{-\lambda_4^3 - \lambda_4^5}{1-\lambda_4} \right| \\ &\iff |2\lambda_4| < |1 + \lambda_4| \end{aligned}$$

holds by Lemma 4.3.3 part (e.).

Therefore, $\lambda_4 \in \partial\mathcal{M}$ is accessible since all the assumption of Theorem 4.1.3 are satisfied. \square

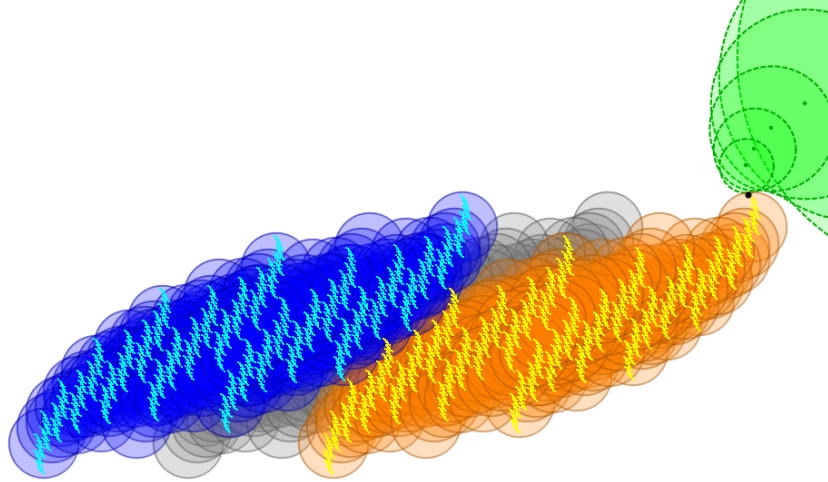


Fig. 4.7. The attractor A_{λ_4} inside $\tilde{\mathcal{I}}^5$. The green discs are part of the chain whose existence is provided by Theorem 4.1.3.

4.4 Thunderstorm in No Man's Land.

In this section we describe a method of proving that an accessible parameter is on the boundary of the component of $\mathbb{D} \setminus \mathcal{M}$ containing 0. Even though we work with a specific parameter $\lambda \in \mathcal{M}$, the idea applies to other accessible parameters.

“No Man’s Land” is the name that Barnsley [14] gave to the largest region \mathbf{H}_0 of the unit disc not in \mathcal{M} . “Thunderstorm” refers to how we prove that an accessible parameter λ is accessible from 0, by constructing “rays” connecting the origin to $\lambda \in \partial\mathcal{M}$.

We will show the following

Proposition 4.4.1 (Pérez-Silvestri) *Let $\lambda_0 \approx -0.366+0.520i$ be the root of $f(z) = 1 + z + z^2 - 2z^3$ then λ_0 is on the boundary \mathbf{H}_0 .*

The proof is structured as follows: in Section 4.4.1 we see how the algebraic nature of λ_0 implies it lies on an infinite system of curves through 0. In Section 4.4.2 we describe the instars of λ_0 at level 1 and 2. In Section 4.4.3 we run Algorithm 1 on λ_0 , and describe the stack contents at each level so that in Section 4.4.4, we may show that a particular segment in each of these curves is in \mathbf{H}_0 . Finally, in Section 4.4.5 we will piece these segments together, thus concluding the proof. We need to remark that there is a technical issue in this last step that remains unfinished. However, we are confident that it is manageable by direct computation.

Note that the parameter λ_0 is one of the landmark points considered in Section 4.3; it should be possible to obtain the same result for the other landmark points with a similar construction. The key property used in the proof is an alignment condition obtained by the fact that the itinerary of λ_0 is preperiodic with preperiod 1. It seems clear that this property is closely connected to membership in $\mathcal{M}_0 \cap \partial\mathbf{H}_0$, but an explicit characterization has not been found.

4.4.1 Alignment Condition

We construct an infinite collection of curves (*rays*) connecting 0 to λ_0 . The function $f(z) = \frac{1+z+z^2-2z^3}{1-z^3}$ has the following power series

$$\frac{(1 - z^3) + (z + z^2 - z^3)}{1 - z^3} = 1 + z + z^2 - z^3 + z^4 + z^5 - z^6 + z^6 + z^8 - z^9 + \dots \quad (*)$$

Since $f(\lambda_0) = 0$, we find that $\lambda_0 \in \mathcal{M}_0$. Moreover, since $(1-z^{3k})f(z) = f_{3k-1}(z) - 2z^{3k}$ for every integer $k \geq 0$, it follows that λ_0 is a root of each polynomial $f_{3k-1}(z) - 2z^{3k}$ (where $f_{3k-1}(z)$ is a truncation of $(*)$).

The geometrical interpretation is that, in the instar \mathbb{I}^{3k} , the nodal discs with centers $\pm f_{3k-1}(\lambda_0) \pm \lambda_0^{3k}$, are aligned and equidistant (see Fig 4.8). Let us define the expressions

$$\Xi_k(z) := \frac{f_{3k-1}(z)}{z^{3k}},$$

so that $\Xi_k(\lambda_0) = 2$ for all $k \geq 1$. This allows us to consider the level curves $\text{Im}(\Xi_k(z)) = 0$ (see Fig 4.9).

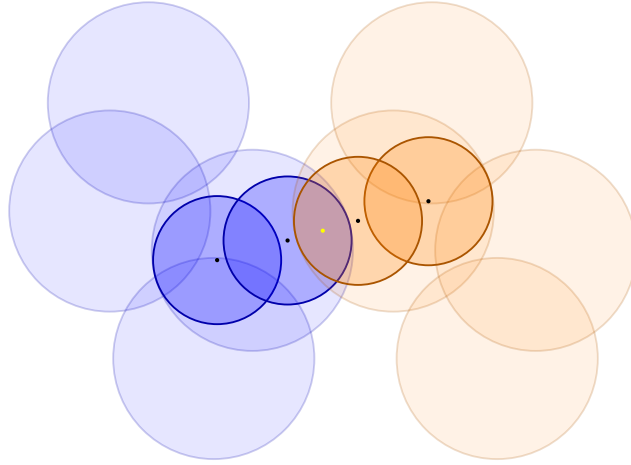


Fig. 4.8. In the background is \mathbb{I}^2 . Highlighted are the nodal discs of level 3 with centers $\pm f_2(\lambda_0) \pm \lambda_0^3$. The origin is colored in yellow.

For a fixed $k \geq 1$, the set of $z \in \mathbb{C}$ such that $\text{Im}(\Xi_k(z)) = 0$ consists of all those curves whose image under Ξ_k is the real line.

Lemma 4.4.1 *For a fixed $k \geq 1$, $\Xi_k^{-1}(\overline{\mathbb{R}}) = \bigcup_{j=1}^{3k} K_j$ where K_j are curves containing the origin.*

Proof Observe that Ξ_k has a single pole of order $3k$ at 0. Hence, $\infty \in \overline{\mathbb{R}}$ has only one preimage with multiplicity $3k$. Therefore, the origin must be in each K_j for every j , since $\Xi_k(K_j) = \overline{\mathbb{R}}$. \square

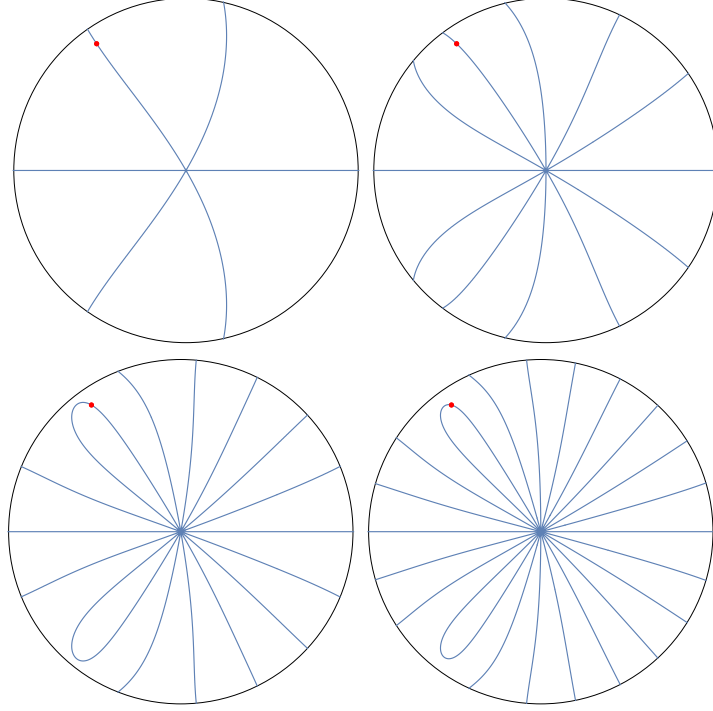


Fig. 4.9. Plots of the level curves $\text{Im}(\Xi_k(z)) = 0$ inside the disc of radius $2^{-1/2}$ for $k = 1, 2, 3, 4$. The parameter λ_0 is drawn in red.

We are only interested in the component \mathcal{C}^k of the level curve that contains λ_0 and, furthermore, in the segment \mathcal{R}^k connecting 0 and λ_0 .

Observe that the level curves are easily rewritten in polar coordinates: let $z = re^{i\theta}$ with $r \neq 0$, then for $k = 1$ we have

$$\begin{aligned} \text{Im}(\Xi_2(z)) &= \text{Im}\left(\frac{1+z+z^2}{z^3}\right) = -\frac{1}{r^3}\sin(3\theta) - \frac{1}{r^2}\sin(2\theta) - \frac{1}{r}\sin(\theta) = 0 \\ \implies \sin(3\theta) + r\sin(2\theta) + r^2\sin(\theta) &= 0; \end{aligned}$$

and in general for $k \geq 1$

$$\text{Im}(\Xi_k(z)) = 0 \implies \sum_{j=0}^{3k-1} c_j r^j \sin((3k-j)\theta) = 0.$$

where the c_j are the coefficients of the polynomial $f_{3k-1}(z)$ which are described by the entries in the itinerary $\mathbf{c} = ++-^\infty$.

Notice that z lying on the level curve \mathcal{C}^k for some $k \geq 1$ implies that it satisfies the equation $f_{3k-1}(z) = Cz^{3k}$ with $C \in \mathbb{R}$. Also $C = 2$ if and only if $z = \lambda_0$, while $C \rightarrow +\infty$ forces $z \rightarrow 0$. The value of C is a measure of overlap between the symmetric discs $D^{c|3k-1}$ and $D^{\bar{c}|3k-1}$: recall that the radius of a nodal disc of level $3k - 1$ for a parameter z is $|z^{3k}|R$, therefore, if $z \in \mathcal{C}^k$ and we look at the ratio of the distance of the centers with the sum of the radii of the two symmetric nodal discs, we obtain

$$\frac{2|f_{3k-1}(z)|}{2|z^{3k}|R} = \frac{C|z^{3k}|}{|z^{3k}|}(1 - |z|) = C(1 - |z|).$$

If the above ratio is greater than 1 (which definitely occurs whenever $C > 3$ since $|z| < 2/3$), we have that the nodal discs do not intersect; if it is equal to 1 they intersect exactly at one point on their boundary, i.e. the origin; otherwise the nodal discs intersect. Hence, we define the ray to be

$$\mathcal{R}^k := \{z \in \mathcal{C}^k \mid \exists C \in [2, \infty) \text{ such that } f_{3k-1}(z) = Cz^{3k}\}.$$

We remark that due to the spiraling structure of $\partial\mathcal{M}$ at λ_0 , the rays \mathcal{R}^k have to intersect \mathcal{M} infinitely often. In particular, we have not yet excluded the possibility that λ_0 is on the boundary of some hole other than \mathbf{H}_0 . To resolve this issue, for each $k \geq 1$, we will consider only the segment of \mathcal{R}^k where we can guarantee that the instar at level $3k - 1$ is disconnected. Then we will argue that the segments in \mathcal{R}^k and \mathcal{R}^{k+1} can be connected by another curve lying completely in \mathbf{H}_0 .

4.4.2 Shape Conditions at λ_0

Let us describe in detail the level 1 and 2 instars for λ_0 . At level 1, D^{++} and D^{--} intersect all other discs, but $D^{-+} \cap D^{+-} = \emptyset$. We call this configuration a “cloud”. The instar of level 2 consists of two cloud copies, N^- and N^+ . Now,

$$|\nu_{+++} - \nu_{---}| = 2|1 + \lambda_0 + \lambda_0^2| = 2|2\lambda_0^3| < \frac{2|\lambda_0^3|}{1 - |\lambda_0|}$$

since $|\lambda_0| < \frac{2}{3}$, which can be interpreted as saying that D^{+++} and D^{---} intersect. It is similarly straightforward to compute, using the rough bounds $\frac{\sqrt{5}-1}{2} < |\lambda_0| < \frac{2}{3}$ and $\arg(\lambda_0) \in (2\pi/3, 23\pi/32)$,

$$\begin{aligned} |\nu_{+++} - \nu_{--+}| &= 2|1 + \lambda_0^2| > \frac{2|\lambda_0^3|}{1 - |\lambda_0|} \\ |\nu_{+++} - \nu_{-++}| &= 2|1| > \frac{2|\lambda_0^3|}{1 - |\lambda_0|} \\ |\nu_{+++} - \nu_{--+}| &= 2|1 + \lambda_0| > \frac{2|\lambda_0^3|}{1 - |\lambda_0|} \\ |\nu_{++-} - \nu_{-++}| &= 2|1 - \lambda_0^2| > \frac{2|\lambda_0^3|}{1 - |\lambda_0|} \\ |\nu_{++-} - \nu_{--+}| &= 2|1 + \lambda_0 - \lambda_0^2| > \frac{2|\lambda_0^3|}{1 - |\lambda_0|} \end{aligned}$$

which say that no other discs of N^- intersect N^+ (and viceversa).

By the self-similarity (Lemma 4.2.1), this exact intersection configuration will repeat locally every third level; i.e. there are two clouds near 0 (subsets of the positive and negative instars), that intersect only at one disc. See Fig. 4.10.

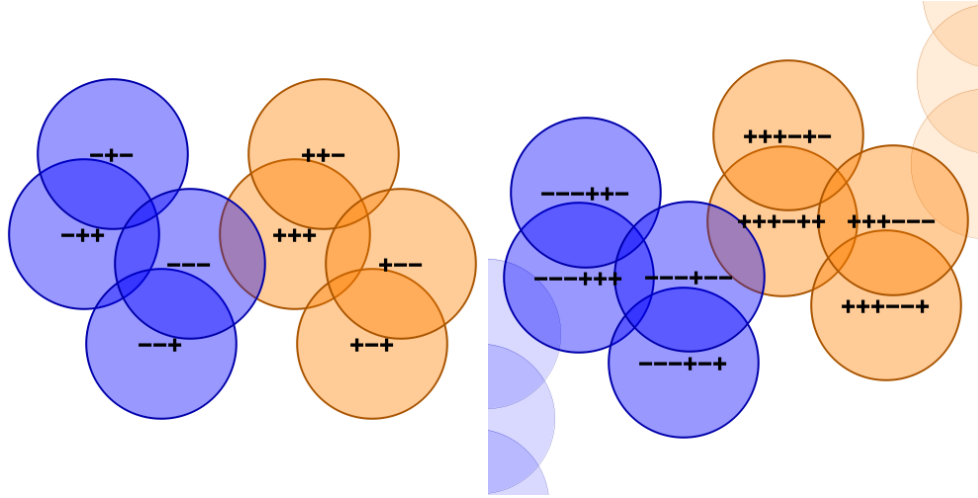


Fig. 4.10. Local picture around the origin of l^2 and l^5 for the parameter λ_0 . The cloud N^- is highlighted in blue, while N^+ is in orange.

4.4.3 Stack Contents of the Disconnectivity Algorithm

A stronger statement is true, because the intersection conditions are exactly the same at every third level. This is the *main property* that allows an iterative argument to proceed. Since $\mathcal{F}_{\lambda_0} = \{f\}$, and the coefficients of f are eventually periodic, the elements in the stack in Algorithm 1 will (eventually) repeat.

This seems surprising at first, since one could expect successive stack entries to consist of ever more complicated expressions in λ_0 . However, let us run the algorithm at λ_0 , starting at level $3j$ (for $j \geq 0$) and tabulate the contents of the stack. In the diagram of Fig. 4.4.3 we show exactly what are these entries and we indicate which nodal disc-intersection is responsible for a particular entry. The fact that $f_{3j}(\lambda_0) = \lambda_0^{3j}$ make it so that the entries in the stack are exactly the same every three levels.

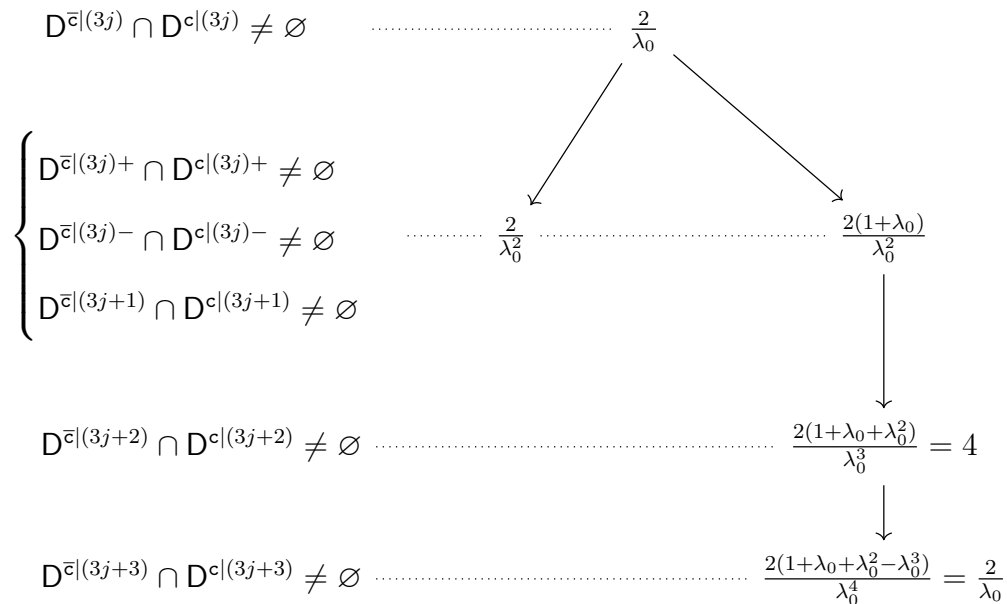


Fig. 4.11. Diagram representing how the stack entries change as we run Algorithm 1 for λ_0 . The integer $j \geq 0$ also indicates the level of the stack.

4.4.4 Different Shapes

Let us now compare the structure of the level 2 instars of λ_0 and three other nearby parameters. Let η_j be the (local) root of $1 + z + z^2 - C_j z^3$ for $C_j = 3, \frac{1}{2}(3 - i), (\frac{7}{5} + i)$, so that $\eta_1 = \frac{1}{3}(-1 + \sqrt{2}i)$, $\eta_2 \approx -0.427 + 0.524i$, $\eta_3 \approx -0.304 + 0.588i$ (see Fig. 4.12).

- a.) The positive and negative instars λ_0 are connected only through the overlap D^{+++} and D^{---} .
- b.) Since $C_1 \in \mathbb{R}$, η_1 is on the ray \mathcal{R}^1 , implying that the discs D^{++++} , D^{+++} , and D^{---+}, D^{----} are aligned. However, $D^{+++} \cap D^{---} = \emptyset$, and, in fact, the positive and negative instars are completely disjoint.
- c.) The values C_2 and C_3 are not real, so $\eta_2, \eta_3 \notin \mathcal{R}^1$. The discs D^{+++} and D^{---} intersect, though. However, the instar structures are different than the λ_0 case because η_2 exhibits the extra intersection of D^{+++} with D^{--+} , while η_3 exhibits the extra intersection of D^{+++} with D^{-+-} .

In order to capture the notion of local shape similarity as parameters approach λ_0 , let us consider the lines through the node ν_{-++} with direction vectors connecting ν_{-++} to ν_{--+} , and ν_{-++} to ν_{+++} :

$$\begin{aligned} \mathcal{L}_{-\lambda_0} &= \left\{ z \in \mathbb{C} \mid \operatorname{Im} \left(\frac{z - \nu_{-++}}{\nu_{--+} - \nu_{-++}} \right) = 0 \right\} = \left\{ z \in \mathbb{C} \mid \operatorname{Im} \left(\frac{z - \nu_{-++}}{-2\lambda_0} \right) = 0 \right\} \\ \mathcal{L}_{\lambda_0^2} &= \left\{ z \in \mathbb{C} \mid \operatorname{Im} \left(\frac{z - \nu_{-++}}{\nu_{+++} - \nu_{-++}} \right) = 0 \right\} = \left\{ z \in \mathbb{C} \mid \operatorname{Im} \left(\frac{z - \nu_{-++}}{2\lambda_0^2} \right) = 0 \right\} \end{aligned}$$

Each line determines a left half-plane in which the node ν_{+++} lies. Thus we can interpret the inequalities

$$\begin{aligned} \operatorname{Im} \left(\frac{\nu_{+++} - \nu_{-++}}{-2\lambda_0} \right) &= \operatorname{Im} \left(\frac{f_0(\lambda_0)}{-\lambda_0} \right) > 0, \\ \operatorname{Im} \left(\frac{\nu_{+++} - \nu_{-++}}{2\lambda_0^2} \right) &= \operatorname{Im} \left(\frac{f_0(\lambda_0)}{\lambda_0^2} \right) > 0, \end{aligned}$$

as describing the relative orientations of the instars l^2 positive and negative clouds.

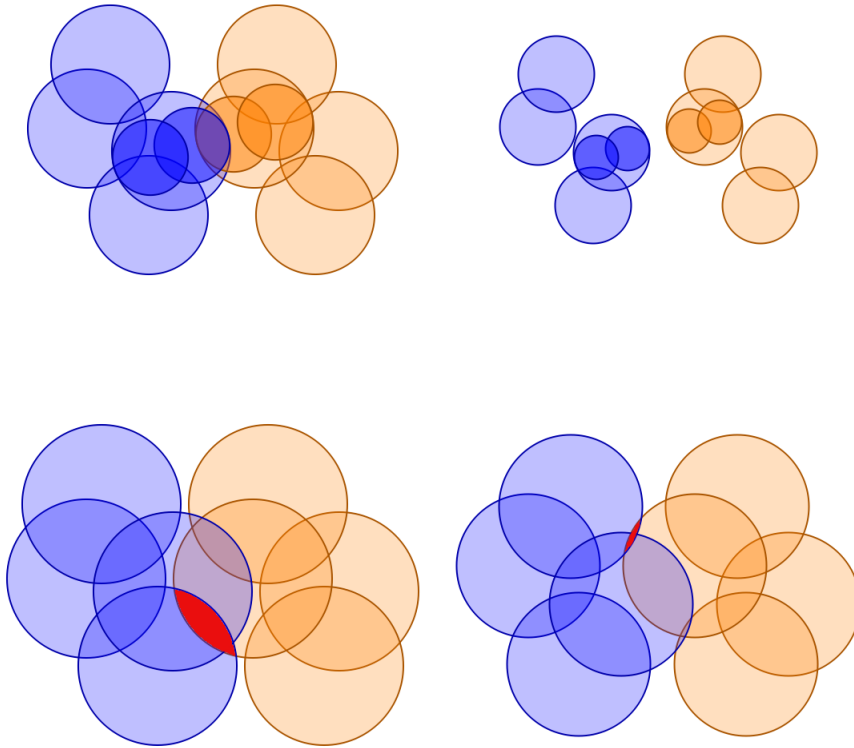


Fig. 4.12. The instar at level 2 for λ_0 (top left), η_1 (top right), η_2 (bottom left), and η_3 (bottom right). The extra intersections are highlighted in red. For λ_0 and η_1 the aligned nodal discs of the next level are also drawn.

The condition for D^{+++} not to intersect the discs D^{-+-} , D^{-++} , or D^{--+} can be written as

$$\begin{aligned}
 |\nu_{+++} - \nu_{--+}| &= 2|1 + \lambda_0^2| > \frac{2|\lambda_0^3|}{1 - |\lambda_0|} \\
 |\nu_{+++} - \nu_{-++}| &= 2|1| > \frac{2|\lambda_0^3|}{1 - |\lambda_0|} \\
 |\nu_{+++} - \nu_{-+-}| &= 2|1 + \lambda_0| > \frac{2|\lambda_0^3|}{1 - |\lambda_0|}
 \end{aligned}$$

As previously mentioned, this arrangement of nodal discs around 0 repeats every three levels. This suggests describing the local shape for other parameters λ in terms of these lines:

$$\begin{aligned}\mathcal{L}_{-\lambda^{3k-2}} &= \left\{ z \in \mathbb{C} \mid \operatorname{Im} \left(\frac{z - \nu_{\bar{c}|(3k-3)++}}{\nu_{\bar{c}|(3k-3)-+} - \nu_{\bar{c}|(3k-3)++}} \right) = 0 \right\} \\ &= \left\{ z \in \mathbb{C} \mid \operatorname{Im} \left(\frac{z - \nu_{\bar{c}|(3k-3)++}}{-2\lambda^{3k-2}} \right) = 0 \right\}\end{aligned}$$

$$\begin{aligned}\mathcal{L}_{\lambda^{3k-1}} &= \left\{ z \in \mathbb{C} \mid \operatorname{Im} \left(\frac{z - \nu_{\bar{c}|(3k-3)++}}{\nu_{\bar{c}|(3k-3)++} - \nu_{\bar{c}|(3k-3)+-}} \right) = 0 \right\} \\ &= \left\{ z \in \mathbb{C} \mid \operatorname{Im} \left(\frac{z - \nu_{\bar{c}|(3k-3)++}}{2\lambda^{3k-1}} \right) = 0 \right\}.\end{aligned}$$

where $\mathbf{c} = +(+ + -)^\infty$ is the itinerary associated to λ_0 .

Now, for a point $\lambda \in \mathcal{R}^k$ we want that, around 0, the arrangements of the nodal discs at level $3k - 1$ resemble the one of λ_0 . The lemma below assumes that λ belongs to the ray \mathcal{R}^k , and proves that the local clouds are oriented correctly with respect to each other **(i.,iii.)**, and that they display no intersections that are not present in A_{λ_0} **(ii.,iv.)**.

Then we prove

Lemma 4.4.2 *Fix $k \geq 1$ and suppose that $f_{3k-1}(\lambda) = C\lambda^{3k}$, i.e. that $\lambda \in \mathcal{R}^k$, and $C > (1 - |\lambda|)^{-1}$. Then the following are satisfied:*

- (i.)** *the left half plane determined by $\mathcal{L}_{-\lambda^{3k-2}}$ contains the node $\nu_{\mathbf{c}|(3k-1)}$;*
- (ii.)** *the discs $D^{\mathbf{c}|(3k-1)}$ and $D^{\bar{\mathbf{c}}|(3k-3)+-}$ do not intersect;*
- (iii.)** *the left half plane determined by $\mathcal{L}_{\lambda^{3k-1}}$ contains the node $\nu_{\mathbf{c}|(3k-1)}$;*
- (iv.)** *the nodal discs $D^{\mathbf{c}|(3k-1)}$ and $D^{\bar{\mathbf{c}}|(3k-3)-+}$ do not intersect.*

Proof The equation $f_{3k-1}(\lambda) = C\lambda^{3k}$ allows us to rewrite each node as follows:

$$\begin{aligned}\nu_{\mathbb{c}|(3k-1)} &= C\lambda^{3k} \\ \nu_{\mathbb{c}|(3k-3)-+} &= 2\lambda^{3k-1} - C\lambda^{3k} \\ \nu_{\mathbb{c}|(3k-3)++} &= 2\lambda^{3k-2} + 2\lambda^{3k-1} - C\lambda^{3k} \\ \nu_{\mathbb{c}|(3k-3)+-} &= 2\lambda^{3k-2} - C\lambda^{3k}\end{aligned}$$

The node $\nu_{\mathbb{a}|(3k-1)}$ belongs to the left half plane defined by the directed line $\mathcal{L}_{-\lambda^{3k-2}}$ if

$$\operatorname{Im}\left(\frac{\nu_{\mathbb{c}|(3k-1)} - \nu_{\mathbb{c}|(3k-3)++}}{-2\lambda^{3k-2}}\right) = \operatorname{Im}(1 + \lambda - C\lambda^2) = \operatorname{Im}(\lambda - C\lambda^2) > 0.$$

The above inequality is equivalent to

$$|\lambda| \sin(\theta) - C|\lambda^2| \sin(2\theta) > 0 \iff 1 - 2C|\lambda| \cos(\theta) > 0$$

which is always satisfied as $\theta = \arg(\lambda) \in (2\pi/3, 23\pi/32)$. Thus, **(i.)** is proved.

The trivial intersection of the discs $\mathbb{D}^{\mathbb{c}|(3k-1)}$ and $\mathbb{D}^{\mathbb{c}|(3k-3)-+}$ is given by the inequality

$$|\nu_{\mathbb{c}|(3k-1)} - \nu_{\mathbb{c}|(3k-3)-+}| = 2|\lambda^{3k-1}| |1 - C\lambda| > 2\frac{|\lambda^{3k}|}{1 - |\lambda|} \iff |1 - C\lambda| > \frac{|\lambda|}{1 - |\lambda|}$$

By the Law of Cosines and the fact that $1 - 2C|\lambda| \cos(\theta) > 0$

$$|1 - C\lambda| = \sqrt{1 + C^2|\lambda|^2 - 2C|\lambda| \cos(\theta)} > C|\lambda| > \frac{|\lambda|}{1 - |\lambda|}$$

where the last inequality is true by assumption. Hence, **(ii.)** is proved.

The node $\nu_{\mathbb{c}|(3k-1)}$ lies in the left half plane defined by the directed line $\mathcal{L}_{-\lambda^{3k-2}}$ if

$$\operatorname{Im}\left(\frac{\nu_{\mathbb{c}|(3k-1)} - \nu_{\mathbb{c}|(3k-3)++}}{2\lambda^{3k-1}}\right) = \operatorname{Im}\left(-\frac{1}{\lambda} - 1 + C\lambda\right) = \operatorname{Im}\left(-\frac{1}{\lambda} + C\lambda\right) > 0.$$

Since $\operatorname{Im}(\lambda) > 0$, then

$$-\operatorname{Im}\left(\frac{1}{\lambda}\right) + C\operatorname{Im}(\lambda) = \frac{1}{|\lambda|^2}\operatorname{Im}(\lambda) + C\operatorname{Im}(\lambda) > 0 \iff C > -\frac{1}{|\lambda|^2}$$

which is clearly true as C is positive. Thus, **(iii.)** is proved.

The trivial intersection of the discs $D^{c|(3k-1)}$ and $D^{\bar{c}|(3k-3)+}$ is given by the inequality

$$|\nu_{c|(3k-1)} - \nu_{\bar{c}|(3k-3)+}| = 2|\lambda^{3k-2}| |1 - C\lambda^2| > 2\frac{|\lambda^{3k}|}{1 - |\lambda|} \iff |1 - C\lambda^2| > \frac{|\lambda^2|}{1 - |\lambda|}$$

Using the Law of Cosines again

$$\begin{aligned} |1 - C\lambda^2| &= \sqrt{1 + C^2 |\lambda^2|^2 - 2C |\lambda^2| \cos(2\pi - 2\theta)} = \sqrt{1 + C^2 |\lambda|^4 - 2C |\lambda|^2 \cos(2\theta)} \\ &= \sqrt{1 + C^2 |\lambda|^4 + 2C |\lambda|^2 - 4C |\lambda|^2 \cos^2(\theta)} \\ &> \sqrt{1 + C^2 |\lambda|^4} > \sqrt{1 + \left(\frac{|\lambda|^2}{1 - |\lambda|}\right)^2} > \frac{|\lambda^2|}{1 - |\lambda|}. \end{aligned}$$

The first inequality in the last line is true because $-\cos^2(\theta) > -1/2$. Hence, **(iv.)** is proved. \square

4.4.5 Proof of the Proposition

Lemma 4.4.2 is the key idea needed to obtain Proposition 4.3.1. When $k = 1$, for parameters $\lambda \in \mathcal{R}^1$ satisfying $f_2(\lambda) = C\lambda^3$ with $C > (1 - |\lambda|)^{-1}$, we can guarantee that the instar at level $3k - 1 = 2$ is disconnected, and hence, $\lambda \in \mathbf{H}_0$. Once $C = (1 - |\lambda|)$, the discs $D^{c|(3k-1)}$ and $D^{\bar{c}|(3k-1)}$ are tangent at 0, which still guarantees $\lambda \in \mathbf{H}_0$. At this point we want to connect to the next level curve, \mathcal{R}^2 .

Remember that $\lambda \in \mathcal{R}^k$ implies that certain nodal discs have their centers on the line through the origin which makes an angle of $\arg(\lambda^{3k})$ with the real axis. The node $\nu_{c|3k+2}$ is inside $D^{c|3k-1}$ and it is in between the lines through the origin which make an angle of $\arg(\lambda^{3k})$ and $\arg(\lambda^{3k+3})$ with the real axis. The points in parameter plane on the curve $\mathcal{C}^{\dagger,k} := \{z \in \mathbb{D} \mid |f_{3k-1}(z)| = |z^{3k}|(1 - |z|)^{-1}\}$ satisfy the tangency condition of the discs $D^{c|(3k-1)}$ and $D^{\bar{c}|(3k-1)}$.

Conjecture 1 *The segment of the curve $\mathcal{C}^{\dagger,k}$ connecting \mathcal{R}^k to \mathcal{R}^{k+1} is in \mathbf{H}_0 .*

Assume the above conjecture is true, and let $\lambda \in \mathcal{R}^{k+1} \cap \mathcal{C}^{\dagger,k}$. Then we claim that the discs $D^{c|(3k+2)}$ and $D^{\bar{c}|(3k+2)}$ are disconnected. If that were not the case, then it would

imply that at level $3k - 1$ there was a non-trivial intersection of the disc $D^{c|(3k-1)}$ and $D^{\bar{c}|(3k-1)}$ contradicting the fact $\lambda \in \mathcal{C}^{\dagger,k}$. Consequently, $\lambda \in \mathcal{R}^{k+1} \cap \mathcal{C}^{\dagger,k}$ satisfies $f_{3k+2}(\lambda) = C\lambda^{3k+3}$ with $C > (1 - |\lambda|)^{-1}$ and Lemma 4.4.2 applies. It follows that $\lambda \in \mathbf{H}_0$.

The proof is therefore complete.

4.5 Connection to Quadratic Dynamics

We end this chapter by describing a fruitful connection between our family of IFS to the quadratic family $z^2 + c$. It is a widely believed, but still open question, to decide whether this connection applies exactly to all parameters in $\partial\mathcal{M} \cap \partial\mathcal{M}_0$. This will only be an overview of known results, and the exposition will follow [11] very closely.

We restrict our attention to those parameters $\lambda \in \mathcal{M}$ for which $O_\lambda = \{0\}$:

$$\mathcal{T} := \{\lambda \in \mathcal{M} \mid |O_\lambda| = 1\}.$$

Lemma 3.4.1 gives that if $\lambda \in \mathcal{T}$, then \mathcal{F}_λ is a singleton $\{f\}$ where the coefficients of f are all nonzero. Consequently, $\mathcal{T} \subset \mathcal{M}_0$. For these parameters λ , A_λ is known to be a *dendrite*, a connected, locally connected, nowhere dense compact set in the plane with connected complement. Bandt [9] observed that it is possible to define quadratic-like dynamics on A_λ for parameters in \mathcal{T} . In this way, from a theorem of Kameyama [27], there exists a conjugacy of this dynamics with the one of $z^2 + c$ for some parameter c .

Observe that A_λ is invariant under $h(z) = -z$. Abusing notation, h flips the signs in $\{-, +\}$ of the itinerary for each point in the attractor. Define on A_λ the piecewise map

$$q_\lambda(z) = \begin{cases} \mathfrak{s}_+^{-1}(z) & z \in A_\lambda^+ \\ (h \circ \mathfrak{s}_-^{-1})(z) & z \in A_\lambda^- \end{cases} = \begin{cases} \frac{z-1}{\lambda} & z \in A_\lambda^+ \\ -\frac{z+1}{\lambda} & z \in A_\lambda^- \end{cases}$$

then q_λ is a well-defined, 2-to-1 map on A_λ that is a local homeomorphism everywhere but at $0 \in O_\lambda$. In fact, the attractor of the IFS $\{\mathfrak{s}_+, \mathfrak{s}_- \circ h\}$ is again A_λ . In terms

of itineraries, q_λ induces as a left shift or a shift-and-a-flip, depending on the first symbol. Recalling from Section 3.1 the definition of the projection $\pi_\lambda : \Sigma^\infty \rightarrow \mathbf{A}_\lambda$, for any word $\mathbf{w} = w_0 w_1 w_2 \cdots \in \Sigma^\infty$

$$q_\lambda(\pi_\lambda(\mathbf{w})) = \begin{cases} \pi_\lambda(\sigma(\mathbf{w})) & \text{if } w_0 = + \\ \pi_\lambda(h(\sigma(\mathbf{w}))) = \pi_\lambda(\sigma(h(\mathbf{w}))) & \text{if } w_0 = - \end{cases}$$

We associate to λ a combinatorial invariant defined as the address of $q_\lambda(0)$ with respect to the partition $\{\{0\}, \mathbf{A}_\lambda^+ \setminus \{0\}, \mathbf{A}_\lambda^- \setminus \{0\}\}$. Assign 0, 1, and \star to $\mathbf{A}_\lambda^- \setminus \{0\}$, $\mathbf{A}_\lambda^+ \setminus \{0\}$, $\{0\}$ respectively. Then if the orbit of $w \in \mathbf{A}_\lambda$ does not come back to 0, we define the address $e(w) = e_0 e_1 \cdots$ of $w = \sum_{j \geq 0} a_j \lambda^j$ recursively as

$$e_0 = a_0 \quad \text{and} \quad e_n = \begin{cases} 1 & a_n \neq a_{n-1}, \\ 0 & a_n = a_{n-1} \end{cases}.$$

The *kneading sequence* $\kappa = \kappa_\lambda$ is the address of $q_\lambda(0)$:

$$\kappa = \kappa_1 \kappa_2 \cdots \quad \text{where} \quad \kappa_n = \begin{cases} e_{n-1}(q_\lambda(0)) & q_\lambda(0) \in \mathbf{A}_\lambda^+ \\ 1 - e_{n-1}(q_\lambda(0)) & q_\lambda(0) \in \mathbf{A}_\lambda^- \end{cases}.$$

Note that by definition, the kneading sequence will always start with 1. Bandt and Rao [24] showed that when $\lambda \in \mathcal{T}$, the orbit of 0 is non-recurrent, so κ is a well-defined sequence in $\{0, 1\}^\infty$.

On the other hand, given a sequence κ in $\{0, 1\}^\infty$, we can obtain a power series $f(z) = \sum_{n \geq 0} a_n z^n$ by

$$a_n = \begin{cases} (-1)^{|\{1 \leq i \leq n \mid \kappa_i = 1\}|} & q_\lambda(0) \in \mathbf{A}_\lambda^+ \\ (-1)^{|\{1 \leq i \leq n \mid \kappa_i = 0\}|} & q_\lambda(0) \in \mathbf{A}_\lambda^- \end{cases}.$$

Note that by [28] the power series so obtained, will have at most one root in the top half of the disc $D_{2^{-1/2}}$. Consequently, the kneading sequence determines a unique $\lambda \in \mathcal{M}_0$.

In the quadratic setting, let $p_c(z) = z^2 + c$, and define the (filled) Julia set for a fixed c to be $J_c = \{z \in \mathbb{C} \mid |p_c^n(z)| \leq 2\}$. If J_c is a dendrite then it is possible (using

external rays) to create a partition $J_c = \{0\} \cup J^0 \cup J^1$ such that $p_c(0) \in J^1$. The kneading sequence of p_c is defined as the address of $p_c(0) = c$.

Proposition 4.5.1 (Eroğlu-Rohde-Solomyak [11]) *Suppose $\lambda \in \mathcal{T}$ and $c \in \mathbb{C}$ is a parameter such that J_c is a dendrite. If the kneading sequences of q_λ and p_c are identical, then the systems (A_λ, q_λ) and (J_c, p_c) are topologically conjugate: there exists a homeomorphism $\varphi : J_c \rightarrow A_\lambda$ such that the following diagram commutes*

$$\begin{array}{ccc} J_c & \xrightarrow{p_c} & J_c \\ \downarrow \varphi & & \downarrow \varphi \\ A_\lambda & \xrightarrow{q_\lambda} & A_\lambda \end{array}$$

This result was later extended by Pilgrim and Haïssinski.

Definition 4.5.1 *A homeomorphism φ between metric spaces (X, d_X) and (Y, d_Y) is quasisymmetric if there is a homeomorphism $\eta : [0, \infty) \rightarrow [0, \infty)$ such that for every $t > 0$ and $a, b, x \in X$,*

$$d_X(a, x) \leq t d_X(b, x) \text{ implies } d_Y(\varphi(a), \varphi(x)) \leq \eta(t) d_Y(\varphi(b), \varphi(x)).$$

Theorem 4.5.1 (Pilgrim-Haïssinski [12]) *Suppose $\lambda \in \mathcal{T}$ and $c \in \mathbb{C}$ is a parameter such that J_c is a dendrite. If the kneading sequences of q_λ and p_c are identical, then the systems (A_λ, q_λ) and (J_c, p_c) are quasisymmetrically conjugate.*

As pointed out in [11], not all dendritic Julia set (i.e. those corresponding to a Misiurewicz parameter c) have a corresponding attractor A_λ . As an example, let $c = i$, then we obtain the kneading sequence $1(10)^\infty$ (from the external ray of angle $\frac{1}{6}$ landing at 0), which gives the power series $(1 - z + z^2)(1 + z^2)^{-1}$. The roots are $\lambda = 4^{-1}(1 \pm \sqrt{7}i)$, but A_λ is not a dendrite, as we have seen at the end of Chapter 3.

The landmark points λ_j for $j = 0, 1, 2$, discussed in Section 4.3, are all elements of \mathcal{T} . Hence, there is a parameter $c_j \in \mathbb{C}$ such that $(A_{\lambda_j}, q_{\lambda_j})$ is quasisymmetrically conjugate to (J_{c_j}, p_{c_j}) .

- The itinerary of 0 for $\lambda_0 \approx 0.366 + 0.52i$ is $+(-++--)^{\infty}$. Thus, the kneading sequence is $1(100)^\infty$, to which we can associate the external ray with angle $\frac{3}{14}$. This lands at $c \approx -0.1558 + 1.112i$.

- The itinerary of 0 for $\lambda_1 \approx 0.596 + 0.254i$ is $+ - -(+)^{\infty}$. Thus, the kneading sequence is $101(0)^{\infty}$, to which we can associate the external ray with angle $\frac{3}{8}$. This lands at $c \approx -1.296 + 0.442i$.
- The itinerary of 0 for $\lambda_2 \approx 0.636 + 0.107i$ is $+ - - -(+)^{\infty}$. Thus, the kneading sequence is $1001(0)^{\infty}$, to which we can associate the external ray with angle $\frac{7}{16}$. This lands at $c \approx -1.771 + 0.066i$.

Pictures of these sets are in Fig 4.13.

From the discussion above, is clear that there is the question of which kneading sequences are admissible for such $\lambda \in \partial\mathcal{M}_0$. Future work will investigate further this issue, as a lot more is known (see [29]) about the admissible kneading sequences for Misiurewicz parameters and the topology of their associated Hubbard tree. In particular, it was pointed out by Henk Bruin that for all the examples above, the α -fixed points of A_{λ} have three arms, and there are no other periodic branch points. Furthermore, the critical value $q_{\lambda}(0)$ is always an endpoint of A_{λ} . The latter remark is indeed true in the case $\lambda \in \mathcal{T}$ is accessible and $0 \in A_{\lambda}$ has a preperiodic itinerary with preperiod 1.

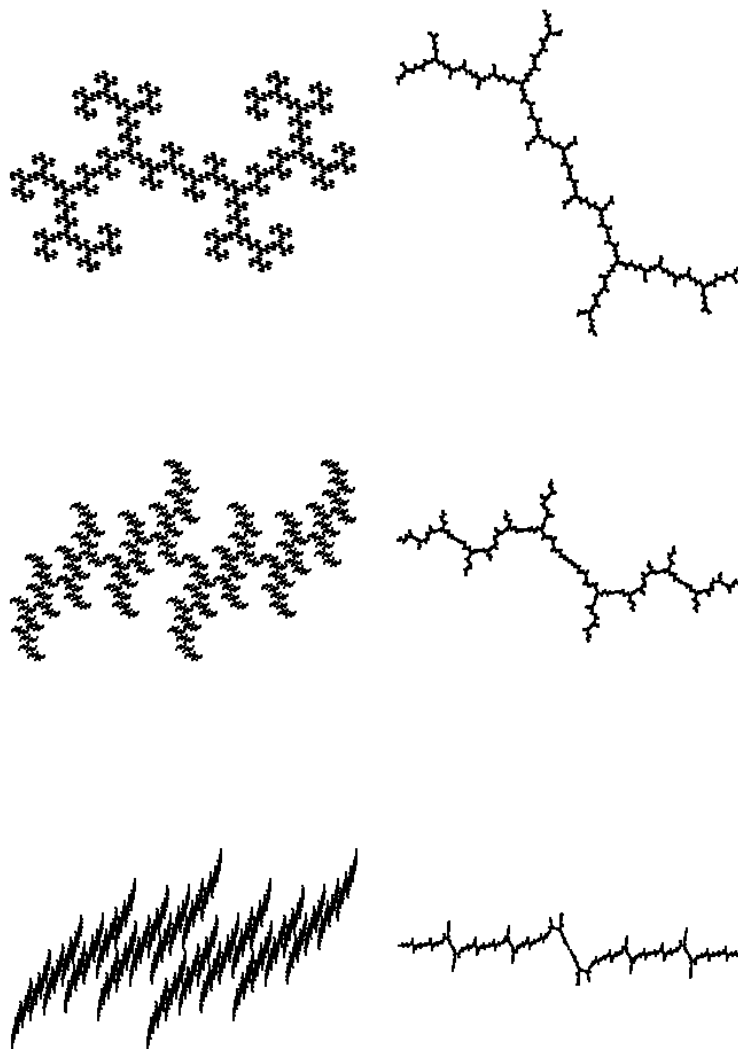


Fig. 4.13. Table illustrating the self similar set A_λ and the corresponding Julia set J_c .

REFERENCES

REFERENCES

- [1] B. Solomyak, “Conjugates of beta-numbers and the zero-free domain for a class of analytic functions,” *Proc. London Math. Soc. (3)*, vol. 68, no. 3, pp. 477–498, 1994.
- [2] D. J. Thompson, “Generalized β -transformations and the entropy of unimodal maps,” *Comment. Math. Helv.*, vol. 92, no. 4, pp. 777–800, 2017.
- [3] W. Thurston, “Entropy in dimension one,” *Frontiers in Complex Dynamics: In Celebration of John Milnor’s 80th Birthday*, pp. 339–384, 2014.
- [4] G. Tiozzo, “Galois conjugates of entropies of real unimodal maps,” *International Mathematics Research Notices*, 2018, accepted.
- [5] P. Erdős, “On a family of symmetric Bernoulli convolutions,” *Amer. J. Math.*, vol. 61, pp. 974–976, 1939.
- [6] Y. Peres, W. Schlag, and B. Solomyak, “Sixty years of Bernoulli convolutions,” *Fractal geometry and stochastics, II (Greifswald/Koserow, 1998)*, vol. 46, pp. 39–65, 2000.
- [7] P. Shmerkin, “On the exceptional set for absolute continuity of Bernoulli convolutions,” *Geom. Funct. Anal.*, vol. 24, no. 3, pp. 946–958, 2014.
- [8] P. Shmerkin and B. Solomyak, “Absolute continuity of complex Bernoulli convolutions,” *Math. Proc. Cambridge Philos. Soc.*, vol. 161, no. 3, pp. 435–453, 2016.
- [9] C. Bandt, “On the mandelbrot set for pairs of linear maps,” *Nonlinearity*, vol. 15, no. 4, pp. 1127–1147, 2002.
- [10] D. Calegari, S. Koch, and A. Walker, “Roots, schottky semigroups, and a proof of bandt’s conjecture,” *Ergodic Theory and Dynamical Systems*, vol. 37, no. 8, pp. 2487–2555, 2017.
- [11] K. I. Eroğlu, S. Rohde, and B. Solomyak, “Quasisymmetric conjugacy between quadratic dynamics and iterated function systems,” *Ergodic Theory and Dynamical Systems*, vol. 30, no. 6, pp. 1665–1684, 2010.
- [12] P. Haïssinsky and K. M. Pilgrim, “Examples of coarse expanding conformal maps,” *Discrete Contin. Dyn. Syst.*, vol. 32, no. 7, pp. 2403–2416, 2012.
- [13] J. E. Hutchinson, “Fractals and self similarity,” *Indiana University Mathematics Journal*, vol. 30, no. 5, pp. 713–747, 1981.
- [14] M. F. Barnsley, *Fractals everywhere*, 2nd ed. Academic Press Professional, Boston, MA, 1993.

- [15] K. Falconer, *Fractal geometry*. John Wiley & Sons, Ltd., Chichester, 1990, mathematical foundations and applications.
- [16] P. A. P. Moran, “Additive functions of intervals and hausdorff measure,” *Mathematical Proceedings of the Cambridge Philosophical Society*, vol. 42, no. 1, pp. 15–23, 1946.
- [17] C. Bandt and D. Mekhontsev, “Elementary fractal geometry: New relatives of the sierpiński gasket,” *Chaos: An Interdisciplinary Journal of Nonlinear Science*, vol. 28, no. 6, pp. 63–104, 2018.
- [18] A. Schief, “Separation properties for self-similar sets,” *Proceedings of the American Mathematical Society*, vol. 122, no. 1, pp. 111–115, 1994.
- [19] C. Bandt and S. Graf, “Self-similar sets vii. a characterization of self-similar fractals with positive hausdorff measure,” *Proceedings of the American Mathematical Society*, pp. 995–1001, 1992.
- [20] M. F. Barnsley and A. N. Harrington, “A mandelbrot set for pairs of linear maps,” *Physica D: Nonlinear Phenomena*, vol. 15, no. 3, pp. 421–432, 1985.
- [21] T. Bousch. (1988) Paires de similitudes. [Online]. Available: <http://topo.math.u-psud.fr/~bousch>
- [22] ——. (1992) Connexité locale et par chemins hölderiens pour les systemes itérés de fonctions. [Online]. Available: <http://topo.math.u-psud.fr/~bousch>
- [23] B. Solomyak, “On the ‘mandelbrot set’ for pairs of linear maps: asymptotic self-similarity,” *Nonlinearity*, vol. 18, no. 5, pp. 1927–1943, 2005.
- [24] C. Bandt and H. Rao, “Topology and separation of self-similar fractals in the plane,” *Nonlinearity*, vol. 20, no. 6, pp. 1463–1474, 2007.
- [25] C. Bandt and N. Hung, “Self-similar sets with an open set condition and great variety of overlaps,” *Proceedings of the American Mathematical Society*, vol. 136, no. 11, pp. 3895–3903, 2008.
- [26] T. Lei, “Similarity between the mandelbrot set and julia sets,” *Communications in mathematical physics*, vol. 134, no. 3, pp. 587–617, 1990.
- [27] A. Kameyama, “Julia sets and self-similar sets,” *Topology Appl.*, vol. 54, no. 1-3, pp. 241–251, 1993.
- [28] F. Beaucloup, P. Borwein, D. W. Boyd, and C. Pinner, “Multiple roots of $[-1, 1]$ power series,” *J. London Math. Soc. (2)*, vol. 57, no. 1, pp. 135–147, 1998.
- [29] H. Bruin and D. Schleicher, “Admissibility of kneading sequences and structure of Hubbard trees for quadratic polynomials,” *J. Lond. Math. Soc. (2)*, vol. 78, no. 2, pp. 502–522, 2008.

VITA

VITA

Stefano was born in the magical and eternal city of Rome, Italy. He has always been fond of mathematics since an early age. When in high-school his teacher Silvana Renzi introduced him to the Mandelbrot set and the theory of fractals, he knew what he wanted to do. Somehow, during his undergraduate studies, he was lucky enough to work with Professor Robert L. Devaney, a leader in the field of Dynamical Systems and Fractals. Through his help and guidance, Stefano managed to enter the graduate school with the largest Dynamical Systems research group in the US. Here, he continued studying this beautiful subject under the supervision of his advisor Professor Rodrigo A. Pérez.

Stefano hopes to continue uncovering the mysterious and fascinating world of Fractals.